LARGE-SCALE DESCRIPTIONS OF THE 1D BOSE GAS & OTHER SELECTED TOPICS IN LOW-DIMENSIONAL QUANTUM MANY-BODY PHYSICS

Jerome Dubail

HABILITATION À DIRIGER LES RECHERCHES

Jérôme Dubail

CNRS et Université de Lorraine
Laboratoire de Physique et Chimie Théoriques

LARGE-SCALE DESCRIPTIONS OF THE 1D BOSE GAS & OTHER SELECTED TOPICS IN LOW-DIMENSIONAL QUANTUM MANY-BODY PHYSICS

DESCRIPTIONS À GRANDE ÉCHELLE DU GAZ DE BOSE 1D & CERTAINS AUTRES PROBLÈMES EN PHYSIQUE QUANTIQUE EN BASSE DIMENSION

Soutenue à Nancy le 6 décembre 2022 devant le jury composé de:

- Rapporteurs

  Fabian Essler, Oxford University

  Thierry Giamarchi, Université de Genève

  Anna Minguzzi, CNRS - Université Grenoble-Alpes

- Examinateurs

  Malte Henkel, Université de Lorraine

  Dragi Karevski, Université de Lorraine

- Membre invité

  Isabelle Bouchoule, CNRS - Université Paris-Saclay

Résumé

Des progrès considérables ont eu lieu ces dernières années concernant la modélisation de la dynamique à grande échelle des systèmes quantiques à N corps en une dimension, quand ceux-ci sont intégrables ou presque intégrables, grâce au développement de l'hydrodynamique généralisée. En particulier, la théorie de l'hydrodynamique généralisée fournit un outil efficace pour la modélisation des expériences sur les gaz de Bose quantiques unidimensionnels. Dans cette thèse d'habilitation je décris les principaux résultats que j'ai obtenus avec mes co-auteurs, à la fois sur les développements de la théorie et sur son application aux expériences d'atomes froids. Je discute également nos tentatives récentes d'incorporer les effets des fluctuations quantiques dans les gaz quantiques hors équilibre dans ce cadre théorique.
Je présente également quelques résultats sur d'autres sujets en physique quantique à N corps en basse dimension. Ceux-ci incluent quelques résultats fondamentaux sur l'"intrication d'opérateurs", un indicateur de la complexité des opérateurs quantiques et de leur approximabilité par des "Matrix Product Operators" dans les systèmes quantiques en une dimension, ainsi que des résultats sur les phases topologiques chirales en deux dimensions (par exemple les états d'effet Hall, les isolants de Chern ou les superfluides p+ip) du point de vue de leurs propriétés d'intrication.

Abstract

Considerable progress has taken place in recent years in modeling the large-scale dynamics of one-dimensional quantum many-body systems that are integrable or nearly integrable, thanks to the advent of Generalized Hydrodynamics. In particular, Generalized Hydrodynamics provides a computationally efficient tool for simulating experiments on one-dimensional Bose gases. In this habilitation thesis I review the main results I obtained with my co-authors, both on theory developments and on the application to cold atom experiments. I also discuss our recent attempts at describing the effects of quantum fluctuations of out-of-equilibrium quantum gases within that framework.
I also present a few results on other topics in low-dimensional quantum many-body physics. These include basic results on 'operator entanglement', an indicator of the complexity of quantum operators and of their approximability by Matrix Product Operators in one-dimensional quantum systems, as well as results on two-dimensional chiral topological phases (e.g. quantum Hall states, Chern bands, or p+ip superfluids) from the point of view of their entanglement properties.

Foreword

Acknowledgments/Remerciements

Je remercie Anna Minguzzi, Fabian Essler et Thierry Giamarchi d'avoir accepté d'être rapporteurs de ce mémoire d'habilitation, et Isabelle Bouchoule, Malte Henkel et Dragi Karevski de participer à mon jury.

Ce mémoire est basé sur des travaux que j'ai effectués dans les dix dernières années en collaboration avec de nombreux collègues physiciens et physiciennes de diverses nationalités et de tous âges. Certains ont été des mentors, d'autres des élèves, beaucoup sont devenus des amis et amies. Je voudrais dire que je les remercie tous et toutes du fond du coeur. J'ai appris énormément d'eux, et j'ai aussi passé de nombreux moments inoubliables. J'espère qu'ils et elles m'excuseront de renoncer à établir une liste nominative ici. J'ai peur d'en oublier certains, et aussi je n'ai pas envie de devoir établir un classement. Je fais simplement une exception pour dire que, au moment d'écrire ces lignes, je pense à Marko Medenjak avec une très grande tristesse.

J'aimerais remercier mes collègues du LPCT, en particulier ceux de l'axe 'dynamique et symétrie' (anciennement 'groupe de physique statistique'), pour toutes les discussions que nous avons eues et pour la bonne ambiance qui régnait dans les couloirs de notre labo pendant ces années. Je remercie ceux qui ont constitué nos équipes de direction successives (Xavier Assfeld, Dragi Karevski, François Dehez) pour tout le travail effectué dont j'ai pu être témoin lorsque j'étais membre de notre comité scientifique, ainsi que notre administratrice Séverine Bonenberger sans qui le LPCT ne pourrait tout simplement pas exister (ainsi que Charlotte Stenger, arrivée plus récemment).

Enfin je remercie ma famille. Ces remerciements-là resteront privés, mais il est évident que rien ne serait possible sans le soutien sans faille et les sacrifices de mes proches.

Scope and organization of this manuscript

This manuscript gives a brief overview of some research directions I have investigated since I obtained my PhD in 2010. It is organized in three main parts.

Part I focuses on the dynamics of the one-dimensional Bose gas, from the perspective

of Generalized Hydrodynamics. It represents my main research activity over the period 2016-2022. The first two chapters of that Part are largely based on a recent review article I co-authored with Isabelle Bouchoule (Bouchoule and Dubail, 2022). I have used selected sections of that review article, which I have reorganized and made more concise. These two chapters provide an introduction to the Lieb-Liniger gas and to its description in terms of Generalized Hydrodynamics. The third chapter of that part is independent from the review article; it discusses developments about the description of quantum fluctuations.

In Part II, I briefly present some results I obtained on two other topics. In the first chapter, I discuss the operator entanglement of quantum operators in spin chains and its implications for their approximability by Matrix Product Operators. This is a research topic I have been investigating since 2016. In the second chapter of that Part, I discuss some older results on entanglement in chiral topological phases, which I obtained over the period 2010-2015, when I was a postdoc with Nick Read and in the following years.

In Part III, I discuss some research perspectives for the next few years.

The Appendices contain reproductions of my main publications, as well as my scientific curriculum.

Contents

Part I

Large-scale descriptions of the 1D Bose gas

This first Part of my manuscript is the longest and most detailed one, as it reflects my main research topic from 2016 to 2022. I give a detailed introduction to results I have obtained on Generalized Hydrodynamics in the 1D Bose gas, as well as on its quantum fluctuations. Some other research topics I have explored over the past decade are presented more succinctly in Part II.

The text of this Part, including its introduction, Chapter 1 and Chapter 2, are largely based on a review article I co-authored with Isabelle Bouchoule very recently (Bouchoule and Dubail, 2022). I have used selected parts of that review article —these parts were all written by myself and not by Isabelle—, which I have reorganized and shortened here. Chapter 3 is independent from the review article and is based on unpublished notes.

Introduction: What is Generalized Hydrodynamics?

Physical systems of many identical particles behave very differently depending on the distance and time scales at which they are probed. In a very dilute gas, on time scales not larger than the typical time between collisions, the particles are essentially non-interacting. Then two clouds of fluid can collide and simply pass through each other; one example of such phenomenon, familiar from astrophysics, is the one of clouds of stars in colliding galaxies. In contrast, on time scales much longer than the collision time, particles typically undergo a very large number of collisions, so that the fluid has time to locally relax to an equilibrium state. This local relaxation gives rise to hydrodynamic behavior, which is typically much more complex, non-linear, than simple free propagation. For example, one can think of two droplets of water that collide: those will not simply pass through each other. More likely their motion will be more complex, for instance they will coalesce.

Fluid dynamics at short times is captured by an evolution equation for the phase-space density of particles $\rho(x,p,t)$ which takes the form of a free transport equation, or collisionless Boltzmann equation. Typically,

$$\frac{\partial}{\partial t}\rho(x,p,t) + v(p)\frac{\partial}{\partial x}\rho(x,p,t) - \frac{\partial V(x)}{\partial x}\frac{\partial}{\partial p}\rho(x,p,t) \;=\; 0. \tag{1}$$

Here we write the equation in one spatial dimension; the extension to higher dimensions is straightforward. In Eq. (1), $v(p)$ is usually the group velocity $\partial\varepsilon(p)/\partial p$ of a particle with momentum p and kinetic energy $\varepsilon(p)$, and $V(x)$ is an external potential. Eq. (1) is obtained, for instance, for N classical particles described by the non-interacting Hamiltonian $\mathcal{H} = \sum_{j=1}^{N}[\varepsilon(p_j)+V(x_j)]$. Then the evolution of the phase-space density $\rho(x,p,t) = \sum_{j=1}^{N}\delta(x-$

$x_j(t))\delta(p - p_j(t))$ follows from the evaluation of the Poisson bracket $\partial\rho/\partial t = \{\mathcal{H}, \rho\}$. Equations similar to Eq. (1) appear in the description of fluids made of both classical particles and quantum particles; we come back to this below.

On time scales much longer than the relaxation time, equation (1) is superseded by a system of hydrodynamic equations. At that scale, the fluid is locally relaxed to an equilibrium state at any time. Local equilibrium states are parametrized by the conserved quantities in the system, whose time evolution is given by continuity equations. A good example is the one of a Galilean fluid with conserved particle number, conserved momentum and conserved energy. Then a coarse-grained hydrodynamic description, valid at large distance and time scales, is obtained by writing three continuity equations for the mass density q_M, the momentum density q_P, and the energy density q_E,

$$\left\{ \begin{array}{rcc} \frac{\partial}{\partial t} q_M(x,t) + \frac{\partial}{\partial x} j_M(x,t) & = & 0 \\ \frac{\partial}{\partial t} q_P(x,t) + \frac{\partial}{\partial x} j_P(x,t) & = & -\frac{1}{m}\frac{\partial V(x)}{\partial x} q_M(x,t) \\ \frac{\partial}{\partial t} q_E(x,t) + \frac{\partial}{\partial x} j_E(x,t) & = & 0, \end{array} \right. \tag{2}$$

where j_M, j_P and j_E are the three associated currents. Here the second line is not quite a continuity equation, unless $\partial V/\partial x = 0$. This is simply because momentum is not conserved in the presence of an external force: the right hand side in this evolution equation for q_P is given by Newton second law.

Because of local equilibration, the currents depend on x and t only through their dependence on the charge densities. In general, a current j is a function of all charge densities q and of their spatial derivatives $\partial_x q$, $\partial_x^2 q$, etc. However, for density variations of very long wavelengths, the dependence on the derivatives can be neglected, and j_M, j_P and j_E are functions of q_M, q_P and q_E only. The zeroth-order hydrodynamic equations obtained in this way are usually called 'Euler scale' hydrodynamics or 'the Euler hydrodynamic limit'. At the Euler scale, the three continuity equations above reduce to the standard Euler equations for a Galilean fluid,

$$\left\{ \begin{array}{rcc} \frac{\partial}{\partial t} n + \frac{\partial}{\partial x}(nu) & = & 0 \\ \frac{\partial}{\partial t} u + u\frac{\partial}{\partial x} u + \frac{1}{mn}\partial_x \mathcal{P} & = & -\frac{1}{m}\frac{\partial V}{\partial x} \\ \frac{\partial}{\partial t} e + u\frac{\partial}{\partial x} e + \frac{1}{n}\mathcal{P}\partial_x u & = & 0. \end{array} \right. \tag{3}$$

Here m is the particles' mass, $n = q_M/m$ is the particle density, $u = q_P/q_M$ is the mean fluid velocity, and $e = (q_E - q_P^2/(2q_M) - nV(x))/n$ is the internal energy per particle. To go from the conservation equations (2) to the system (3), one uses the fact that $j_M = q_P$ because of Galilean invariance. Moreover, at the Euler scale, $j_P = q_P^2/q_M + \mathcal{P}$ and $j_E = (q_E + \mathcal{P})q_P/q_M$, where $\mathcal{P} = \mathcal{P}(n, e)$ is the equilibrium pressure.

To close the system of equations (3), one needs to know the equilibrium pressure $\mathcal{P}(n, e)$, which is a function of n and e that depends on the microscopic details of the system. In some simple models such as the ideal gas, a simple analytic expression for the pressure

is available, but usually there is none. For the one-dimensional Bose gas with contact repulsion, which is at the center of this review article, $\mathcal{P}(n, e)$ can be tabulated numerically.

To conclude this brief discussion of hydrodynamic equations, we mention that it is of course possible to go 'beyond the Euler scale', and to do first-order hydrodynamics by keeping the dependence of the currents on gradients of charge densities. This results in Navier-Stokes-like hydrodynamic equations, which include dissipative terms. In this review article we mostly focus on Euler scale (zeroth order) hydrodynamics.

'Generalized Hydrodynamics' is about the peculiar fluid-like behavior that emerges in 1D classical and quantum integrable systems. It is peculiar in the sense that it is simultaneously of the form (2,3) and of the form (1), on time scales much longer than the inverse collision rate. This behavior has become known as 'Generalized Hydrodynamics' or 'GHD' since 2016 (Castro-Alvaredo et al., 2016; Bertini et al., 2016). Here the word 'Generalized' is used in the same way as it is in 'Generalized Gibbs Ensemble' (Rigol et al., 2007, 2008): it designates the extension of a concept ('Gibbs Ensemble' or 'Hydrodynamics') from the case with a small, finite, number of conserved quantities to the case with infinitely many of them.

To illustrate the emergence of 'Generalized Hydrodynamics' in a system with infinitely many conserved quantities, it is instructive to think about N identical billiard balls of diameter $|\Delta|$ whose motion is restricted to a one-dimensional line, see Fig. 1. Here we take $\Delta < 0$. [This funny convention ensures that the hydrodynamic equations for the hard core gas (4) are almost the same as the ones for the Lieb-Liniger gas, see Eq. (1.55). Δ is positive in the repulsive one-dimensional Bose gas, see Subsection 1.1.1.] This model for a classical one-dimensional gas is known as the 'hard rod gas' in the statistical physics literature, see e.g. (Percus, 1976; Lebowitz and Percus, 1967; Aizenman et al., 1975; Boldrighini et al., 1983; Spohn, 2012; Boldrighini and Suhov, 1997; Doyon and Spohn, 2017*b*; Cao et al., 2018). The balls are at position x_j and move at velocity v_j, $j = 1, \ldots, N$. When two balls collide elastically, they exchange their velocities, so the set of velocities is conserved at any time. Thus, this many-particle system has infinitely many conserved quantities that are independent in the thermodynamic limit $N \to \infty$. Indeed, for any function f of the velocity, the charge $Q[f] := \sum_{j=1}^{N} f(v_j)$ is conserved.

One can introduce a coarse-grained phase-space density of balls $\rho(x, v) = \sum_{j=1}^{N} \delta_\ell(x - x_j)\delta_\sigma(v - v_j)$, where δ_ℓ and δ_σ are smooth distributions with weight one peaked around the origin, for instance two Gaussians of width ℓ and σ. When ℓ and σ are large enough so that the phase space volume $[x, x+\ell] \times [v, v+\sigma]$ contains a very large number of balls, but small enough so that the density stays constant through the volume, the coarse-grained

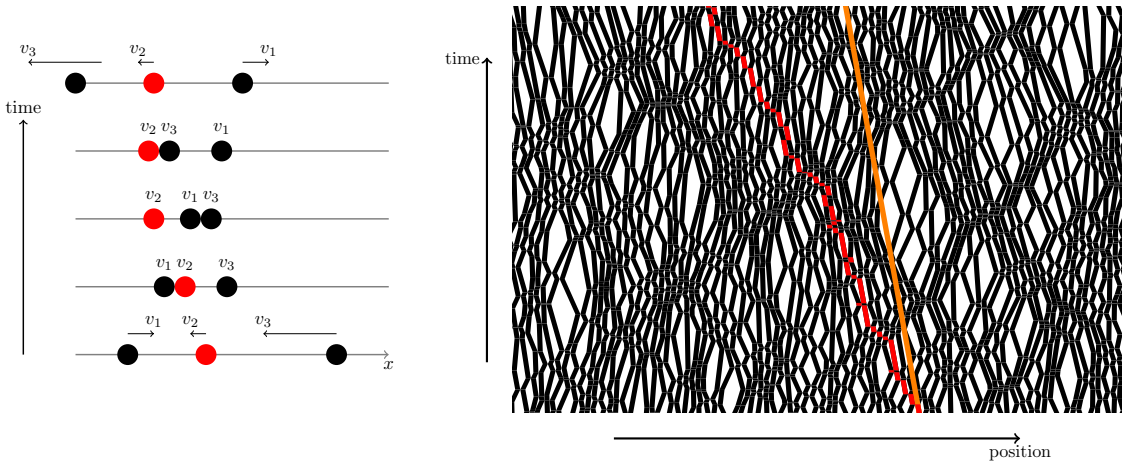

Figure 1: *[From the review article (Bouchoule and Dubail, 2022)]* The simplest system that exhibits 'Generalized Hydrodynamics' is arguably the classical hard rod gas, i.e. identical billiard balls whose motion is restricted to a line. Left: the balls collide elastically and exchange their velocities. One can re-index the balls after each collision so that the 'bare' velocity v_j is constant (here the red ball is the one with velocity v_2 at any time). Right: at large distance and time scales, the effective velocity of the red ball v^{eff} (red trajectory) is different from its 'bare' velocity v (orange trajectory). The 'Generalized Hydrodynamics' description of the hard rod gas (4) is an Euler hydrodynamic limit where the interactions between the particles enter through the effective velocity.

density evolves according to the two equations

$$\begin{cases} \partial_t \rho(x,v,t) + \partial_x \left(v^{\text{eff}}[\rho](v)\, \rho(x,v,t) \right) - \dfrac{1}{m} \dfrac{\partial V(x)}{\partial x} \partial_v \rho(x,v,t) \;=\; 0, \\ v^{\text{eff}}[\rho](v) = v - \Delta \displaystyle\int_{-\infty}^{\infty} \left(v^{\text{eff}}[\rho](v) - v^{\text{eff}}[\rho](w) \right) \rho(w) dw, \end{cases} \tag{4}$$

where we have included an external potential $V(x)$. These are the Generalized Hydrodynamics equations for the hard rod gas, initially derived by Percus (1976), and proved by Boldrighini et al. (1983) for $V(x) = 0$. The inclusion of the trapping potential, and its breaking of the conservation laws, was investigated more recently by Cao et al. (2018).

The first equation (4) is similar to the transport equation (1), although two important differences need to be stressed. The first difference lies in the range of applicability of Eq. (4): it is a coarse-grained description of the hard rod gas based on local relaxation, which is valid only at the Euler scale. The free transport equation (1), on the other hand, does not rely on hydrodynamic assumptions. The second difference is that, instead of the single-particle group velocity, Eq. (4) involves an 'effective velocity'. That effective velocity

is a functional of the density $\rho(v)$ at a given position x and time t, defined by the second equation (4). It has a simple interpretation, see Fig. 1. At each collision, the labels of the colliding balls can be switched, so that each velocity v_j stays constant, but the position x_j changes instantaneously by $\pm|\Delta|$ (the diameter of the balls). For a finite density of balls, these jumps result in a modification of the propagation velocity of the ball with velocity v_j through the gas, $v_j \to v^{\text{eff}}[\rho](v_j)$.

The Generalized Hydrodynamics equations (4) are also analogous to the Euler hydrodynamic equations (2)-(3), but for infinitely many charges. All the charges are conserved in the absence of an external potential ($V(x) = 0$), while for $V(x) \neq 0$ only the conservation of mass and energy are expected to survive, generically. To see this, consider the aforementioned charges $Q[f] = \sum_{j=1}^{N} f(v_j)$, and their associated charge densities $q[f](x,t) = \int_{-\infty}^{\infty} f(v)\rho(x,v,t)dv$. Those charge densities evolve according to

$$\begin{aligned} &\frac{\partial}{\partial t} q[f](x,t) + \frac{\partial}{\partial_x} j[f](x,t) \;=\; -\frac{1}{m}\frac{\partial V(x)}{\partial x}\int_{-\infty}^{\infty} f'(v)\rho(x,v,t)dv, \\ &\text{with} \qquad j[f](x,t) = v^{\text{eff}}[\rho](v)q[f](x,t). \end{aligned} \tag{5}$$

When $V(x) = 0$, the first equation is a continuity equation that expresses the conservation of $Q[f]$. The second line gives the expectation value of the current as a function of the charge densities under the hydrodynamic assumptions.

Thus, as claimed above, Generalized Hydrodynamics captures a peculiar fluid-like behavior which resembles both a fluid obeying the free transport equation (1), and one obeying the Euler hydrodynamic equations (2,3).

Remarkably, the Generalized Hydrodynamics equations (4) have reappeared in 2016, in the context of quantum integrable one-dimensional systems (Castro-Alvaredo et al., 2016; Bertini et al., 2016). In the decade that preceded this 2016 breakthrough, tremendous progress had been made on out-of-equilibrium quantum dynamics, largely driven by advances in cold atom experiments. To name but one example, the 2006 Quantum Newton Cradle experiment of Kinoshita et al. (2006), where two one-dimensional clouds of interacting atoms in a harmonic potential $V(x)$ undergo thousands of collisions, seemingly escaping convergence towards thermal equilibrium, had become an important source of inspiration and a challenge for quantum many-body theorists. Many important conceptual advances on the thermalization (or absence thereof) of isolated quantum systems, in particular the developments around the notion of Generalized Gibbs Ensemble, occurred between 2006 and 2016. Yet, a quantitatively reliable modeling of the Quantum Newton Cradle setup, with experimentally realistic parameters, had remained completely out of reach. As usual with quantum many-body systems, the exponential growth of the Hilbert space with the number of atoms N seemingly prevented direct numerical simulations of the dynamics.

The 2016 breakthrough of Generalized Hydrodynamics has completely changed this state of affairs. Realizing that the dynamics of one-dimensional ultracold quantum gases

in experiments such as the Quantum Newton Cradle is captured by Generalized Hydrodynamics equations of the form (4) has ushered in a new era for their theory description.

Chapter 1

The 1D Bose gas: from the exact solution by Bethe Ansatz to Generalized Hydrodynamics

1.1 The Lieb-Liniger model and the rapidities

In the absence of an external potential, the Hamiltonian of one-dimensional bosons with delta repulsion is, in second quantized form,

$$H = \int \Psi^\dagger(x) \left[-\frac{\hbar^2 \partial_x^2}{2m} - \mu + \frac{g}{2} \Psi^\dagger(x) \Psi(x) \right] \Psi(x)\, dx. \tag{1.1}$$

Here $\Psi^\dagger(x)$ and $\Psi(x)$ are the boson creation/annihilation operators that satisfy the canonical commutation relations $\left[\Psi(x), \Psi^\dagger(x')\right] = \delta(x - x')$, m is the mass of the bosons, $g > 0$ is the 1D repulsion strength, and μ is the chemical potential. The total number of particles in the system is $N = \int \left\langle \Psi^\dagger(x)\Psi(x) \right\rangle dx$. In the literature, it is customary to define the parameter $c = mg/\hbar^2$, homogeneous to an inverse length. In a box of length L, the ratio of c to the particle density $n = N/L$ gives the dimensionless repulsion strength, or Lieb parameter,

$$\gamma = \frac{c}{n} = \frac{mg}{\hbar^2 n}. \tag{1.2}$$

In the rest of this section we review some basic facts about the exact solution of the model (1.1) of Lieb and Liniger (1963), see (Korepin et al., 1997; Gaudin, 2014) for introductions. In particular, we emphasize the crucial concept of the *rapidities*, and we review a number of results that have proved useful in the recent developments of Generalized Hydrodynamics. We set $\hbar = m = 1$.

1.1.1 The scattering shift (or Wigner time delay)

It is instructive to start with the case of $N = 2$ particles on an infinite line. In first quantization, using center-of-mass and relative coordinates $X = (x_1 + x_2)/2$ and $Y = x_1 - x_2$, the Hamiltonian (1.1) splits into a sum of two independent one-body problems,

$$H \;=\; -\frac{1}{2}\partial_{x_1}^2 - \frac{1}{2}\partial_{x_2}^2 + c\,\delta(x_1 - x_2) \;=\; -\frac{1}{4}\partial_X^2 - \partial_Y^2 + c\,\delta(Y). \tag{1.3}$$

The eigenstates of the center-of-mass Hamiltonian $-\frac{1}{4}\partial_X^2$ are plane waves, and the Hamiltonian for the relative coordinate Y is the one of a particle of mass $1/2$ in the presence of a delta potential at $Y = 0$. Because of that delta potential, the first derivative of the wavefunction $\varphi(Y)$ must have a discontinuity at $Y = 0$: $\varphi'(0^+) - \varphi'(0^-) - c\,\varphi(0) = 0$. Coming back to the original coordinates, one sees that the two-body wavefunction $\varphi(x_1, x_2) = \langle 0|\,\Psi(x_1)\Psi(x_2)\,|\varphi\rangle$ satisfies

$$\lim_{x_2 \to x_1^+} [\partial_{x_2}\varphi(x_1, x_2) - \partial_{x_1}\varphi(x_1, x_2) \;-\; c\,\varphi(x_1, x_2)] = 0. \tag{1.4}$$

The same condition holds for x_1 exchanged with x_2, since the wavefunction is symmetric. Thus the eigenstates of (1.3) are

$$\varphi(x_1, x_2) \;\propto\; \begin{cases} (\theta_2 - \theta_1 - ic)e^{ix_1\theta_1 + ix_2\theta_2} - (\theta_1 - \theta_2 - ic)e^{ix_1\theta_2 + ix_2\theta_1} & \text{if} \quad x_1 < x_2 \\ (x_1 \leftrightarrow x_2) & \text{if} \quad x_1 > x_2, \end{cases} \tag{1.5}$$

corresponding to the eigenvalues $(\theta_1^2 + \theta_2^2)/2$. For $\theta_1 > \theta_2$, the two terms $e^{ix_1\theta_1 + ix_2\theta_2}$ and $e^{ix_1\theta_2 + ix_2\theta_1}$ correspond to the in-coming and out-coming pairs of particles in a two-body scattering process. The ratio of their amplitudes is the two-body scattering phase,

$$e^{i\phi(\theta_1 - \theta_2)} := \frac{\theta_1 - \theta_2 - ic}{\theta_2 - \theta_1 - ic}. \tag{1.6}$$

An equivalent expression for that phase, often used in the literature and which we also use below, is $\phi(\theta) = 2\arctan(\theta/c) \in [-\pi, \pi]$.

It was pointed out by Eisenbud (1948) and by Wigner (1955) that the scattering phase may be viewed semiclassically as a 'time delay'. Let us briefly sketch the argument of Wigner (1955). First, we note that, for a single particle, a simple substitute for a wavepacket is a superposition of two plane waves with momenta θ and $\theta + \delta\theta$,

$$e^{ix\theta} + e^{ix(\theta + \delta\theta)}. \tag{1.7}$$

Such a superposition evolves in time as $e^{ix\theta - it\varepsilon(\theta)} + e^{ix(\theta+\delta\theta) - it\varepsilon(\theta+\delta\theta)}$, where $\varepsilon(\theta) = \theta^2/2$ is the energy. The center of this 'wave packet' is at the position where the phases of the two terms coincide, namely the point where $x\delta\theta - t[\varepsilon(\theta + \delta\theta) - \varepsilon(\theta)] = 0$, which gives $x \simeq vt$ with the group velocity $v = d\varepsilon/d\theta = \theta$. So this is indeed a 'wave packet' moving at speed

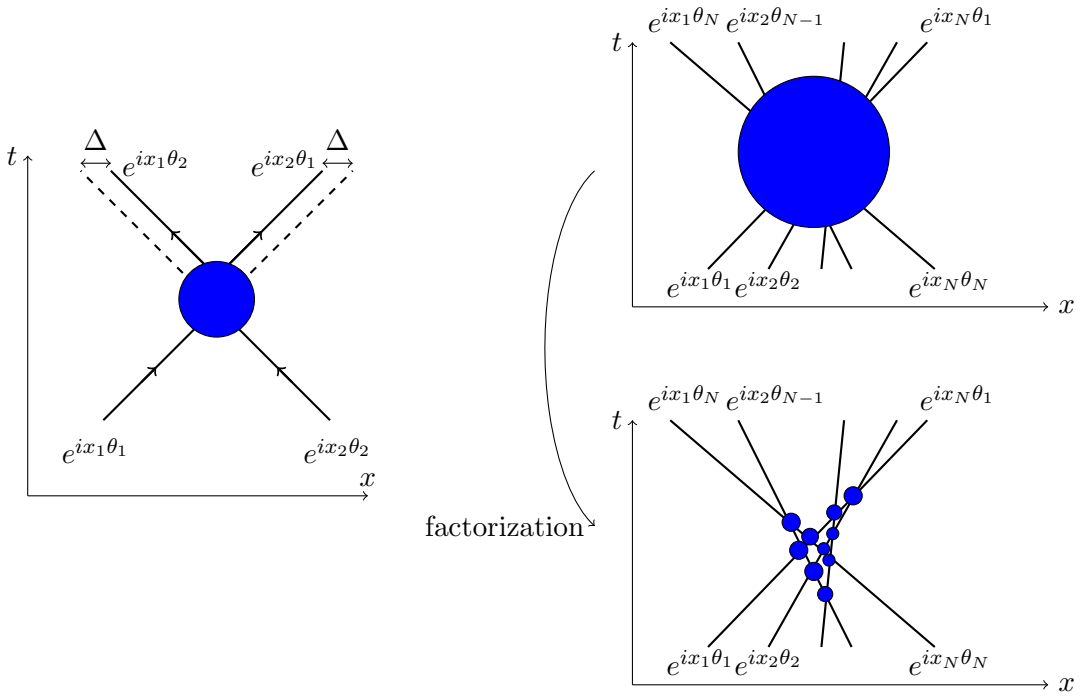

Figure 1.1: *[From the review article (Bouchoule and Dubail, 2022)]* Left: the wavefunction (1.5) on the infinite line corresponds to a two-body scattering process. Semiclassically, the scattering phase in that two-body process is reflected in the scattering shift (1.11): after the collision, the position of the particle has been shifted by a distance $\Delta(\theta_1 - \theta_2)$. Right: the Bethe wavefunction (1.12) on the infinite line corresponds to an N-body scattering process which factorizes into two-body processes (the scattering shift Δ is also present here, but it is not drawn in the cartoon). In that N-body process, the rapidities θ_j are the asymptotic momenta of the bosons.

θ. Next, consider two incoming particles in a state such that the center of mass $(x_1+x_2)/2$ has momentum $\theta_1+\theta_2$, while the relative coordinate x_1-x_2 is in a 'wave packet' moving at velocity $(\theta_1-\theta_2)/2$,

$$\begin{aligned}\psi_{\text{inc.}}(x_1,x_2) &\propto e^{i\frac{x_1+x_2}{2}(\theta_1+\theta_2)}\left(e^{i(x_1-x_2)\frac{\theta_1-\theta_2}{2}}+e^{i(x_1-x_2)(\frac{\theta_1-\theta_2}{2}+\delta\theta)}\right)\\ &= e^{ix_1\theta_1+ix_2\theta_2}+e^{ix_1(\theta_1+\delta\theta)+ix_2(\theta_2-\delta\theta)}.\end{aligned} \tag{1.8}$$

According to Eqs. (1.5)-(1.6), the corresponding out-coming state would be

$$\begin{aligned}\psi_{\text{outc.}}(x_1,x_2) &\propto -e^{i\phi(\theta_1-\theta_2)}e^{ix_1\theta_2+ix_2\theta_1}-e^{i\phi(\theta_1-\theta_2+2\delta\theta)}e^{ix_1(\theta_2-\delta\theta)+ix_2(\theta_1+\delta\theta)}\\ &= e^{i\frac{x_1+x_2}{2}(\theta_1+\theta_2)}\left(-e^{i\phi(\theta_1-\theta_2)}e^{i(x_2-x_1)\frac{\theta_1-\theta_2}{2}}-e^{i\phi(\theta_1-\theta_2+2\delta\theta)}e^{i(x_2-x_1)(\frac{\theta_1-\theta_2}{2}+\delta\theta)}\right).\end{aligned} \tag{1.9}$$

Then, repeating the previous argument of phase stationarity, one finds that the relative coordinate is at position $x_1-x_2\simeq\frac{\theta_1-\theta_2}{2}t-2d\phi/d\theta$ at time t. Since the center of mass is not affected by the collision and moves at the group velocity $(\theta_1+\theta_2)/2$, we see that the position of the two semiclassical particles after the collision will be

$$x_1\simeq\theta_1 t-\Delta(\theta_2-\theta_1),\qquad x_2\simeq\theta_2 t+\Delta(\theta_2-\theta_1), \tag{1.10}$$

where the scattering shift $\Delta(\theta)$ is given by the derivative of the scattering phase,

$$\Delta(\theta):=\frac{d\phi(\theta)}{d\theta}=\frac{2c}{c^2+\theta^2}. \tag{1.11}$$

The two particles are delayed: their position after the collision is the same as if they were late by a time $\delta t_1=\Delta(\theta_2-\theta_1)/v_1$ and $\delta t_2=\Delta(\theta_2-\theta_1)/v_2$ respectively.

1.1.2 The Bethe wavefunction, and the rapidities as asymptotic momenta

For more particles, the eigenstates of the Hamiltonian (1.1) on the infinite line are Bethe states $|\{\theta_a\}\rangle$ labeled by a set of N numbers $\{\theta_a\}_{1\le a\le N}$, called the rapidities. In the domain $x_1<x_2<\cdots<x_N$, the wavefunction is (Lieb and Liniger, 1963; Korepin et al., 1997; Gaudin, 2014)

$$\begin{aligned}\varphi_{\{\theta_a\}}(x_1,\dots,x_N) &= \langle 0|\,\Psi(x_1)\dots\Psi(x_N)\,|\{\theta_a\}\rangle\\ &\propto \sum_\sigma(-1)^{|\sigma|}\left(\prod_{1\le a<b\le N}(\theta_{\sigma(b)}-\theta_{\sigma(a)}-ic)\right)e^{i\sum_j x_j\theta_{\sigma(j)}},\end{aligned} \tag{1.12}$$

and it is extended to other domains by symmetry $x_i\leftrightarrow x_j$. Here the sum runs over all permutations σ of N elements (so there are $N!$ terms) and $(-1)^{|\sigma|}$ is the signature of the

permutation. The momentum and energy of the eigenstate (1.12) are

$$P = \sum_{a=1}^{N} \theta_a, \qquad E = \sum_{a=1}^{N} \frac{\theta_a^2}{2}. \tag{1.13}$$

The rapidities θ_a are conveniently thought of as the asymptotic momenta in an N-body scattering process. For $\theta_1 > \theta_2 > \cdots > \theta_N$, the combination of two terms

$$e^{ix_1\theta_1+\cdots+ix_N\theta_N} + \left(\prod_{1\leq a<b\leq N} -e^{i\phi(\theta_a-\theta_b)}\right) e^{ix_1\theta_N+\cdots+ix_N\theta_1} \tag{1.14}$$

that appears in (1.12) can be viewed as the sum of in-coming ($e^{ix_1\theta_1+\cdots+ix_N\theta_N}$) and out-coming states ($e^{ix_1\theta_N+\cdots+ix_N\theta_1}$) in an N-body scattering process, see Fig. 1.1. Their respective amplitude $\prod_{1\leq a<b\leq N} -e^{i\phi(\theta_a-\theta_b)}$ is a many-body phase, which depends on all in-coming rapidities. Crucially, this many-body phase factorizes into a product of two-body scattering phases (1.6): this is a central property of all quantum integrable systems.

The fact that the rapidities are the asymptotic momenta in a scattering process implies that they can be measured by letting the bosons expand freely along the infinite line (Rigol and Muramatsu, 2005; Minguzzi and Gangardt, 2005; Buljan et al., 2008; Jukić et al., 2008; Del Campo, 2008; Bolech et al., 2012; Campbell et al., 2015; Mei et al., 2016; Caux et al., 2019; Wilson et al., 2020; Malvania et al., 2020). Here we follow the argument of (Campbell et al., 2015).

Consider a state $|\psi_t\rangle$ of N bosons confined to some interval around the origin at time t. This could be, for instance, the ground state in a trapping potential $V(x)$, or some out-of-equilibrium state produced by some quench protocol, also in a trapping potential to ensure that the bosons are initially confined. This many-body state can be expanded in the basis of Bethe states,

$$\begin{aligned} |\psi_t\rangle &= \int_{\theta_1>\theta_2>\cdots>\theta_N} d\theta_1 d\theta_2 \ldots d\theta_N \ \langle\{\theta_a\}|\psi_t\rangle \ |\{\theta_a\}\rangle \\ &= \frac{1}{N!}\int d\theta_1 d\theta_2 \ldots d\theta_N \ \langle\{\theta_a\}|\psi_t\rangle \ |\{\theta_a\}\rangle\,, \end{aligned} \tag{1.15}$$

where the Bethe states on the infinite line are normalized such that $\langle\{\theta_a\}|\{\theta'_a\}\rangle = \prod_{a=1}^{N}\delta(\theta_a-\theta'_a)$ (assuming that both sets of rapidities are ordered, $\theta_1 > \cdots > \theta_N$ and $\theta'_1 > \cdots > \theta'_N$). The integral is restricted to the domain $\theta_1 > \theta_2 > \cdots > \theta_N$ in the first line to avoid double-counting. Notice that, with the definition (1.12), the Bethe states are anti-symmetric under exchange of two rapidities $\theta_a \leftrightarrow \theta_b$. Then, plugging (1.12) into (1.15), and using this anti-symmetry, one obtains (Campbell et al., 2015)

$$\langle 0|\,\Psi(x_1)\ldots\Psi(x_N)\,|\psi_t\rangle \propto \int d\theta_1 \ldots d\theta_N \ \langle\{\theta_a\}|\psi_t\rangle \ e^{i\sum_{a<b}\phi(\theta_a-\theta_b)} e^{i\sum_a x_a\theta_{N+1-a}}, \tag{1.16}$$

for $x_1 < x_2 < \cdots < x_N$. This expression is particularly convenient to analyze the expansion. When the trapping potential $V(x)$ is switched off at time t, and the bosons are let to evolve freely along the infinite line, the probability to find them at positions $x_1, x_2, \ldots, x_N$ after an expansion time $t_{\rm exp}$ is

$$\begin{aligned} P_{\rm exp}(x_1,\ldots,x_N) &= |\langle 0|\,\Psi(x_1,t_{\rm exp})\ldots\Psi(x_N,t_{\rm exp})\,|\psi_t\rangle|^2 \\ &\propto \left|\int d\theta_1\ldots d\theta_N\ \langle\{\theta_a\}\,|\psi_t\rangle\ e^{i\sum_{a<b}\phi(\theta_a-\theta_b)} e^{i\sum_a (x_a\theta_{N+1-a} - i\frac{t}{2}\theta_{N+1-a}^2)}\right|^2 \\ &\underset{t_{\rm exp.}\to\infty}{=} \frac{1}{t_{\rm exp}^N}\,|\langle\{x_N/t_{\rm exp},\ldots,x_1/t_{\rm exp}\}\,|\psi_t\rangle|^2\,. \end{aligned} \tag{1.17}$$

From the second to the third line, we have used the stationary phase approximation, taking the limit $t_{\rm exp}\to\infty$ while keeping the ratios $x_1/t_{\rm exp},\ldots,x_N/t_{\rm exp}$ fixed. The proportionality factor is fixed by imposing that $\int_{x_1<\cdots<x_N} P(x_1,\ldots,x_N)dx_1\ldots dx_N = 1$.

In conclusion, we see from (1.17) that the joint probability distribution of the positions of the atoms after a large 1D expansion time directly reflects the distribution of rapidities in the state $|\psi_t\rangle$ just before the expansion. This is very important because it means that the rapidities can be measured experimentally, by performing such 1D expansions. This has been done experimentally for the first time by Wilson et al. (2020).

1.1.3 Finite density and the Bethe equations

In the two previous subsections, we have focused on a finite number of bosons on the infinite line, corresponding to a vanishing density of particles. But, to understand the thermodynamic properties of the model, one needs to work with a finite density N/L. This can be done by imposing periodic boundary conditions, identifying the points $x = 0$ and $x = L$ in the system. Imposing periodic boundary conditions on the Bethe wavefunction (1.12), i.e. $\varphi_{\{\theta_a\}}(x_1,\ldots,x_{N-1},L) = \varphi_{\{\theta_a\}}(0,x_1,\ldots,x_{N-1})$, leads to the Bethe equations

$$e^{i\theta_a L}\prod_{b\neq a} e^{i\phi(\theta_a-\theta_b)} = (-1)^{N-1}, \qquad a = 1,\ldots,N, \tag{1.18}$$

where the two-body scattering phase $\phi(\theta_a-\theta_b)$ is defined in Eq. (1.6). Taking the logarithm on both sides, one gets the following system of N coupled non-linear equations

$$\theta_a + \frac{1}{L}\sum_{b\neq a} 2\,\arctan\left(\frac{\theta_a-\theta_b}{c}\right) = p_a, \qquad \text{where} \quad \begin{cases} p_a \in \frac{2\pi}{L}\mathbb{Z} & \text{for} \quad N \quad \text{odd} \\ p_a \in \frac{2\pi}{L}(\mathbb{Z}+\frac{1}{2}) & \text{for} \quad N \quad \text{even.} \end{cases} \tag{1.19}$$

It is convenient to think of the numbers p_a as the momenta of N non-interacting fermions (with periodic or anti-periodic boundary conditions, depending on the parity of N). These fermion momenta have the following interpretation. For fixed N and L, one can adiabatically follow each eigenstate $|\{\theta_a\}_{1\leq a\leq N}\rangle$ as one varies the repulsion strength c. In the

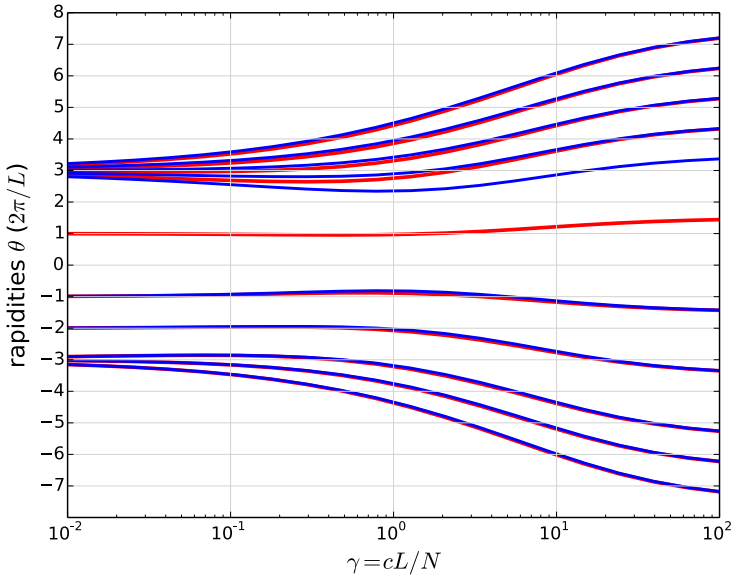

Figure 1.2: *[From the review article (Bouchoule and Dubail, 2022)]* Blue curves: rapidities θ_a obtained by solving the Bethe equations (1.19) with $N = 10$ and $(p_a)_{1\leq a\leq 10} = \frac{2\pi}{L}(7.5, 6.5, 5.5, 4.5, 3.5, -1.5, -3.5, -5.5, -6.5, -7.5)$, or the equivalent form (1.22) with $(p_a^{(\mathrm{B})})_{1\leq a\leq 10} = \frac{2\pi}{L}(3, 3, 3, 3, 3, -1, -2, -3, -3, -2)$. The rapidity θ_a interpolates between $p_a^{(\mathrm{B})}$ (when $c \to 0$) and p_a ($c \to \infty$). Red curves: rapidities obtained after the modification $(p_5 = 3.5) \to (p_5 = 1.5)$. It shows that the rapidities are all coupled: changing only one of the p_a's results in small shifts of all the other rapidities.

infinite repulsion limit $c \to +\infty$, the bosonic wavefunction (1.12) is, up to multiplication by a sign $\prod_{a<b} \mathrm{sign}(x_b - x_a)$, equal to the Slater determinant of N non-interacting fermions, i.e. $\det\left[e^{ix_a\theta_b}\right]_{1\leq a,b\leq N}$ (Girardeau, 1960). In that limit, the rapidities are nothing but the momenta of these non-interacting fermions: $\theta_a = p_a$. Importantly, the fermions in the $c \to +\infty$ limit must obey the Pauli exclusion principle, so all momenta should be different: $p_a \neq p_b$ if $a \neq b$. In the following we order both the rapidities and the fermion momenta as

$$\theta_1 > \theta_2 > \cdots > \theta_N, \qquad p_1 > p_2 > \cdots > p_N. \tag{1.20}$$

It is natural to wonder what happens in the opposite limit of non-interacting bosons, $c \to 0$. This is easily answered by introducing the 'boson momenta' $p_a^{(\mathrm{B})}$, related to the fermion momenta p_a as

$$p_a^{(\mathrm{B})} = p_a + \frac{2\pi}{L}\left(a - \frac{N+1}{2}\right) \in \frac{2\pi}{L}\mathbb{Z}, \qquad a = 1, \ldots, N. \tag{1.21}$$

Notice that $p_1^{(\mathrm{B})} \geq p_2^{(\mathrm{B})} \geq \cdots \geq p_N^{(\mathrm{B})}$; in particular, two or more boson momenta can

coincide. Using the fact that $\arctan(\mathrm{u}) = \frac{\pi}{2}\,\mathrm{sign}(u) - \arctan(1/\mathrm{u})$, Eq. (1.19) is equivalent to

$$\theta_a - \frac{1}{L}\sum_{b\neq a} 2\,\arctan\left(\frac{c}{\theta_a-\theta_b}\right) = p_a^{(\mathrm{B})}, \qquad a = 1,\dots,N. \tag{1.22}$$

For $c > 0$, The 'momenta' $p_a^{(B)}$ are just another way of parameterizing the solutions of the Bethe equations; they should not be confused with the momenta of the atoms, which would be obtained by computing the momentum distribution $\langle\{\theta_a\}|\,\Psi_p^\dagger\Psi_p\,|\{\theta_a\}\rangle$, where $\Psi_p^\dagger = \frac{1}{\sqrt{L}}\int e^{ipx}\Psi^\dagger(x)dx$ is the Fourier mode of the creation operator $\Psi^\dagger(x)$. However, in the limit of vanishing repulsion $c \to 0$, the rapidities are nothing but the boson momenta, $\theta_a \to p_a^{(\mathrm{B})}$. Moreover, in that limit, the Bethe wavefunction (1.12) is nothing but the permanent $\mathrm{per}[e^{ix_a\theta_b}]_{1\leq a,b\leq N}$, i.e. the wavefunction of N non-interacting bosons. So, in that limit, the rapidities coincide with the atom momenta.

Away from these two limits, the rapidities θ_a correspond to an adiabatic interpolation between the non-interacting fermion ($c \to +\infty$) and boson ($c \to 0$) momenta, obtained by solving the Bethe equations (1.19).

In general, the Bethe equations (1.19) cannot be solved analytically, but they can easily be solved numerically. One efficient way of doing this is to use the Newton-Raphson method.

1.2 Conserved charges and currents

The eigenstates of the Lieb-Liniger Hamiltonian (1.1) are Bethe states $|\{\theta_a\}_{1\leq a\leq N}\rangle$ labeled by their sets of rapidities. This allows to define a family of charge operators $Q[f]$, diagonal in the eigenbasis and parameterized by functions $f : \mathbb{R} \to \mathbb{R}$, such that

$$Q[f]\,|\{\theta_a\}\rangle = \left(\sum_{b=1}^{N} f(\theta_b)\right)|\{\theta_a\}\rangle\,. \tag{1.23}$$

Both the momentum operator and the Hamiltonian are of that form, with $f(\theta) = \theta$ and $f(\theta) = \theta^2/2$ respectively, see Eq. (1.13). It is the integrability of the model, reflected in the structure of the eigenstates (1.12), which allows us to consider the more general conserved charges (1.23). By construction, all these operators commute: $[Q[f_1], Q[f_2]] = 0$. In general, an explicit expression for $Q[f]$ in second-quantized form (like $Q[\theta^2/2]$ given by Eq. (1.1)) is not known, and typically regularization issues appear when one tries to write it (Davies, 1990; Davies and Korepin, 2011). Nevertheless, even in the absence of such direct expressions for the charges, the conserved charges $Q[f]$ defined formally by Eq. (1.23) prove to be very useful. There are other ways to do calculations with these charges, that do not require to know their explicit second-quantized form, in particular the algebraic Bethe Ansatz, see e.g. (Korepin et al., 1997) for an introduction.

From their definition (1.23), one expects the $Q[f]$ charges to be extensive with N, and to be the integral of a charge density

$$Q[f] = \int_0^L q[f](x)dx. \tag{1.24}$$

For f sufficiently regular, the charge density $q[f](x)$ is sufficiently local, meaning that it acts as the identity far away from the point x. [In the hard core limit $g \to +\infty$, this is a consequence of the Paley-Wiener theorem. At finite repulsion strength g, and more generally in interacting integrable models, the locality properties of charge densities are an advanced topic that is beyond the scope of this review; see e.g. (Ilievski et al., 2016; Doyon, 2017; Palmai and Konik, 2018) for introductions.] By definition, the expectation value of the charge density in a Bethe state (normalized as $\langle\{\theta_a\}|\{\theta_a\}\rangle = 1$) is

$$\langle\{\theta_a\}|\, q[f](x)\,|\{\theta_a\}\rangle = \frac{1}{L}\sum_{b=1}^{N} f(\theta_b). \tag{1.25}$$

It is independent of x because the Bethe state is translation invariant.

To the charge density $q[f]$, one associates a current operator $j[f]$ through the continuity equation,

$$\frac{\partial}{\partial t}q[f](x) + \frac{\partial}{\partial x}j[f](x) = i\,[H, q[f](x)] + \frac{\partial}{\partial x}j[f](x) = 0. \tag{1.26}$$

As sketched in the introduction, continuity equations are the basic ingredient of hydrodynamics. To write useful hydrodynamic equations, however, one must be able to evaluate the currents in given stationary states. Until very recently, it was not known how to evaluate the expectation values of the current $j[f]$. However, thanks to developments in integrability, in particular in form factor techniques and algebraic Bethe Ansatz, a remarkable exact formula has just been discovered by Borsi et al. (2020) for the expectation value of $j[f]$ in a Bethe state (see also (Pozsgay, 2020*a*,*b*; Borsi et al., 2021),

$$\langle\{\theta_a\}|\, j[f](x)\,|\{\theta_a\}\rangle = \frac{1}{L}\sum_{a,b} \varepsilon'(\theta_a)[\mathcal{G}^{-1}]_{ab} f(\theta_b). \tag{1.27}$$

Here $\varepsilon'(\theta) = \theta$ is the derivative of $\varepsilon(\theta) = \theta^2/2$, and $\mathcal{G}$ is the Jacobian matrix of the transformation from the p_a's to the θ_b's defined by Eq. (1.19), known as the Gaudin matrix,

$$\mathcal{G}_{ab} = \frac{\partial p_a}{\partial \theta_b} \tag{1.28}$$

(where the p_a's in Eq. (1.19) are no longer restricted to be in $\frac{2\pi}{L}\mathbb{Z}$). The Gaudin matrix is symmetric, $\mathcal{G}^T = \mathcal{G}$, as a consequence of the fact that the scattering phase ϕ depends on the rapidities θ_a and θ_b only through the difference $\theta_a - \theta_b$, see Eq. (1.11).

Let us mention that the remarkable formula (1.28) is a particular case of a more general result, also obtained in (Borsi et al., 2020; Pozsgay, 2020*a*,*b*). One can define generalized currents $j[h,f](x)$ through the generalization of the continuity equation (1.26):

$$i\,[Q[h],q[f](x)] + \frac{\partial}{\partial x} j[h,f](x) = 0. \tag{1.29}$$

Then the general formula for the expectation value reads

$$\langle\{\theta_a\}|\, j[h,f](x)\,|\{\theta_a\}\rangle = \frac{1}{L}\sum_{a,b} h'(\theta_a)[\mathcal{G}^{-1}]_{ab} f(\theta_b), \tag{1.30}$$

and the above physical current is the special case $h(\theta) = \varepsilon(\theta) = \theta^2/2$. We note that such generalized currents had also been considered in (Castro-Alvaredo et al., 2016) in the thermodynamic limit.

The discovery and proof of formula (1.29) or its generalization (1.30) required advanced techniques (Borsi et al., 2020; Pozsgay, 2020*a*,*b*), however the result is simple and its physical interpretation is quite clear. The b^{th} boson, with rapidity θ_b, carries an amount of charge density $\frac{1}{L}f(\theta_b)$. In the absence of other particles, it would travel at the single-particle group velocity $v_b = \partial\varepsilon(\theta_b)/\partial p(\theta_b) = \partial\varepsilon(\theta_b)/\partial\theta_b$ (or its generalization $v_b = \partial h(\theta_b)/\partial p(\theta_b)) = \partial h(\theta_b)/\partial\theta_b$), resulting in the current $j[h,f] = \frac{1}{L}v_b f(\theta_b)$.

In the presence of other particles, the group velocity of the b^{th} boson is modified. To compute it, one can consider a small variation of the fermion momentum $p_b \to p_b + \delta p_b$ in Eq. (1.19). This results in a small change of the total momentum $\delta P = \delta p_b$, and of the total energy $\delta E = \delta\left(\sum_{a=1}^N \varepsilon(\theta_a)\right) = \sum_a \frac{\partial\varepsilon(\theta_a)}{\partial p_b}\delta p_b = \sum_a \varepsilon'(\theta_a)[\mathcal{G}^{-1}]_{ab}\delta p_b$ (more generally, of the total charge $\delta Q[h] = \sum_a \frac{\partial h(\theta_a)}{\partial p_b}\delta p_b = \sum_a h'(\theta_a)[\mathcal{G}^{-1}]_{ab}\delta p_b)$). Thus, the modified group velocity is $\delta E/\delta p_b = \sum_a \varepsilon'(\theta_a)[\mathcal{G}^{-1}]_{ab}$ resulting in formula (1.27), or more generally $\delta Q[h]/\delta p_b = \sum_a h'(\theta_a)[\mathcal{G}^{-1}]_{ab}$ resulting in (1.30).

For further discussions of the physical interpretation of Eqs. (1.27,1.30), see (Borsi et al., 2020), and also (Bonnes et al., 2014; Bertini et al., 2016; Castro-Alvaredo et al., 2016; Doyon et al., 2018; Doyon, 2019*b*), where similar discussions had been given previously for the thermodynamic version of these formulas (see Eq. (1.41) below). See also the review articles (Borsi et al., 2021; Cubero et al., 2021).

1.3 Thermodynamic limit

So far we have focused on a finite number of bosons N, first on an infinite line, and then in a periodic box of length L. To do hydrodynamics, one needs first to understand the thermodynamic properties of the system. In this subsection, we briefly review the techniques for taking the thermodynamic limit $N, L \to \infty$, keeping the density of bosons $n = N/L$ fixed.

The key idea is to focus on an infinite sequence of eigenstates $(|\{\theta_a\}_{1\leq a\leq N}\rangle)_{N\in\mathbb{N}}$ of the Lieb-Liniger Hamiltonian (1.1), with $L = N/n$, such that the limit of the distribution of rapidities

$$\rho(\theta) := \lim_{N\to\infty} \frac{1}{L}\sum_{a=1}^{N} \delta(\theta - \theta_a) \tag{1.31}$$

is well defined and is a (piecewise) smooth function of θ. The thermodynamic properties of the system (such as its energy density, pressure, etc.) then become particular functionals of that rapidity density $\rho(\theta)$, and the goal is to find these functionals and to evaluate them. In what follows, we write '$\lim_{\text{therm.}}$' for this limiting procedure.

For example, consider the expectation values of the charge densities (1.25): in the thermodynamic limit, these become

$$\lim_{\text{therm.}} \langle\{\theta_a\}|\, q[f]\,|\{\theta_a\}\rangle \;=\; \int_{-\infty}^{\infty} f(\theta)\rho(\theta)d\theta. \tag{1.32}$$

In particular, the density of particles, the momentum density, and the energy density are, respectively, $n = \langle q[1]\rangle = \int \rho(\theta)d\theta$, $\langle q[\theta]\rangle = \int \theta\rho(\theta)d\theta$ and $\langle q[\theta^2/2]\rangle = \int \frac{\theta^2}{2}\rho(\theta)d\theta$.

1.3.1 Thermodynamic form of the Bethe equations

Crucially, since all the states in the infinite sequence $(|\{\theta_a\}_{1\leq a\leq N}\rangle)_{N\in\mathbb{N}}$ are Bethe states, each set of rapidities $\{\theta_a\}_{1\leq a\leq N}$ must satisfy the Bethe equations (1.19). To implement that constraint, it is customary to consider the set of fermion momenta $\{p_a\}_{1\leq a\leq N}$ associated to the set of rapidities $\{\theta_a\}_{1\leq a\leq N}$, both of them ordered as in (1.20), and to define the density of states $\rho_{\text{s}}(\theta)$ as

$$2\pi\rho_{\text{s}}(\theta) := \lim_{\text{therm.}} \frac{|p_a - p_{a+1}|}{|\theta_a - \theta_{a+1}|}, \tag{1.33}$$

where the sequence of indices a in the r.h.s is chosen so that $\lim_{\text{therm.}}\theta_a = \theta$. Because the fermion momenta p_a must satisfy the Pauli exclusion principle (they must all be different), it is clear that $|p_a - p_{a+1}| \geq \frac{2\pi}{L}$. Also, notice that, by definition, $\lim_{\text{therm.}} \frac{1}{L|\theta_a-\theta_{a+1}|} = \rho(\theta)$. Consequently, the Fermi occupation ratio

$$\nu(\theta) := \frac{\rho(\theta)}{\rho_{\text{s}}(\theta)} \tag{1.34}$$

must always satisfy

$$0 \leq \nu(\theta) \leq 1. \tag{1.35}$$

Moreover, the rapidity density $\rho(\theta)$ and the density of states $\rho_{\text{s}}(\theta)$ are related by the thermodynamic version of the Bethe equation (1.19). Plugging Eq. (1.19) into the definition

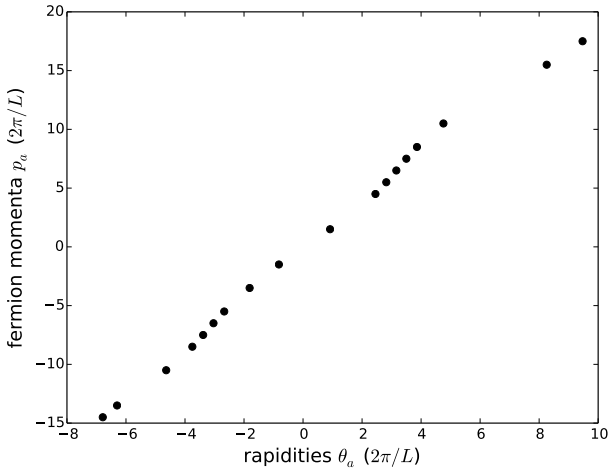

Figure 1.3: *[From the review article (Bouchoule and Dubail, 2022)]* Fermion momenta p_a plotted against the rapidities θ_a for the solution of the Bethe equations (1.19) defined by $p_a = \frac{2\pi}{L}(-14.5, -13.5, -10.5, -8.5, -7.5, -6.5, -5.5, -3.5, -1.5, 1.5, 4.5, 5.5, 6.5, 7.5, 8.5, 10.5, 15.5, 17.5)$ with $\gamma = 0.2$. As the density of momenta p_a and of rapidities θ_a increases, this becomes a smooth curve, whose slope is 2π times the density of states $\rho_{\rm s}(\theta)$, see Eq. (1.33).

(1.33) leads to the constitutive equation

$$\begin{aligned} 2\pi\rho_{\rm s}(\theta) &= \lim_{\rm therm.} \frac{1}{\theta_a - \theta_{a+1}} \left[\left(\theta_a + \frac{1}{L}\sum_b 2\,\arctan\left(\frac{\theta_a - \theta_b}{2}\right)\right) \right. \\ &\qquad \left. - \left(\theta_{a+1} + \frac{1}{L}\sum_b 2\,\arctan\left(\frac{\theta_{a+1} - \theta_b}{2}\right)\right)\right] \\ &= 1 + \int_{-\infty}^{\infty} \Delta(\theta - \theta')\rho(\theta')d\theta', \end{aligned} \tag{1.36}$$

where $\Delta(\theta - \theta')$ is the differential two-body scattering shift (1.11).

In practice, to construct interesting thermodynamic states, one can specify the Fermi occupation ratio $\nu(\theta)$, and then use the constitutive equation (1.36) to reconstruct the rapidity density $\rho(\theta)$ and the density of states $\rho_{\rm s}(\theta)$. One important example of this is the ground state of the Lieb-Liniger Hamiltonian, which corresponds to an occupation ratio which is a rectangular function: $\nu(\theta) = 1$ for $\theta \in [-\theta_{\rm F}, \theta_{\rm F}]$, and $\nu(\theta) = 0$ otherwise. Here $\theta_{\rm F}$ is the Fermi rapidity, which is a function of the density of particles n. In that case, the constitutive equation becomes the Lieb equation (Lieb and Liniger, 1963) (also known as the Love equation (Love, 1949); for studies of this particular equation see e.g. Takahashi

(1975); Popov (1977); Lang et al. (2017); Prolhac (2017); Marino and Reis (2019)). Another important example is the one of a thermal equilibrium distribution $\rho(\theta)$ obtained by solving the Yang-Yang equation (Eq. (1.52) below).

In general, the constitutive equation cannot be solved analytically, however, since it is linear, it is easily solved numerically by discretizing the integral.

1.3.2 The dressing

In thermodynamic manipulations, it turns out that the following operation is ubiquitous: to a function $f(\theta)$, one has to associate its 'dressed' counterpart $f^{\rm dr}(\theta)$, defined by the integral equation

$$f^{\rm dr}(\theta) = f(\theta) + \int \frac{d\theta'}{2\pi} \Delta(\theta-\theta')\nu(\theta') f^{\rm dr}(\theta'). \tag{1.37}$$

Although it is not explicit in the notation, $f^{\rm dr}(\theta)$ is always a functional of the rapidity distribution, through its dependence on the Fermi occupation ratio. For instance, with this definition, the constitutive equation (1.36) is recast as

$$2\pi\rho_{\rm s}(\theta) = 1^{\rm dr}(\theta), \tag{1.38}$$

where $1(\theta) = 1$ is the constant function.

Another example where the dressing (1.37) pops out is in manipulations that involve the Gaudin matrix. This is important, because to establish hydrodynamic equations one needs the thermodynamic limit of the expectation value of the current, see Eq. (1.27). The following identity holds:

$$\frac{f^{\rm dr}(\theta)}{2\pi\rho_s(\theta)} = \lim_{\rm therm.} \sum_{b=1}^{N} [\mathcal{G}^{-1}]_{ab} f(\theta_b), \tag{1.39}$$

where, again, the relation between θ in the l.h.s and the rapidity θ_a in the r.h.s is $\theta = \lim_{\rm therm.}\theta_a$. This identity is easily derived as follows. Using the definition (1.28),

$$\begin{aligned}\sum_b \mathcal{G}_{ab} h(\theta_b) &= \left(1 + \frac{1}{L}\sum_{b\neq a}\Delta(\theta_a-\theta_b)\right) h(\theta_a) - \frac{1}{L}\sum_{b\neq a}\Delta(\theta_b-\theta_a)h(\theta_b) \\ &\underset{\text{therm. lim.}}{\longrightarrow} 2\pi\rho_s(\theta)\,h(\theta) - \int\frac{d\theta'}{2\pi}\Delta(\theta-\theta')n(\theta')2\pi\rho_s(\theta')h(\theta') \\ &= [2\pi\rho_s\, h]^{\rm undr}(\theta),\end{aligned} \tag{1.40}$$

where the 'undressing' is the inverse of the dressing, i.e. $(f^{\rm undr})^{\rm dr}(\theta) = f(\theta)$. Inverting this formula gives Eq. (1.39).

We will see a few more examples of physical quantities whose computation involves the dressing operation below. References where this operation is used extensively include e.g.

the original derivation of the GHD equations in integrable quantum field theories (Castro-Alvaredo et al., 2016), the calculation of Drude weights and other two-point correlations of charge and currents in the Lieb-Liniger model (Doyon and Spohn, 2017*a*), the inclusion of force fields (Doyon and Yoshimura, 2017) or adiabatically varying interactions (Bastianello et al., 2019) or diffusive corrections (De Nardis et al., 2018; Gopalakrishnan et al., 2018; De Nardis et al., 2019) into the GHD equations.

1.3.3 Expectation values of the currents in the thermodynamic limit

We now present the central ingredient of Generalized Hydrodynamics. The thermodynamic expectation value of the current $j[f]$ (see subsection 1.2) is

$$\lim_{\text{therm.}} \langle\{\theta_a\}|\, j[f]\,|\{\theta_a\}\rangle \;=\; \int v^{\text{eff}}[\rho](\theta) f(\theta)\rho(\theta)d\theta, \tag{1.41}$$

where the 'effective velocity' is a functional of the rapidity distribution defined by

$$v^{\text{eff}}[\rho](\theta) \;:=\; \frac{(\varepsilon')^{\text{dr}}(\theta)}{2\pi\rho_{\text{s}}(\theta)} \;=\; \frac{\text{id}^{\text{dr}}(\theta)}{1^{\text{dr}}(\theta)}, \tag{1.42}$$

with $\varepsilon'(\theta) = \text{id}(\theta) = \theta$ and $1(\theta) = 1$. The remarkable result (1.41) was first obtained by (Castro-Alvaredo et al., 2016; Bertini et al., 2016), and it was the key observation that triggered all the later developments of GHD in quantum integrable systems. Bertini et al. (2016) relied partially on (Bonnes et al., 2014), where the formula for the effective velocity (1.42) had first appeared in the context of a quantum integrable system. In retrospect, the thermodynamic result (1.41) can be viewed as a consequence of the finite-size formula (1.27) of (Borsi et al., 2020; Pozsgay, 2020*a*,*b*), using the fact that the dressing is the thermodynamic limit of the Gaudin matrix, see Eq. (1.39). Historically though, the thermodynamic result was discovered before its finite-size counterpart. Since 2016, several works have aimed at establishing the validity of the thermodynamic formula (1.41) in various models, by relying on various approaches. Let us mention the form factor approaches of (Vu and Yoshimura, 2019; Cubero and Panfil, 2020; Cubero, 2020) for quantum field theories, arguments based on the symmetry of the charge-current correlations (Yoshimura and Spohn, 2020), or exact results in the classical integrable model of the Toda chain (Bulchandani et al., 2019; Cao et al., 2019; Doyon, 2019*a*; Spohn, 2020). See also the review articles (Borsi et al., 2021; Cubero et al., 2021).

The effective velocity (1.42) solves the equation

$$v^{\text{eff}}[\rho](\theta) = \theta - \int_{-\infty}^{\infty} \Delta(\theta-\theta') \Big(v^{\text{eff}}[\rho](\theta) - v^{\text{eff}}[\rho](\theta')\Big)\, \rho(\theta')d\theta'. \tag{1.43}$$

This is analogous to Eq. (4) in the introduction, which defines the effective velocity in the hard rod gas. The main difference is that the scattering shift $\Delta(\theta-\theta')$ is now rapidity-dependent, while in the hard rod gas Δ is a constant equal to minus the diameter of the

balls. The physical interpretation of Eq. (1.43) is analogous to the one in Fig. 1: a 'tracer' quasiparticle with rapidity (asymptotic momentum) θ, which would normally travel at constant speed θ in the vacuum, finds its velocity modified by the presence of a finite density $\rho(\theta')$ of other quasiparticles. From time t to $t+\delta t$, the tracer typically scatters against a number $\delta t \times |v^{\rm eff}[\rho](\theta) - v^{\rm eff}[\rho](\theta')|\rho(\theta')$ of quasiparticles with rapidity θ'. At each collision, the tracer is shifted backwards by an amount $\Delta(\theta-\theta')$: this is the physical effect that is encoded by formula (1.43).

To check that the effective velocity (1.42) solves Eq. (1.43) as claimed, one can use the definition of the dressing and the constitutive relation:

$$\begin{aligned}
&\int_{-\infty}^{\infty} \Delta(\theta-\theta') \left(v^{\rm eff}[\rho](\theta) - v^{\rm eff}[\rho](\theta') \right) \rho(\theta') d\theta' \\
&= v^{\rm eff}[\rho](\theta) \int_{-\infty}^{\infty} \Delta(\theta-\theta')\rho(\theta')d\theta' - \int_{-\infty}^{\infty} \frac{d\theta'}{2\pi} \Delta(\theta-\theta')\nu(\theta'){\rm id}^{\rm dr}(\theta') \\
&= v^{\rm eff}[\rho](\theta)\,(2\pi\rho_{\rm s}(\theta)-1) - ({\rm id}^{\rm dr}(\theta) - {\rm id}(\theta)) = \theta - v^{\rm eff}[\rho](\theta).
\end{aligned}$$

1.3.4 Entropy maximization: the Yang-Yang equation

In the previous Subsection we illustrated how physical observables, such as the expectation values of charges and currents, become functionals of the rapidity distribution $\rho(\theta)$ in the thermodynamic limit. We did no explain how to construct physically meaningful rapidity distributions though (except for the ground state of the Lieb-Liniger Hamiltonian, for which $\nu(\theta)$ is a rectangular function, see Subsection 1.3).

For instance, what is the rapidity distribution corresponding to a thermal equilibrium state at non-zero temperature? This question was answered in the pioneering work of Yang and Yang (1969), which we now briefly review.

First, we observe that there are many different choices of sequences of eigenstates $(\{\theta_a\}_{1\leq a\leq N})_{N\in\mathbb{Z}}$ that lead to the same thermodynamic rapidity distribution (1.31). The description of the system in terms of a rapidity distribution $\rho(\theta)$ is only a coarse-grained description: one should think of the rapidity distribution $\rho(\theta)$ as characterizing a macrostate of the system, corresponding to a very large number of possible microstates $|\{\theta_a\}\rangle$. To do thermodynamics, one needs to estimate the number of such microstates.

To estimate that number, one focuses on a small rapidity cell $[\theta, \theta+\delta\theta]$, which contains $L\rho(\theta)\delta\theta$ rapidities. The Bethe equations (1.19) relate these rapidities to fermion momenta p_a in a momentum cell $[p, p+\delta p]$, where $\delta p/\delta\theta \simeq 2\pi\rho_{\rm s}(\theta)$, see Eq. (1.33). Importantly, the fermion momenta p_a satisfy the Pauli exclusion principle. Then the number of microstates is evaluated by counting how many configurations of mutually distinct $L\rho(\theta)\delta\theta$ fermion momenta can fit into the box $[p, p+\delta p]$. Since the minimal spacing between two momenta is $\frac{2\pi}{L}$, the answer is

$$\#{\rm conf.} \;\simeq\; \frac{[L\rho_{\rm s}(\theta)\delta\theta]!}{[L\rho(\theta)\delta\theta]![L(\rho_{\rm s}(\theta)-\rho(\theta))\delta\theta]!}. \tag{1.44}$$

The total number of microstates is the product of all such configurations over all the rapidity cells $[\theta, \theta + \delta\theta]$. Taking the logarithm, and replacing the sum by an integral over $d\theta$, we obtain the Yang-Yang entropy

$$\begin{aligned} &\log\left(\,\#\text{microstates}\,\right) \;\simeq\; L\, S_{\rm YY}[\rho], \\ &S_{\rm YY}[\rho] \;:=\; \int_{-\infty}^{\infty} \left(\rho_{\rm s}\log\rho_{\rm s} - \rho\log\rho - (\rho_{\rm s}-\rho)\log(\rho_{\rm s}-\rho)\right) d\theta. \end{aligned} \tag{1.45}$$

The notation indicates that the Yang-Yang entropy is a functional of ρ only, and not of $\rho_{\rm s}$; this is because $\rho_{\rm s}$ must always be obtained from ρ by the constitutive equation (1.36).

Now let us consider the thermal equilibrium density matrix at temperature T,

$$\hat\rho_{\rm thermal} \;\propto\; e^{-H/T} \;=\; \sum_{|\theta_a\rangle} e^{-\sum_a (\varepsilon(\theta_a)-\mu)/T}\, |\{\theta_a\}\rangle\, \langle\{\theta_a\}|\,, \tag{1.46}$$

where the sum runs over all eigenstates. In fact, a straightforward generalization consists in considering the Generalized Gibbs Ensemble (Rigol et al., 2007, 2008) density matrix

$$\hat\rho_{\rm GGE}[f] \;\propto\; e^{-Q[f]} \;=\; \sum_{|\theta_a\rangle} e^{-\sum_a f(\theta_a)}\, |\{\theta_a\}\rangle\, \langle\{\theta_a\}|\,, \tag{1.47}$$

for some function f. We would like to compute expectation values w.r.t this density matrix, e.g.

$$\langle\mathcal{O}\rangle_{\rm GGE} \;:=\; \frac{{\rm tr}[\mathcal{O}e^{-Q[f]}]}{{\rm tr}[e^{-Q[f]}]} \;=\; \frac{\sum_{|\theta_a\rangle} \langle\{\theta_a\}|\,\mathcal{O}\,|\{\theta_a\}\rangle\, e^{-\sum_a f(\theta_a)}}{\sum_{|\theta_a\rangle} e^{-\sum_a f(\theta_a)}} \tag{1.48}$$

for some observable $\mathcal{O}$. When the observable $\mathcal{O}$ is sufficiently local, it is believed that the expectation value $\langle\{\theta_a\}|\,\mathcal{O}\,|\{\theta_a\}\rangle$ does not depend on the specific microstate of the system, so that it becomes a functional of ρ in the thermodynamic limit,

$$\lim_{\rm therm.} \langle\{\theta_a\}|\,\mathcal{O}\,|\{\theta_a\}\rangle \;=\; \langle\mathcal{O}\rangle_{[\rho]}\,. \tag{1.49}$$

This assumption is related to a 'Generalized Eigenstate Thermalization Hypothesis', see e.g. (Cassidy et al., 2011; Pozsgay, 2011; He et al., 2013; Pozsgay, 2014; Vidmar and Rigol, 2016; Dymarsky and Pavlenko, 2019). Under that assumption, one can replace the above sum over all eigenstates by a functional integral over the coarse-grained rapidity distribution ρ,

$$\lim_{\rm therm.} \langle\mathcal{O}\rangle_{\rm GGE} \;=\; \frac{\int \mathcal{D}\rho\; \langle\mathcal{O}\rangle_{[\rho]}\, e^{L(S_{\rm YY}[\rho] - \int f(\theta)\rho(\theta)d\theta)}}{\int \mathcal{D}\rho\, e^{L(S_{\rm YY}[\rho] - \int f(\theta)\rho(\theta)d\theta)}}. \tag{1.50}$$

The functional integral is then dominated by the root distribution which minimizes a (generalized) free energy functional:

$$\frac{\delta}{\delta\rho}\left[\int f(\theta)\rho(\theta)d\theta - S_{\rm YY}[\rho]\right] \;=\; 0. \tag{1.51}$$

Using the definition of the Yang-Yang entropy and the constitutive equation (1.19), one obtains the following relation between the function $f(\theta)$ defining the diagonal density matrix (1.47) and the rapidity distribution $\rho(\theta)$ dominating the functional integral (1.50):

$$f(\theta) = \log\left(\frac{\rho_{\rm s}(\theta)}{\rho(\theta)} - 1\right) - \int \frac{d\theta'}{2\pi}\Delta(\theta-\theta')\log\left(1-\frac{\rho(\theta')}{\rho_{\rm s}(\theta')}\right). \tag{1.52}$$

This equation is known as the (Generalized) Yang-Yang equation, or (Generalized) Thermodynamic Bethe Ansatz equation. Again, the term 'Generalized' refers to the replacement of the thermal equilibrium density matrix by a Generalized Gibbs Ensemble, (1.46)→(1.47), see e.g. (Caux and Konik, 2012; Wouters et al., 2014). Like most of the equations encountered so far, in general the Yang-Yang equation cannot be solved analytically, but it can be efficiently solved numerically, by iteration. In particular, this allows to compute the rapidity distribution $\rho(\theta)$ at thermal equilibrium.

This is particularly useful in applications discussed later in this review, because in experiments, one often assumes that the system is (at least initially) at thermal equilibrium.

For instance, using the Yang-Yang equation, it is possible to tabulate the equilibrium pressure $\mathcal{P}(n,e)$ as a function of the particle density n and the energy per particle e. To do this, one needs to first solve numerically Eq. (1.52) with $f(\theta) = (\varepsilon(\theta)-\mu)/T$, and Eq. (1.36), to get $\rho(\theta)$ and $\rho_{\rm s}(\theta)$. Then the equilibrium pressure is given by (Yang and Yang, 1969; Korepin et al., 1997)

$$\mathcal{P} = -\left(\frac{\partial F}{\partial L}\right)_T = -T\int\frac{d\theta}{2\pi}\log\left(1-\frac{\rho(\theta)}{\rho_{\rm s}(\theta)}\right), \tag{1.53}$$

where the free energy is $F/L = \int(\varepsilon(\theta)-\mu)\rho(\theta)d\theta - TS_{\rm YY}[\rho]$. This gives the thermodynamic equilibrium pressure at density $n = \int\rho(\theta)d\theta$ and energy per particle $e = \int\frac{\theta^2}{2}\rho(\theta)d\theta/n$. Alternatively, the pressure can be identified with the momentum current $j_P = j[\mathrm{id}]$ (with $\mathrm{id}(\theta)=\theta$) as we did in the introduction, see Eq. (3). Thus, according to Eq. (1.41), we must also have

$$\mathcal{P} = \lim_{\rm therm.}\langle j[\mathrm{id}]\rangle = \int v^{\rm eff}(\theta)\,\theta\,\rho(\theta)d\theta. \tag{1.54}$$

The equivalence between the two formulas (1.53) and (1.54) follows from manipulations of the dressing operation (1.37). [To elaborate: with the definition of the effective velocity, formula (1.54) is equivalent to $\mathcal{P} = \int\theta\nu(\theta)\mathrm{id}^{\rm dr}(\theta)\frac{d\theta}{2\pi}$, while differentiating (1.52) w.r.t. θ and using the definition of the dressing operation leads to $\mathrm{id}^{\rm dr}(\theta) = T\frac{1}{\nu(\theta)}\frac{d}{d\theta}\log(1-\nu(\theta))$.]

1.4 Generalized Hydrodynamics equations for the 1D Bose gas

We just reviewed the thermodynamic properties of the homogeneous Lieb-Liniger gas. In particular, we emphasized the key role of the distribution of rapidities $\rho(\theta)$. In the

thermodynamic limit, expectation values of physical observables, like charge densities or currents, become functionals of the rapidity distribution.

We now turn to Euler scale hydrodynamics, whichs follow from this thermodynamics. As in any hydrodynamic approach, the starting point is the assumption of separation of scales, see Fig. 1.4. When the charge densities in the gas vary sufficiently slowly in space and in time, one can view the gas as a continuum of fluid cells, each of which contains a thermodynamically large number of particles that have relaxed to a stationary state.

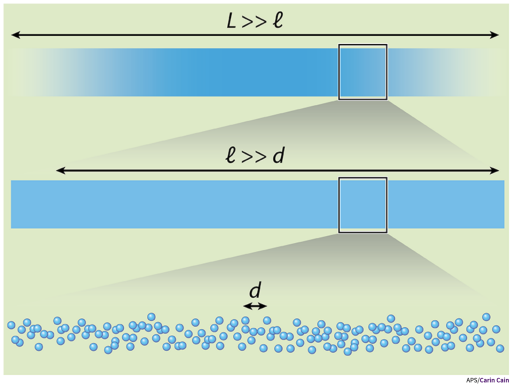

Figure 1.4: *[From (Dubail, 2016); reproduced in the review article (Bouchoule and Dubail, 2022)]* Like any other hydrodynamic approach, Generalized Hydrodynamics applies in the limit where separations of distance and time scales hold. When the characteristic distance L over which densities vary is much larger than the microscopic length scale d, one can view the system as a continuum of locally homogeneous fluid cells of size ℓ ($d \ll \ell \ll L$) which contain a thermodynamically large number of particle. Similarly, assuming slow variation in time, each fluid cell is locally relaxed to a stationary state. In standard hydrodynamics, this local stationary state is a thermal equilibrium state, while in Generalized Hydrodynamics it is a Generalized Gibbs Ensemble.

Under the assumption of separation of scales, the gas is described by its distribution of rapidities $\rho(x, \theta, t)$ within each fluid cell $[x, x + dx]$ at time t. This time- and position-dependent rapidity density evolves according to the Generalized Hydrodynamic equations,

$$\begin{aligned} &\partial_t \rho(x,\theta,t) + \partial_x \left(v^{\text{eff}}[\rho](\theta)\, \rho(x,\theta,t) \right) - (\partial_x V(x)) \partial_\theta \rho(x,\theta,t) \;=\; 0 \\ &v^{\text{eff}}[\rho](\theta) = \theta - \int_{-\infty}^{\infty} \Delta(\theta - \theta') \left(v^{\text{eff}}[\rho](\theta) - v^{\text{eff}}[\rho](\theta') \right) \rho(\theta') d\theta'. \end{aligned} \tag{1.55}$$

These equations were first derived for quantum integrable systems by Castro-Alvaredo et al. (2016); Bertini et al. (2016) (more precisely, they were derived in the absence of an external potential $V(x)$; the additional term, which corresponds to Newton's second law, was added later by Doyon and Yoshimura (2017)). These equations are of the same

form as Eqs. (4) for the classical integrable gas discussed in the introduction, with two main nuances. The first is that it is the density of rapidities, or asymptotic momenta, that enters the equations; not a 'bare' velocity as in the hard rod gas. The second is that $\Delta(\theta - \theta') = \frac{2mg/\hbar}{(mg/\hbar)^2+(\theta-\theta')^2}$ is now the scattering shift (1.11), which depends on the rapidities, while Δ in the classical gas in the introduction was just a constant equal to minus the diameter of the balls. The effective velocity that solves the second equation (1.55) can be written as $v^{\text{eff}}[\rho](\theta) = \text{id}^{\text{dr}}(\theta)/1^{\text{dr}}(\theta)$, as discussed in Subsection 1.3.3.

Chapter 2

Generalized Hydrodynamics in the 1D Bose gas: specific setups and experiments

2.1 Modeling the quantum Newton Cradle

The GHD equations (1.55) allow to describe situations that are very far from thermal equilibrium. Arguably, the most paradigmatic such out-of-equilibrium situation is the quantum Newton Cradle setup of Kinoshita et al. (2006). There, the atoms, which are initially at equilibrium in a harmonic potential, are suddenly given a large momentum $\pm q_{\text{Bragg}}$ by a Bragg pulse. Half of the atoms move to the right, the other half move to the left. Because of the harmonic trapping potential, the two packets of atoms oscillate in the trap, colliding twice during each oscillation cycle.

Let us stress that, before the advent of GHD, a direct simulation of the Quantum Newton Cradle setup with experimentally realistic parameters (in particular, a number of atoms numbers of atoms $N \sim 10^2 - 10^3$) was completely out of reach. This is of course because of the exponential growth of the Hilbert space in many-body quantum systems, which makes all direct approaches, such as an exact diagonalization of (a dicretized version of) the Lieb-Liniger Hamiltonian (1.1), numerically untractable for more than a dozen of atoms. Thanks to the discovery of GHD in 2016, this situation has now completely changed. Nowadays, it is very easy to model the 1D Bose gas in a quantitatively reliable way.

Bulchandani et al. (2017) used GHD to model two packets of atoms colliding against each other on an infinite line. Then, a complete study of the Newton Cradle setup, including the trapping potential that gives rise to oscillations of the packets and therefore multiple collisions, was performed by Caux et al. (2019), see Fig. 2.1. The numerical solution of the GHD equation in that reference was obtained by a classical molecular dynamics simulation

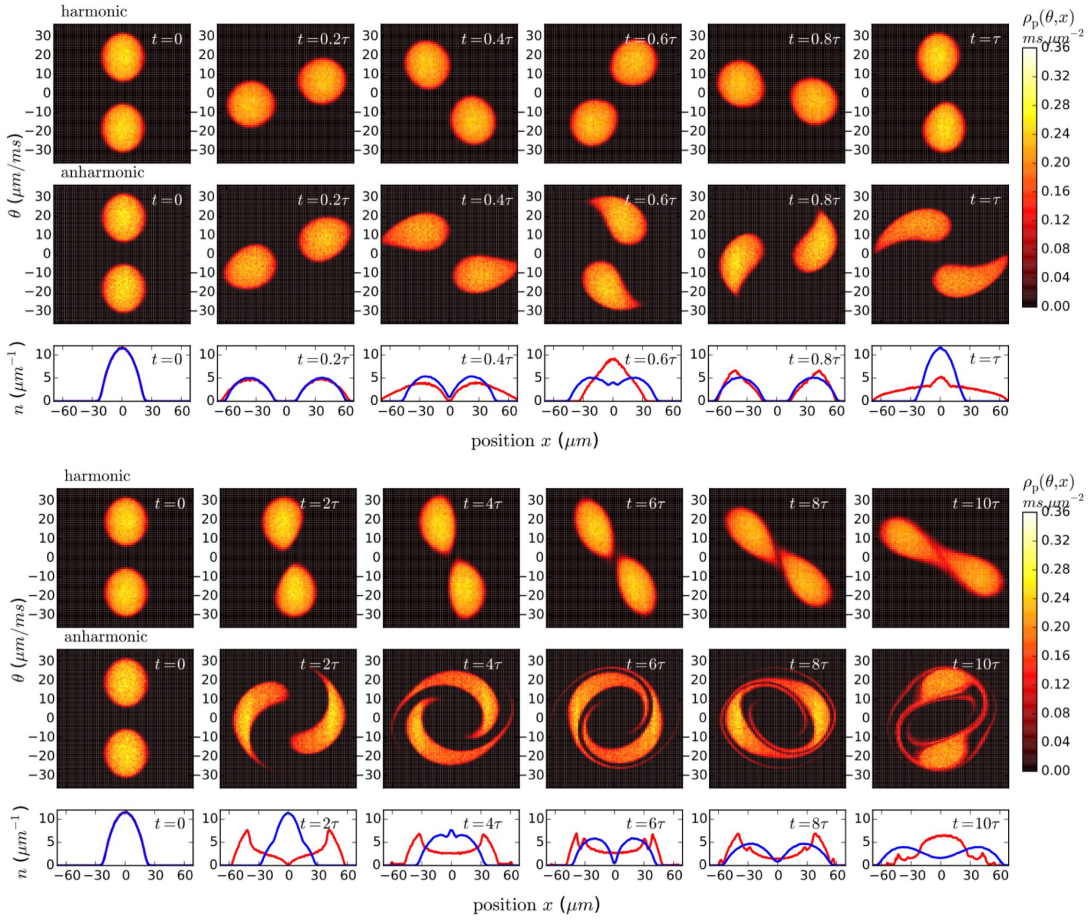

Figure 2.1: *[From (Caux et al., 2019); reproduced in the review article (Bouchoule and Dubail, 2022)]* GHD simulation of the 1D Bose gas in the Newton Cradle setup. Top figure: the evolution of the phase-space rapidity density $\rho(x, \theta, t)$ during the first oscillation cycle is shown for a harmonic trap with period τ (first row), and a quasi-harmonic trap with a small anharmonicity (second row). The corresponding density profiles $n(x,t) = \int \rho(x, \theta, t) d\theta$ are shown in blue and red respectively (third row). Bottom: same as the top one, but on longer time scales.

of the so-called flea gas model (Doyon et al., 2018), which is an extension of the classical hard rod gas that incorparates the scattering shift discussed in Subsection 1.1.1. There are other ways of numerically solving the GHD equations, which have been discussed, to some extent, in (Bulchandani et al., 2017, 2018; Doyon et al., 2017; Bastianello et al., 2019; Møller and Schmiedmayer, 2020; Bastianello, De Luca, Doyon and De Nardis, 2020; Møller et al., 2021; Bastianello et al., 2021). Møller and Schmiedmayer (2020) also made their code 'ifluid' publicly available.

In Fig. 2.1, one can observe the evolution of the rapidity distribution predicted by GHD in a harmonic potential $V(x) = \frac{1}{2}m\omega^2 x^2$ (with oscillation period $\tau = 2\pi/\omega$), and also in a potential with a small anharmonicity potential $V(x) = \frac{m\omega^2}{\pi^2\ell^2}(1-\cos\frac{\pi x}{\ell})$. The initial state is constructed so as to mimic the effect of the Bragg pulse sequence that imparts their initial momentum to the atoms. Before the sequence, the gas is described in a hydrostatic (or local density) approximation by its local distribution of rapidities $\rho(x,\theta,t<0) = \rho_{\rm thermal}(x,\theta)$, obtained by solving the Yang-Yang equation (1.52) for a thermal equilibrium distribution. Then momentum $\pm q_{\rm Bragg}$ is imparted in a random fashion to all quasiparticles in the system. This results in a distribution of rapidities at $t = 0$

$$\rho(x,\theta,t=0) \simeq \frac{1}{2}\rho_{\rm thermal}(x,\theta - q_{\rm Bragg}) + \frac{1}{2}\rho_{\rm thermal}(x,\theta + q_{\rm Bragg}). \tag{2.1}$$

This simple Ansatz for the initial state can be justified using results of (Van den Berg et al., 2016), which showed that the momentum distribution function of the bosons is affected in this way by a Bragg pulse, and to a good approximation the same holds for the rapidities. The rapidity distribution is evaluated at later times by solving the GHD equation (1.55). One observes that the two blobs, initially well separated in momentum space for sufficiently large $q_{\rm Bragg}$, evolve by performing a deformed rotation-like movement around the origin of phase space. In the harmonic case, over the first two or three oscillations cycles, their evolution is not drastically affected by the collisions. However at later times, the two blobs ultimately merge due to inter-cloud interactions. With a small anharmonicity, the two blobs get deformed much more quickly and the distribution $\rho(x,\theta,t)$ gets more and more stirred up after few periods. This dephasing effect would also be present for the single particle in an anharmonic trap, see e.g. (Bastianello et al., 2017). Many-body dephasing is also present: without interactions, the original blobs would disintegrate into long spiraling filaments; instead, here the filaments merge and high-energy (longer-period) tails scatter to lower energies, leading to the reformation of new blobs.

Importantly, the ability to perform GHD modeling of the Newton Cradle setup has opened the possibility to study theoretically one fundamental question raised by the experiment of Kinoshita et al. (2006). If one waits long enough, does the gas in the trap ultimately reach thermal equilibrium?

This question is non-trivial because, although the Lieb-Liniger gas is integrable, its integrability is broken by the trapping potential $V(x)$. Yet, at the Euler scale, the potential $V(x)$ varies very slowly compared to microscopic scales, so the breaking of integrability by

the external potential is weak. It is not obvious how much of the original conservation laws should be reflected in the stationary state.

Cao et al. (2018) studied this question for the classical hard rod gas in a trapping potential, and found that the answer is negative: the gas exhibits 'incomplete thermalization'. It reaches a stationary state of the GHD equation (1.55), namely a rapidity distribution $\rho_{\text{stat.}}(x,\theta)$ which satisfies

$$\partial_x \Big(v^{\text{eff}}[\rho_{\text{stat.}}](\theta)\, \rho_{\text{stat.}}(x,\theta) \Big) - (\partial_x V)\partial_\theta \rho_{\text{stat.}}(x,\theta) = 0, \tag{2.2}$$

but this distribution does not need to be a thermal equilibrium distribution in the trap. The possibility of GHD-stationary distributions of the form (2.2) that are not thermal has also been discussed in (Doyon and Yoshimura, 2017). Caux et al. (2019) arrived at the same conclusion for the 1D Bose gas in the Newton Cradle setup, within the framework of the aforementioned flea gas model. In (Caux et al., 2019), the existence of non-thermal stationary states was argued to be a consequence of the conservation of certain quantities $S[f]$ under evolution generated by the Euler-scale GHD equation (1.55), even in the presence of an external potential $V(x)$. The conservation of these quantities is incompatible with convergence towards thermal equilibrium. These quantities can be constructed out of the Fermi occupation ratio $\nu(x,\theta,t)$, and read

$$S[f] \;=\; \int dx\, d\theta\, \rho_{\text{s}}(x,\theta,t) f(\nu(x,\theta,t)), \tag{2.3}$$

for arbitrary functions f. We stress that these quantities are different from the standard conserved charges of the form (1.23). Instead, the quantities $S[f]$ look more like generalizations of the Yang-Yang entropy: the Yang-Yang entropy, integrated over space, corresponds to the specific choice $f(\nu) = -\nu\log\nu - (1-\nu)\log(1-\nu)$, see Eq. (1.44). The fact that

$$\frac{d}{dt} S[f] \;=\; 0 \tag{2.4}$$

can be checked directly using the GHD equation (1.55), see (Caux et al., 2019). We stress that the Yang-Yang entropy, and more generally the quantities $S[f]$, are conserved only at the Euler scale. When higher-order terms are included into the hydrodynamic equations (1.55), as discussed in Subsection 2.2.4 below, the entropy increases with time, and the other quantities $S[f]$ are no longer constant. In particular, it has been argued recently by (Bastianello, De Luca, Doyon and De Nardis, 2020) that the inclusion of a Navier-Stokes-like higher order term in (1.55) does lead to 'complete thermalization'.

2.2 Brief overview of other theory results in the 1D Bose

In this section we briefly review some other physically relevant setups in the 1D Bose gas that have been theoretically investigated with the new toolbox provided by GHD, or some variations/extensions of GHD.

2.2.1 Bipartite quench with 1D clouds.

De Nardis and Panfil (2018) considered the case of two atom clouds that are prepared at different temperatures $T_1 \neq T_2$, put in the same trapping potential. At the junction between the two clouds, the local state displays an edge singularity in its response function and quasilong-range order.

2.2.2 Infinite box trap: reflection of quasi-particless against boundaries.

Dubessy et al. (2021) studied the Lieb-Liniger gas in an infinite flat box potential (Fig. 2.2). Initially the gas is in its ground state. At time $t = 0$, it is instantaneously boosted by a momentum k_0, a protocol that can be realized experimentally by phase imprinting. Then the particles in the gas start reflecting against the two infinite walls at $x = 0$ and $x = L$. This is modeled in GHD by the following boundary condition,

$$\rho(x = 0, \theta) \;=\; \rho(x = 0, -\theta). \tag{2.5}$$

The same boundary condition holds at $x = L$. Dubessy et al. (2021) used a trick to implement easily these boundary conditions: the system can be glued together with its mirror image, to give a periodic system of length $2L$. The rapidity distribution in that periodic system of size $2L$ is related to the one in the infinite box potential by

$$\rho_{\text{periodic}}(x, \theta) = \begin{cases} \rho(x, \theta) & \text{if} \quad 0 < x < L \\ \rho(2L - x, -\theta) & \text{if} \quad L < x < 2L. \end{cases} \tag{2.6}$$

With this trick, they studied the formation of shock waves that oscillate in the box for several periods, with a period fixed by the sound velocity in the gas, see Fig. 2.2.

2.2.3 Adiabatically varying interactions.

The original formulation of GHD of (Castro-Alvaredo et al., 2016; Bertini et al., 2016) was for a time-independent, translation invariant, Hamiltonian acting on a spatially inhomogeneous state. In particular, no external potential term $-(\partial_x V)(\partial_\theta \rho)$ was included originally. Doyon and Yoshimura (2017) considered the addition of generalized potentials to the Hamiltonian $H \to H + \int V_f(x) q[f](x) dx$, where $q[f](x)$ is the charge density of the charge operator (1.23). This includes, in particular, the case of a standard external potential $H \to H + \int V(x) \Psi^\dagger(x) \Psi(x) dx$, corresponding to the simplest choice $q[f] = 1$, which results in the form (1.55) of the GHD equation with the acceleration term $-\partial_x V \partial_\theta \rho$. This is the form of the GHD equation that is most relevant for the description of existing experiments. However we stress that the results of (Doyon and Yoshimura, 2017) are in principle more general.

A further extension of the original GHD equation was obtained by Bastianello et al. (2019), who considered the case of a non-uniform repulsion strength $g(x, t)$ through the

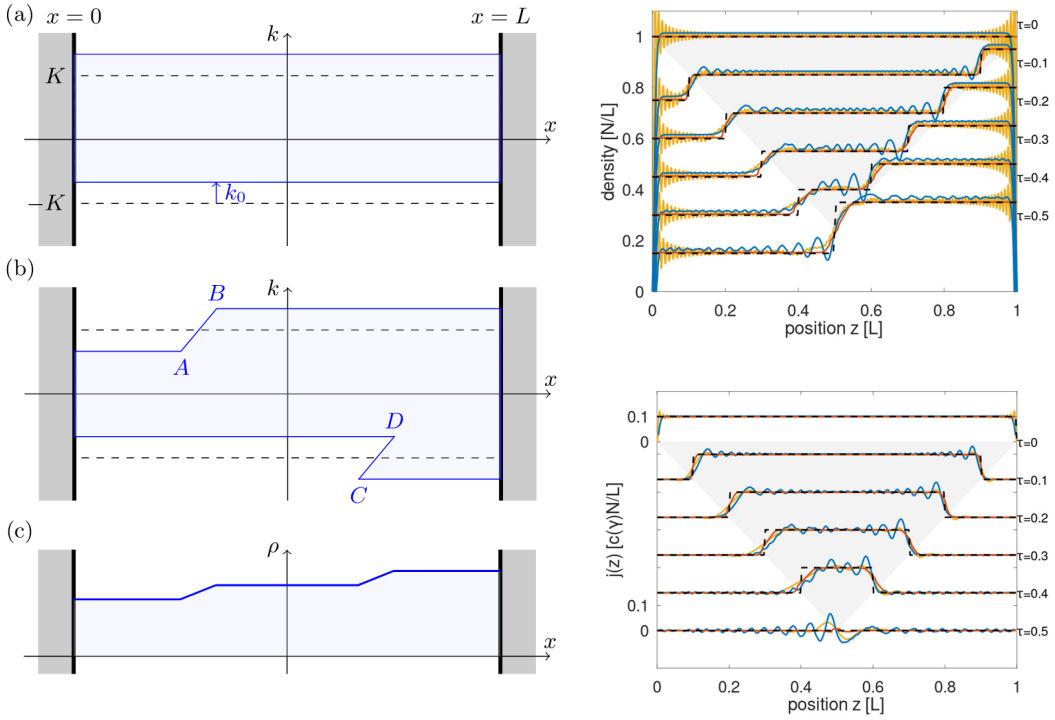

Figure 2.2: *[From (Dubessy et al., 2021); reproduced in the review article (Bouchoule and Dubail, 2022)]* Left: GHD simulation of a gas in an infinite box trap. (a) The initial state is the ground state, on which a boost of $+k_0$ is applied at $t = 0$. The blue region is the region of phase space where the Fermi occupation ratio $\nu(x, \theta, t) = \rho(x, \theta, t)/\rho_s(x, \theta, t)$ is one. (b) After some time the contour of the blue region gets Outside this region, it is zero. (c) The corresponding real-space density profile $n(x, t) = \int \rho(x, \theta, t) d\theta$. Right: evolution of the particle density (top) and current (bottom). Here $\tau = t/(vL)$ where v is the sound velocity. The blue curve is obtained with the Gross-Pitaevskii equation (valid for small γ), the yellow curve is obtained from a free fermion calculation in the $\gamma \to \infty$ limit, and the red curve is the GHD simulation at $\gamma = 1$. The dashed black line correspond to an effective model, see (Dubessy et al., 2021).

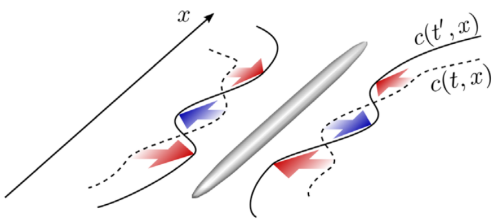

Figure 2.3: *[From (Bastianello et al., 2019); reproduced in the review article (Bouchoule and Dubail, 2022)]* The GHD equations (1.55) can be extended to include an repulsion strength $c(x,t)$ that varies slowly in time or in space, which would correspond to slowly varying the transverse trapping frequency in an experimental setup.

gas, see Fig. 2.3. Under the assumption of slow variation of $g(x,t)$ (or of $c(x,t) = \frac{mg(x,t)}{\hbar^2}$) in position and time, they found the following additional term:

$$\partial_t \rho + \partial_x \left(v^{\text{eff}} \rho \right) - (\partial_x V) \partial_\theta \rho + \partial_\theta \left(\frac{(\partial_t c) F^{\text{dr}} + (\partial_x c) \Lambda^{\text{dr}}}{1^{\text{dr}}} \rho \right) = 0, \tag{2.7}$$

where we have dropped the dependence on x, θ and t for better readability, and where the functions F and Λ are

$$F(\theta) := \int \frac{\partial \phi(\theta - \theta')}{\partial c} \rho(\theta') d\theta', \qquad \Lambda(\theta) := \int \frac{\partial \phi(\theta - \theta')}{\partial c} v^{\text{eff}}(\theta') \rho(\theta') d\theta'.$$

For a derivation of this result, see the original paper (Bastianello et al., 2019).

2.2.4 Beyond the Euler scale: Navier-Stokes diffusive corrections

As mentioned in the introduction, Euler-scale hydrodynamic equations are but the zeroth-order in a gradient expansion. More precisely, under the assumption of local relaxation, the expectation value of the currents $\langle j(x) \rangle$ are functions of the charges $\langle q(x) \rangle$ and of their derivatives. Schematically: $\langle j(x) \rangle = F(\langle q(x) \rangle, \partial_x \langle q(x) \rangle, \partial_x^2 \langle q(x) \rangle, \dots)$, which is then expanded as $\langle j(x) \rangle = F(\langle q(x) \rangle, 0, 0, \dots) + \frac{\partial F}{\partial(\partial_x \langle q \rangle)}(\langle q(x) \rangle, 0, 0, \dots) \partial_x \langle q(x) \rangle + \dots$ The zeroth order gives the Euler-scale hydrodynamic equations, while the next order gives the hydrodynamic equation at the diffusive scale. These hydrodynamic equations include a diffusive, entropy-producing (or Navier-Stokes) term.

The 'Navier-Stokes' GHD equation, with the diffusive term, was obtained in (De Nardis et al., 2018). The result reads

$$\partial_t \rho + \partial_x \left(v^{\text{eff}} \rho \right) - (\partial_x V) \partial_\theta \rho = \frac{1}{2} \partial_x \left(\mathfrak{D} \partial_x \rho \right), \tag{2.8}$$

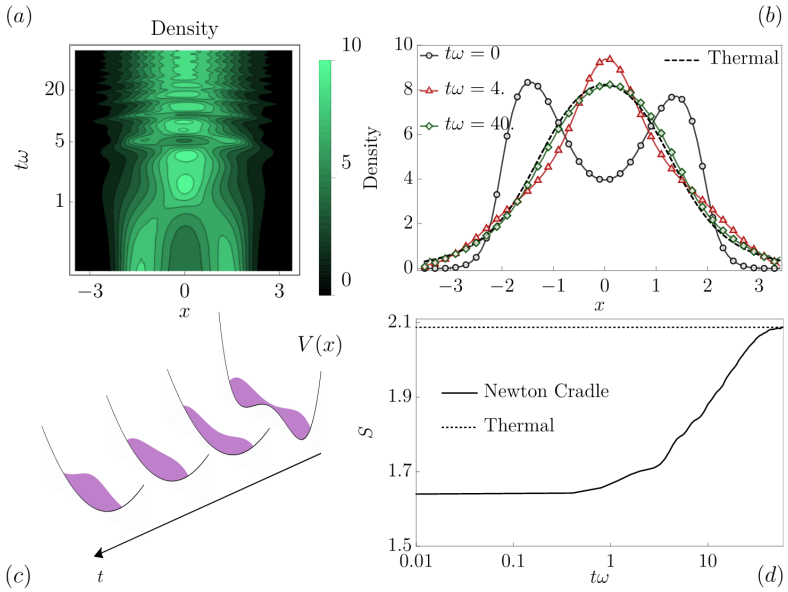

Figure 2.4: *[From (Bastianello, De Luca, Doyon and De Nardis, 2020); reproduced in the review article (Bouchoule and Dubail, 2022)]* When the Navier-Stokes term (2.8) is included in the GHD equation, it is found that the 1D Bose gas in the quantum Newton Cradle does reach thermal equilibrium. Bottom left: cartoon of the quench protocol (quench from double-well to harmonic potential). Top: evolution of the density profile $n(x,t)$ under GHD-Navier-Stokes evolution. In the top right plot, one sees that the density goes to the thermal equilibrium density at long times. Bottom right: the entropy invreases and ultimately reaches its thermal equilibrium value.

where $\mathfrak{D}$ is a kernel (i.e. $\mathfrak{D}f(\theta) = \int \mathfrak{D}(\theta,\theta')f(\theta')d\theta'$) describing a Markov process of random momentum exchanges via two-body collisions (Gopalakrishnan et al., 2018; De Nardis et al., 2019). It is defined by the relation

$$[\mathfrak{D}(\theta,.)]^{\mathrm{dr}}(\theta')\rho_{\mathrm{s}}(\theta') \;=\; [\rho_s(.)\tilde{\mathfrak{D}}(.,\theta')]^{\mathrm{dr}}(\theta), \tag{2.9}$$

with

$$\begin{aligned}
\rho_{\mathrm{s}}(\theta)^2\tilde{\mathfrak{D}}(\theta,\theta') &= \left(\int W(\alpha,\theta)d\alpha\right)\delta(\theta-\theta') - W(\theta,\theta'),\\
W(\theta,\alpha) &= \rho(\theta)(1-\nu(\theta))(\Delta^{\mathrm{dr}}(\theta-\alpha))^2\left|v^{\mathrm{eff}}(\theta)-v^{\mathrm{eff}}(\alpha)\right|.
\end{aligned}$$

For a detailed derivation of these equations, see (De Nardis et al., 2019).

As mentioned above, interestingly, taking into account the diffusive correction changes the conclusion about thermalization in the quantum Newton Cradle setup, see (Bastianello,

De Luca, Doyon and De Nardis, 2020) and Fig. 2.4. With the inclusion of the Navier-Stokes term, the quantities (2.3) are no longer conserved, and it is found that the gas ultimately reaches thermal equilibrium, contrary to what had been observed previously in (Cao et al., 2018; Caux et al., 2019). For more studies of diffusion in the Lieb-Liniger gas, see e.g. (Panfil and Pawełczyk, 2019; Medenjak et al., 2020).

2.2.5 Boltzmann kinetic equation for Bose gases at the 1D-3D crossover.

Taking inspiration from the developments of GHD, Møller et al. (2021) studied a 3D Bose gas at the crossover to the 1D regime, and introduced a phenomenological description of the gas dynamics at that crossover. The idea is the following. The atoms lie in the 3D potential $V(x) + V_\perp(r_\perp)$, where $r_\perp = \sqrt{y^2+z^2}$ is the distance from the axis at $y = z = 0$. The transverse potential is harmonic, $V_\perp(y,z) = m\omega_\perp^2 r_\perp^2/2$, so that the wavefunction of each atom $\psi(x, r_\perp)$ can be expanded on the eigenstates $\psi_n(r_\perp)$ of the transverse harmonic oscillator, see Eq. (**??**) below. Strictly in the 1D regime (i.e. when $\hbar\omega_\perp$ is much larger than all other energy scales), the transverse ground state ($n = 0$) is the only state that is occupied. But if the transverse confinement is not strong enough, transverse excited states will also be occupied. Møller et al. (2021) consider the first three transverse states ($n = 0, 1, 2$) (their degeneracy is neglected), and regard the resulting system as a three-component 1D Bose gas, with a Hamiltonian of the form

$$\begin{aligned} H &= H_0 + \text{excitation terms}, \\ H_0 &= \sum_{a=0,1,2} \int dx\, \Psi_a^\dagger \left(-\frac{\partial_x^2}{2m} + V(x) + \frac{g_a}{2}\Psi_a^\dagger \Psi_a \right) \Psi_a + \sum_{0\le a<b\le 2} \int dx\, g_{ab} \Psi_a^\dagger \Psi_a \Psi_b^\dagger \Psi_b. \end{aligned} \tag{2.10}$$

Here the excitation terms are of the form $\int dx \left((\Psi_a^\dagger(x))^2 \Psi_b^2(x) + \text{h.c.} \right)$ and correspond, for instance, to a two-body collision where two atoms in the transverse ground state get excited to the first excited state. The coupling constants g_a and g_{ab} ($a, b = 0, 1, 2$) are effective 1D coupling constants resulting from the 3D interaction. Møller et al. (2021) assume that they are equal: $g_a = g_{ab} = g$; under that assumption, the multi-component Bose gas with $V(x) = 0$ is integrable (Yang, 1967; Gaudin, 2014; Caux et al., 2009; Klauser and Caux, 2011; Klümper and Pâţu, 2011; Pâţu and Klümper, 2015; Robinson et al., 2016; Robinson and Konik, 2017), however the description of its thermodynamic limit is considerably more complicated than the one of the Lieb-Liniger model reviewed in Section 1.1.

By a sequence of approximations, **?** ultimately arrive at a phenomenological description that resembles the GHD equation of the 1D Bose gas, where the excitation terms in the Hamiltonian (2.10) are introduced in the form of a Boltzmann collision integral:

$$\partial_t \rho + \partial_x [v^{\text{eff}} \rho] - (\partial_x V)\partial_\theta \rho = \mathcal{I}. \tag{2.11}$$

That collision integral $\mathcal{I}$ is constructed phenomenologically, by considering a simple model for two-body collisions. This phenomenological approach does not incorporate interactions with the other particles, contrary to what usually happens in exact Bethe Ansatz calculations (where the interaction effects appear through the dressing of the various quantities that enter all the formulas). Within the framework of that very simple model, the probability for two colliding atoms with momenta $p_1 = \hbar k_1$, $p_2 = \hbar k_2$ initially in the same transverse state to get excited to a different transverse state is estimated as $P_{\updownarrow}(k,q) \simeq 4c^2kq/[k^2q^2 + c^2(k+q)^2]$ where $k = |k_1 - k_2|$ and $q = \sqrt{|k_1 - k_2|^2 - 8m\omega_\perp/\hbar}$. Then the authors assume that the atom momenta may be replaced by the rapidities, and arrive at a closed expression for $\mathcal{I}$, see (Møller et al., 2021) for more details. The various approximations involved in the construction of the effective Boltzmann equation (2.11) are particularly meaningful in the ideal Bose gas regime, where the interactions between atoms are negligible. There, this phenomenological approach is expected to work well. Notice that in the ideal Bose gas regime, the GHD dynamics reduces to that of free Bosons, with the effective velocity appearing in Eq. (2.11) reducing to the bare velocity $v^{\text{eff}}(\theta) = \theta/m$. In that regime the aforementioned assumption that all intra- and inter-component coupling strengths are equal is actually no longer necessary for the gas to be integrable. Beyond the ideal Bose gas regime, the accuracy of the description of the 1D-3D crossover by Eq. (2.11) remains to be investigated.

Motivated by the recent experiment in the Newton Cradle setup of Li et al. (2020), which observed thermalization attributed to excitations of the transverse modes, Møller et al. (2021) simulated the Newton Cradle with Eq. (2.11) in the ideal Bose gas regime, and found that excitations to the transverse modes do indeed induce thermalization.

2.3 Experimental tests of Generalized Hydrodynamics

2.3.1 Techniques for 1D confinement of Bose gases

Confining potentials for cold atoms can be realized in different ways (Pethick and Smith, 2008), see below. In order to create 1D systems, the 3D confinement must be very anisotropic: locally, the potential is quasi-harmonic,

$$V_{3\text{D}}(x,y,z) \simeq \frac{1}{2}m\omega_\parallel^2 x^2 + \frac{1}{2}m\omega_\perp^2(y^2+z^2) \tag{2.12}$$

with

$$\omega_\perp \gg \omega_\parallel. \tag{2.13}$$

The 1D regime is reached when the transverse confinement is large enough so that the transverse energy gap $\hbar\omega_\perp$ is much larger than the typical energy per atom. Then the transverse degrees of freedom are frozen, and the resulting dynamics in effectively one-dimensional, along the direction x.

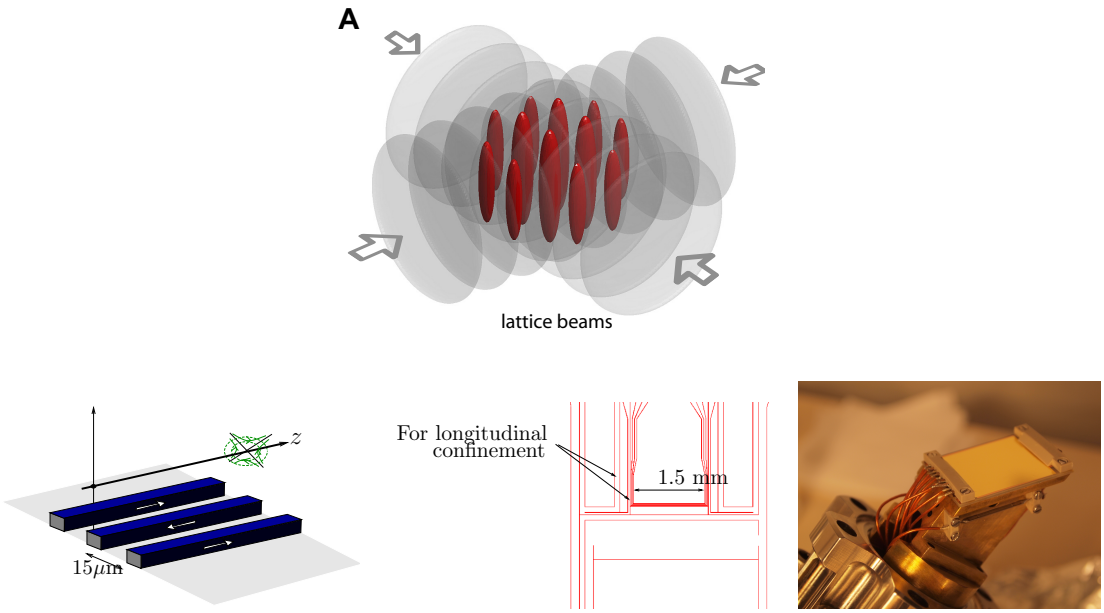

Figure 2.5: *[From the review article (Bouchoule and Dubail, 2022)]* Creating 1D gases in cold atom experiments. **A.** A 2D optical lattice produces an array of 1D tubes. **B.** Guiding atoms along a 3-wire guide on an atom-chip [pictures from the atom-chip experiment of Isabelle Bouchoule]. (a) Three parallel wires, running current in alternate directions, guide the atoms along a line above the central wire. (b) Chip layout (wires edges shown). In addition to the 3-wire guide, other wires are used for the longitudinal confinement and for preparation stages. (c) The atom-chip, covered with a gold mirror.

In that regime, the effective delta interaction between the atoms in 1D comes from their 3D short-range interaction, whose strength is set by the 3D scattering length $a_{3\mathrm{D}}$. The precise relation between the $1D$ coupling constant g and $a_{3\mathrm{D}}$ was worked out by Olshanii (1998),

$$g = \frac{2\hbar\omega_\perp a_{3\mathrm{D}}}{1 - \mathcal{C}a_{3\mathrm{D}}/a_\perp}, \tag{2.14}$$

where $a_\perp = \sqrt{2\hbar/(m\omega_\perp)}$ is the width of the transverse ground state and $\mathcal{C} \simeq 1.46$. In many experimental realizations, $a_{3\mathrm{D}} \ll a_\perp$, so that Olshanii's relation (2.14) reduces to $g_{1\mathrm{D}} = 2\hbar\omega_\perp a_{3\mathrm{D}}$. Formula (2.14) shows a resonant behavior when $\mathcal{C}a_{3D}/a_\perp \simeq 1$, which can be interpreted as a Feshbach resonance involving a bound state related to a transversely excited state Bergeman et al. (2003).

There are two main technologies to realize 1D gases in experiments (Fig. 2.5).

1. The confining potential is created by laser fields: the interaction between the induced atomic dipole and the laser field results in a force acting on the center-of-mass motion of the atom, which is conservative if the laser frequency is sufficiently far from any atomic resonance and which is proportional to the laser intensity gradient. The strong transverse confinement is realized by lasers with large intensity gradients resulting from interference, and a 2D optical lattice formed by lasers far-detuned from the atomic transitions realizes a 2D array of 1D tubes for the atoms where the 1D regime can be created (Kinoshita et al., 2005; Haller et al., 2009; Fabbri et al., 2011). Such 'optical trapping' setups possess several nice features:

   - very strong transverse confinements can be obtained, since the light intensity is modulated on distances as small as the laser wavelength. This allows to realize 1D gases with string repulsion, see Olshanii's formula (2.14)
   - cold atoms are loaded in optical lattices adiabatically from a 3D BEC, which gives very cold 1D gases
   - the magnetic field is a free parameter that can be tuned to approach Feshbach resonances and thus adjust the interaction strength between atoms (Haller et al., 2009).

   On the other hand, optical trapping setups also have some drawbacks, the main one being that all measurements are automatically ensemble-averaged over all the 1D tubes, which greatly complicates the data analysis.

2. The confining potential is created by spatially-varying magnetic fields, exploiting the non-vanishing magnetic moment of the atoms. Strong magnetic gradients are obtained in the vicinity of microwires on 'atom chips' (Reichel et al., 1999; Folman et al., 2000; Reichel and Vuletic, 2011), and the 1D regime can be reached (van Amerongen et al., 2008; Armijo et al., 2011; Jacqmin et al., 2011). The main advantages of atom chip setups are:

- a single 1D gas is realized, which allows for direct comparison with theoretical predictions. This also allows to study fluctuations and correlations, see for instance (Fang et al., 2016).
- the guiding of atoms can be realized on very long distances, as the transverse confinement is invariant along the whole microwire.

The main drawbacks are that the effective 1D coupling constants that can be reached are small, and that the 1D gases are prepared and cooled down directly in the 1D geometry, resulting in temperatires that are much higher than those obtained in 2D optical lattices. For studies of the phenomena limiting the temperatures in atom chip setups, see (Rauer et al., 2016; Schemmer and Bouchoule, 2018; Bouchoule and Schemmer, 2020).

2.3.2 Test of GHD in an atom chip setup

A first experimental demonstration of the validity and relevance of GHD was carried out by Schemmer et al. (2019). In this experiment, a 1D gas is realized on an atom chip. The initial cloud is at equilibrium in a regime close to the quasicondensate regime. Dynamics is initiated by a quench of the longitudinal potential, and the time evolution of the density profiles is recorded. For all situations considered, the results are in very good agreement with the predictions of the GHD theory.

The data are also compared to predictions of standard hydrodynamics, given by the Euler equations (3) of the introduction, with the pressure term corresponding to the Lieb-Liniger model. In contrast with GHD, this standard hydrodynamic approach assumes that the gas is locally at thermal equilibrium. A clear failure of standard hydrodynamics is found when the 1D gas is prepared at equilibrium in a double-well potential, and the double-well is suddenly switched off and the gas is let to expand freely in 1D, see Fig. 2.6.

The origin of the failure of standard hydrodynamics in the above scenario is revealed by the following simple picture (Fig. 2.6, bottom). During the time evolution, the two clouds that were initially in each of the potential wells spread, the negative rapidities moving to the left and the positive ones to the right. After some expansion time, at the central position, the positive rapidities from the left cloud meet negative rapidities coming from the right cloud. The resulting rapidity distribution is then double peaked. The standard hydrodynamic theory cannot capture this feature, because it assumes local thermal equilibrium and the rapidity distribution of thermal states are single-peaked. This striking difference between GHD and conventional Euler hydrodynamics is clearly visible in Fig. 2.6, where the calculated Fermi occupation ratio $\nu(x, \theta)$ is displayed for both theories.

2.3.3 Test of GHD in an optical trapping setup

In the experiment of Schemmer et al. (2019), GHD is tested in a very large atom cloud that contains thousands of atoms, and whose longitudinal size, of the order of 100μm, is

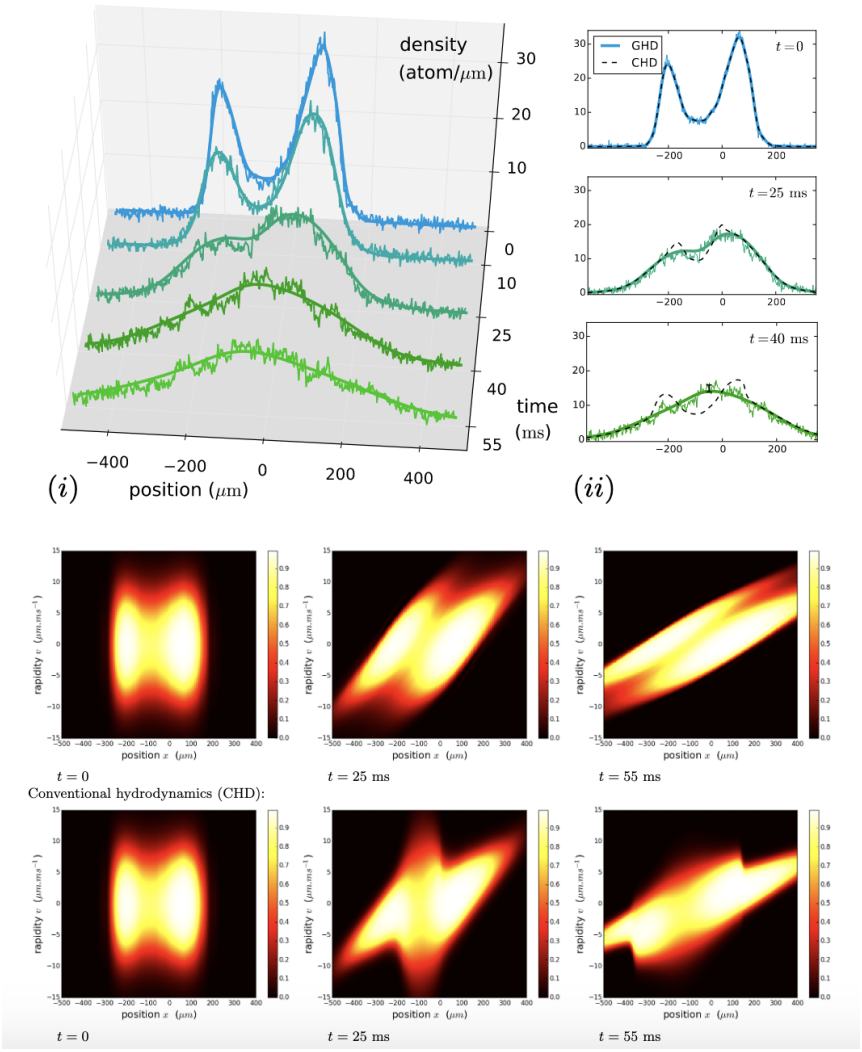

Figure 2.6: Top. *[From (Schemmer et al., 2019); ; reproduced in the review article (Bouchoule and Dubail, 2022)]* Experimental test of GHD theory. The density profiles after a quench from a double well potential to a flat potential are shown. The experimental date (noisy curves) are in very good agreement with GHD predictions (smooth solid lines). The standard hydrodynamics (dashed lines on the right figures) fails to capture the experimental dynamics. Bottom. *[From Supplemental Material of (Schemmer et al., 2019)]* Calculations of the expected rapidity distributions after a release from a double-well potential. The figures show the evolution of the Fermi occupation ratio $\nu(x, \theta)$, which is in one-to-one correspondence with the rapidity distribution $\rho(x, \theta)$ (see Subsection 1.3). The top line shows prediction from GHD theory, and the bottom line shows prediction from standard Euler hydrodynamics. The GHD predicts the appearance a of double peaked rapidity distribution around the center of the cloud (clearly visible on the plot at $t = 55$ms). Standard Euler hydrodynamics, on the other hand, assumes that at each point x the rapidity distribution $\rho(x, \theta)$ is the one at thermal equilibrium, which is a single peaked function. This theory is thus unable to capture the correct physics.

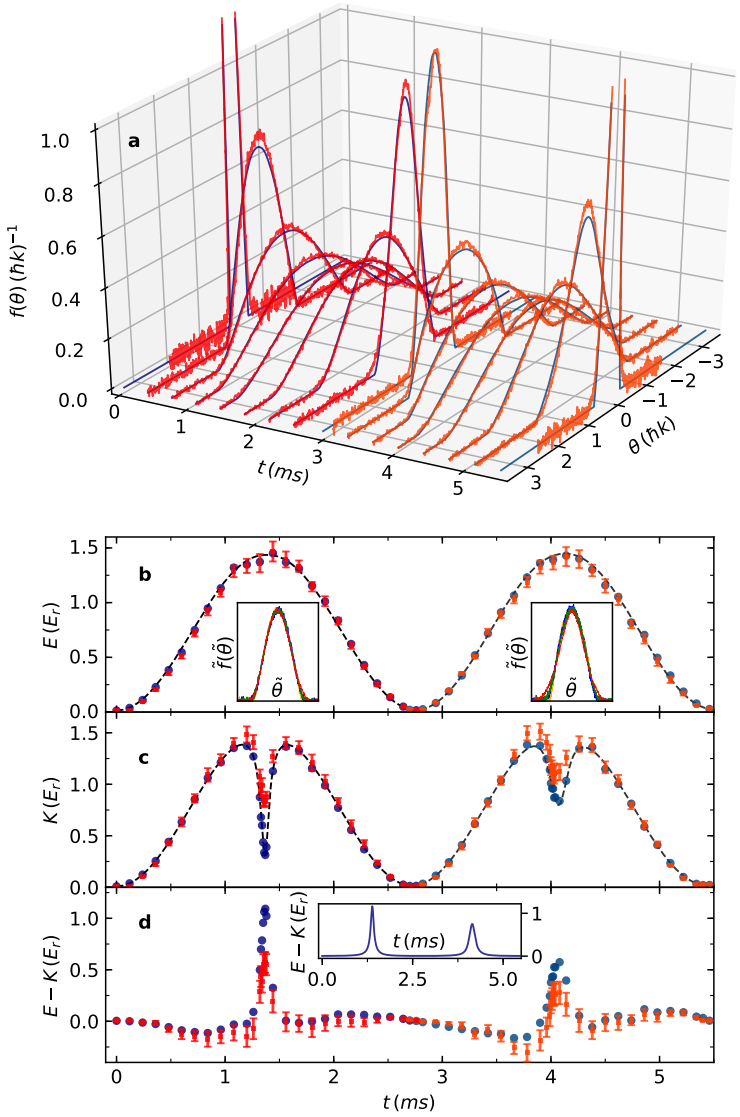

Figure 2.7: *[From (Malvania et al., 2020); reproduced in the review article (Bouchoule and Dubail, 2022)]* Test of GHD using strongly interacting gases. The dynamics is generated by a sudden increase of the depth of the Gaussian longitudinal confinement by a factor 100. The first two compression cycles are shown. Experimental data (red curves in (a) and red dots in (b-d)) are compared to GHD predictions for a gas initially in the ground state (blue lines in (a)). The blue dots in (b-c) are the GHD calculation using the measured atom number at each time, while the dashed line in (b-c) is the theory using the average atom number. **a** Measured rapidity distribution $f(\theta)$, integrated over positions x and averaged over all 1D tubes, compared to the GHD prediction. **b** Rapidity energy E, *i.e.* $\int d\theta f(\theta)(\theta^2/(2m))$, in units of the recoil energy $E_{\rm r}$. **c** Evolution of the kinetic energy, obtained from the measured momentum distribution $w(p)$: $K = \int dp w(p)(p^2/(2m))$. **d** Interaction energy $E - K$.

very large compared to microscopic scales. In these conditions, GHD is clearly expected to be valid. In a more recent experiment by Malvania et al. (2020), GHD is tested in a setup that uses a 2D lattice of 1D gases. In this experiment, the typical atom number N is as low as 10 to 20 per 1D gas. Moreover, the (quasi)harmonic longitudinal potential $V(x)$ can be quenched very dramatically: at time $t = 0$, the amplitude of the trap can be increased by a factor as large as 100, so the atom cloud is very strongly compressed. The validity of GHD is severely challenged in this situation. Yet, the experimental data, which are averaged over all the 1D tubes, are still correctly described by GHD over the first few oscillation cycles. We now discuss the results of Malvania et al. (2020) in more detail.

The 1D clouds are prepared from a 3D Bose-Einstein condensate by adiabatically increasing the depth of the 2D lattice. When the 2D lattice depth is large enough, the gas decouples into independent 1D tubes. The temperature is extremely low, so that each 1D gas is close to the ground state of the Lieb-Liniger Hamiltonian in each tube. The dynamics is generated by suddenly increasing the longitudinal potential $V(x)$ felt by the atoms in each tube. The longitudinal potential $V(x)$, realized using an optical beam, has a Gaussian shape and its depth is increased by a large factor, 10 or 100 depending on the experimental data set. In sharp contrast with (Schemmer et al., 2019), the initial cloud lies in the hard-core regime, with mean γ, averaged over the distribution of linear densities, as large as 9. Malvania et al. (2020) measure the time evolution of the rapidity distribution (Fig. 2.7), using the technique of (Wilson et al., 2020). This measurement is a global measurement: the rapidity distribution is integrated over positions x within each tube, and averaged over all the tubes.

The results are shown in Fig. 2.7, for a quench of the 1D trap amplitude by a factor 100. They are in excellent agreement with GHD predictions, which use the Lieb-Liniger ground state within the local density approximation as the initial state and the GHD equations (1.55). In the theory calculation, it is found that, for a an increase of the trap depth of the quasi-harmonic (Gaussian) potential by a factor 100, the dimensionless repulsion strength γ, taken to be initially of order 1 in the center of the cloud, drops to a value of order 0.1 at the maximum of the compression. Thus, the variation of γ as a function of position and time over one compression cycle is very large.

The measurement of the rapidity distribution, integrated over all atoms, allows to monitor the evolution of the 'rapidity energy', defined as $E = \int \rho(x,\theta)\theta^2/(2m)dxd\theta$ for a single 1D cloud —and it is averaged over all clouds in the measurement—. The rapidity energy is the total energy, which is conserved, minus the potential energy associated to the confining potential. Since the potential energy oscillates as the cloud breathes, so does the rapidity energy E, as seen in Fig. 2.7.b. Moreover, besides the rapidity distribution, Malvania et al. (2020) also measure the momentum distribution, from which the kinetic energy K can be extracted. The time-evolution of the kinetic energy is shown in Fig.2.7.c. The difference between the rapidity energy E and the kinetic energy K is the interaction energy. If the gas remained in the hard-core regime at all times, then one would always have $K = E$: the atoms would never be at the same position, so the contact interaction energy

would be zero and the rapidity energy would be entirely in the form of kinetic energy. The narrow dip of K at the time when the cloud is most compressed clearly demonstrates that, at this time, the cloud leaves the hard core regime.

To conclude this Chapter, we stress that the good agreement found by (Malvania et al., 2020) between experimental data with small atom number per tube and the predictions of GHD is a topic that deserves further investigation. As discussed in the Supplemental Material of (Malvania et al., 2020), the averaging over 1D tubes results in a smoothing of small atom number effects, which may explain the good agreement with the hydrodynamic theory, to some extent. It would be interesting to investigate the question of the accuracy of GHD for single 1D clouds of a few atoms more systematically. On the theory side, this could be done by performing numerical simulations of a single 1D gas for very small atom numbers (similarly to the numerical results shown in Fig. 3.5, but for longer times).

Chapter 3

Quantum fluctuations

3.1 Ground state quantum fluctuations from the effective field theory viewpoint

In this section I discuss zero point quantum fluctuations of an Euler fluid at zero temperature, and correlation functions from the perspective of effective field theory. This is of course nothing but Luttinger liquid theory, which can be presented in several other ways, see e.g. (Haldane, 1981; Giamarchi, 2003; Cazalilla, 2004; Tsvelik, 2007).

I find that the effective field theory perspective, even though it is less constructive than some other approaches —for instance, than Haldane's one (Haldane, 1981)—, does have its own merits. In particular, in my opinion, it makes a very clear distinction between what is universal (i.e. field theory data) and what is not (i.e. all dimensionful data that are needed to connect objects in the microscopic system to field theory ones). This is why I prefer to introduce the theory in this slightly non-standard way here, inspired by (Abanov, 2006).

3.1.1 Standard Euler equations for the classical Galilean fluid: reduction to two equations

In this Section we consider first a classical Galilean fluid. It is described by the three Euler equations discussed in the introduction,

$$\left\{ \begin{array}{rcl} \frac{\partial}{\partial t} n + \frac{\partial}{\partial x}(nu) & = & 0 \\ \frac{\partial}{\partial t} u + u \frac{\partial}{\partial x} u + \frac{1}{mn} \partial_x \mathcal{P} & = & -\frac{1}{m} \frac{\partial V}{\partial x} \\ \frac{\partial}{\partial t} e + u \frac{\partial}{\partial x} e + \frac{1}{n} \mathcal{P} \partial_x u & = & 0. \end{array} \right. \tag{3.1}$$

Here we want to study this fluid near equilibrium at zero temperature. It turns out that, at zero temperature, only the first two partial different equations in (3.1) are needed; the third one is redundant. The reason is as follows. As discussed in the introduction, the third equation in (3.1) comes from conservation of energy. Equivalently, it can be recast

to express the fact that entropy moves with the flow, namely

$$\partial_t s + u\partial_x s = 0, \tag{3.2}$$

where s is the entropy per particle. At zero temperature, $s = 0$ everywhere in the fluid, so that equation is always trivially satisfied.

To see that (3.2) is equivalent to the third equation in (3), one way is to use the thermodynamic relation between the internal energy per unit mass and s, $de = \frac{T}{m}ds - \mathcal{P}d\,(1/n)$. Then

$$\begin{aligned} \frac{T}{m}(\partial_t + u\partial_x)s &= (\partial_t + u\partial_x)e - \frac{\mathcal{P}}{n^2}(\partial_t + u\partial_x)n \\ &= (\partial_t + u\partial_x)e + \frac{\mathcal{P}}{n}\partial_x u, \end{aligned}$$

where we used the first equation in (3.1) to go from the first to the second line.

To summarize, our classical Galilean fluid at zero temperature is described by two equations,

$$\begin{aligned} \partial_t n + \partial_x(nu) &= 0 \\ \partial_t u + u\partial_x u + \tfrac{1}{n}\partial_x \mathcal{P} &= -\tfrac{1}{m}\partial_x V, \end{aligned} \tag{3.3}$$

where $V(x)$ is the external potential, and $\mathcal{P}(n)$ is the zero-temperature pressure of the fluid which depends on the microscopic details.

The function $\mathcal{P}(n)$ —i.e. the equation of state of the fluid— might be very different depending on whether the underlying microscopic system is classical or quantum. For instance, in a classical gas of non-interacting particles, the particles would simply freeze at zero temperature and the pressure would vanish, while this can never be true with quantum particles which always have zero point fluctuations. Nevertheless, apart from the equation of state which may be sensitive to quantum effects, what we have done so far is *classical hydrodynamics*.

Next, we argue that the quantization of the classical fluid (3.3) is a Luttinger liquid.

3.1.2 An action for the standard Euler fluid

Formally, there are various ways of quantizing the Euler equations at zero temperature (3.3), but in the end they are roughly equivalent. One way, which we follow here, is to write an action whose minimization leads to the classical equations (3.3), and then write a path integral.

Our starting point is then to find a variational principle for the Euler equations (3.3). To do that, one has to treat the two equations (3.3) on a different footing. We look at the first one (the continuity equation for the mass density) as a *constraint*, which by definition is always satisfied exactly by the couple (n, j). The second one (the Euler equation for u)

results from the variational principle, by minimizing $\mathcal{S}[n,j]$ under the constraint $\partial_t n + \partial_x j = 0$. We choose the action (Abanov, 2006)

$$\mathcal{S}[n,j] = \int dxdt \left[\frac{j^2}{2n} - \rho_E(n) - nV\right], \tag{3.4}$$

where $\rho_E(n)$ is the ground state energy density.

To vary this action under the constraint $\partial_t n + \partial_x j = 0$, one can imagine that one has a configuration $(n(x,t), j(x,t))$ which satisfies the continuity equation, and represent fluctuations around that configuration by a "height field" $h(x,t)$,

$$\delta n(x,t) = \frac{m}{2\pi}\partial_x h(x,t), \qquad \delta j(x,t) = -\frac{m}{2\pi}\partial_t h(x,t), \tag{3.5}$$

such that $(n+\delta n, j+\delta j)$ automatically satisfies the constraint. Then, varying the action to first order in $\delta n, \delta j$ (substituting (3.5) and integrating by parts), one gets

$$\begin{aligned}\delta\mathcal{S}^{(1^{\text{st}}\text{ order})} &= \int dxdt \left[\frac{j\delta j}{n} - \frac{j^2}{2n^2}\delta n - \delta n \partial_n \rho_E - \delta n\ V\right] \\ &= \frac{m}{2\pi}\int dxdt \left[\partial_t\left(\frac{j}{n}\right) + \partial_x\left(\frac{j^2}{2n^2}\right) + \partial_x(\partial_n\rho_E + V)\right] h.\end{aligned}$$

The expression inside the bracket must vanish; using $u = j/\rho$ and $\partial_x(\partial_n\rho_E) = \frac{1}{n}\partial_x P$ [this follows from the thermodynamic relations (at $T=0$) $d\rho_E = \mu dn$ and $d\mathcal{P} = n\ d\mu$], this gives precisely the second equation in (3.3), as required. So the action (3.4) is indeed a "good" action for the Euler equations (3.3).

3.1.3 Quadratic effective field theory

Now that an action has been identified, one can turn classical hydrodynamics into "quantum hydrodynamics" simply by putting the action inside an exponential, and by integrating over all configurations (n,j) that satisfy the constraint. This can be done directly in terms of the height field: given a reference configuration (ρ, j) which satisfies the continuity equation, one can write the path integral as

$$\int [dh]\ \exp\left(\frac{i}{\hbar}\mathcal{S}\left[n + \frac{m}{2\pi}\partial_x h, j - \frac{m}{2\pi}\partial_t h\right]\right). \tag{3.6}$$

Such path integrals are typically approximated by the saddle-point method, by expanding to second order in h around classical configurations (ρ, j) —configurations which are solutions to the Euler equations (3.3)—, leading to a gaussian path integral.

Expanding the action to second order gives

$$\begin{aligned}\delta\mathcal{S}^{(2^{\text{nd}}\text{ order})} &= \frac{1}{2}\int dxdt \left[\frac{1}{\rho}(\delta j)^2 - 2\frac{j}{\rho^2}(\delta\rho)(\delta j) + (\frac{j^2}{\rho^3} - \partial_\rho^2\rho_E)(\delta\rho)^2\right] \\ &= \frac{\hbar}{8\pi}\int dxdt \begin{pmatrix} \partial_t h & \partial_x h \end{pmatrix} \cdot A \cdot \begin{pmatrix} \partial_t h \\ \partial_x h \end{pmatrix}\end{aligned}$$

for some 2×2 symmetric matrix A. This gives a quadratic action for the quantum fluctuations around a classical hydrodynamic solution. Of course, there should also be higher order terms, but those are irrelevant in the renormalization group sense in two spacetime dimensions, so one usually omits them. One concludes that quantum fluctuations of 1d liquids are captured by a quadratic action. This effective theory is known as Luttinger (or Tomonaga-Luttinger) liquid theory.

3.1.4 The parameters in the effective action: mean fluid velocity u, sound velocity v, Luttinger parameter K

To elaborate, the above symmetric matrix A can be checked to be of the form

$$A = \frac{1}{K} \times \begin{pmatrix} \frac{u^2}{v} - v & -\frac{u}{v} \\ -\frac{u}{v} & \frac{1}{v} \end{pmatrix}^{-1},$$

where $u = j/n$ is the local mean velocity of the fluid, and the sound velocity v and the dimensionless Luttinger parameter K are given by

$$v = \sqrt{n\, \partial_n^2 \rho_E} \qquad \text{and} \qquad K = \frac{\pi \hbar n}{m^2 v}. \tag{3.7}$$

In terms of these parameters, the above quadratic action for the fluctuations of h becomes

$$\mathcal{S}[h] \equiv \delta \mathcal{S}^{(2^{\text{nd}} \text{ order})} = \frac{\hbar}{8\pi} \int \frac{\sqrt{-g}\, d^2\mathrm{x}}{K} g^{ab} (\partial_a h)(\partial_b h) \tag{3.8}$$

where $\mathrm{x}^0 = t, \mathrm{x}^1 = x$, and the metric g_{ab} is

$$\begin{aligned} ds^2 &= g_{ab} d\mathrm{x}^a d\mathrm{x}^b \\ &= (dx - (u+v)\, dt)(dx - (u-v) dt). \end{aligned} \tag{3.9}$$

The action (3.8) is the one of the free massless boson, also called Gaussian Free Field (GFF), in the metric g. The physical meaning of g is that it is the natural metric in which sound waves propagate. Indeed, the sound waves propagating on top of the fluid correspond to low-energy excitations of the GFF, which propagate along the null geodesics of g, and those are precisely the right- and left-moving sound waves which propagate at velocity $u \pm v$.

3.1.5 Equal-time correlation functions

The effective field theory allows to compute ground state correlation functions in the fluid. The idea is that any local observable $\hat{O}(x)$ in the microscopic model should have an expansion in terms of the field theory operators $\phi(x)$ that appear in the effective field theory,

$$O(x) = \sum_{\phi} \mathcal{A}_{O\phi}(x)\ \phi(x), \tag{3.10}$$

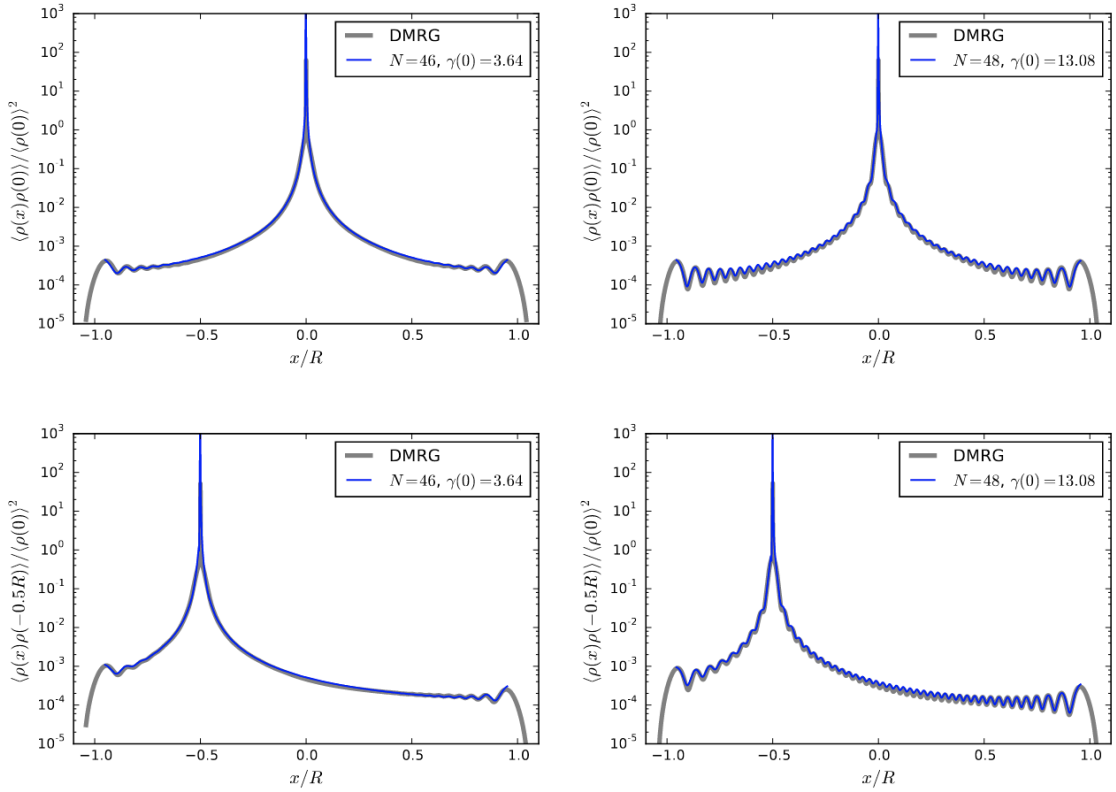

Figure 3.1: *[From (Brun and Dubail, 2018).]* Connected part of the density-density correlation function $\langle 0|\, n(x)n(y)\, |0\rangle$ in the ground state $|0\rangle$ of the harmonically trapped 1D Bose gas with N particles, with Lieb interaction parameter $\gamma(x)$ —the gas is inhomogeneous, so the Lieb parameter depends on position—. The blue curve corresponds to the expansion (3.10)-(3.11) in terms of field theory correlators, while the gray line is the numerically exact simulation (obtained with DMRG in the lattice gas at very low particle density).

where the $\mathcal{A}_{O\phi}(x)$ are scalar coefficient discussed in detail below (Subsec. 3.1.6). As it stands, Eq. (3.10) is meaningless: the left hand side is an operator acting on the Hilbert space of the microscopic quantum system, while the right hand side is a sum over operators in some field theory. Formula (3.10) must be understood as a statement about *all long-distance correlation functions*. The statement is that, for any set of local operators $O_1(x_1)$, $O_2(x_2)$, ..., $O_p(x_p)$, their expectation value in the ground state $|0\rangle$ has an asymptotic expansion in terms of the field theory (FT) correlators,

$$\langle 0|\, O_1(x_1)O_2(x_2)\dots O_n(x_n)\,|0\rangle \;=\; \sum_{\phi_1,\dots\phi_n} \left(\prod_{j=1}^{n} \mathcal{A}_{O_j\phi_j}(x_j)\right) \langle \phi_1(x_1)\phi_2(x_2)\dots\phi_n(x_n)\rangle_{\rm FT}\,. \tag{3.11}$$

This asymptotic expansion holds in the limit when the points x_1, x_2, ..., x_p are separated by large distances. The terms in the right hand side can be ordered according to the scaling dimensions of the field theory operators: the larger the scaling dimension, the faster they decay as a function of the distance between the points x_1, x_2, ...

The point is that, since the effective field theory is a free boson theory, the correlators $\langle \phi_1(x_1)\phi_2(x_2)\dots\phi_n(x_n)\rangle_{\rm FT}$ can be computed efficiently. In the special case when the Luttinger parameter K is independent of position —in particular, when the fluid is homogeneous, or when the microscopic model can be mapped to non-interacting fermions—, then all field theory correlators are easily computed by exploiting conformal invariance, see e.g. Francesco et al. (2012) for an introduction. When the Luttinger parameter K is not constant, the theory is not conformally invariant, however one can still express all correlation functions in terms of three fundamental two-point functions only, which correspond to the Green's functions of the Laplacian for different combinations of boundary conditions (Dirichlet/Dirichlet, Neumann/Neumann, Dirichlet/Neumann), see (Brun and Dubail, 2018) for details.

As an example of an application, in Fig. 3.1 we show the connected density-density correlation function in the ground state of the harmonically trapped 1D Bose gas with $N \simeq 40$ particles, compared to numerical results obtained with DMRG. The results are in excellent agreeement, although only the first three leading operators are included in the expansion (3.10) of the density operator,

$$\delta n(x) \;=\; n(x) - \langle 0|\, n(x)\,|0\rangle \;=\; \frac{1}{2\pi}\partial_x h(x) + \mathcal{A}_{\delta n\ \mathcal{V}_{1,0}}(x)\mathcal{V}_{1,0}(x) + \mathcal{A}_{\delta n\ \mathcal{V}_{-1,0}}(x)\mathcal{V}_{-1,0}(x) + \dots, \tag{3.12}$$

where $\mathcal{V}_{a,b}(x)$ is the so-called 'electric-magnetic operator' with 'electric' charge a and 'magnetic charge' b. The scaling dimensions of the operator $\partial_x h(x)$ is 1, and the scaling dimensions of $\mathcal{V}_{\pm 1,0}$ is equal to the Luttinger parameter K. They are the three lowest operators with zero magnetic charge; operators with non-zero magnetic charge are not allowed in the expansion of the density operator because they correspond to operators that change the total number of particles N.

In summary, the correlation functions of observables in the microscopic quantum model are given in terms of the correlators in the effective field theory by expansions of the form (3.10)-(3.11). The correlators in the effective field theory can be easily obtained, either fully analytically in the conformally invariant case (when the Luttinger parameter K is constant), or in terms of only three fundamental Green's functions that are easily obtained numerically.

The difficulty of computing ground state correlation functions then boils down to computing the non-universal prefactors $\mathcal{A}_{O\phi}(x)$; we now turn to that problem.

3.1.6 Computing the non-universal coefficients from exact form factor formulas

The non-universal coefficients $\mathcal{A}_{O\phi}(x)$ can be computed using the following method, see also (Shashi et al., 2011, 2012; Kitanine et al., 2011, 2012; Bondesan et al., 2015; Brun and Dubail, 2018; Scopa et al., 2020). The coefficients are extracted from the homogeneous system —here, the 1D Bose gas— with periodic boundary conditions. The effective field theory is conformally invariant, and one relies on the operator-state correspondence, namely that the local operators $\phi(x)$ in the conformal field theory (CFT) are in correspondence with eigenstates of the CFT hamiltonian $|\phi\rangle$.

One makes the following assumptions:

- for sufficiently large system sizes L, the low-energy excited states of the microscopic hamiltonian H can be unambiguously identified with the ones of the CFT Hamiltonian. In particular, the ground state of H for a system of size L, $|0\rangle_L$, is viewed as a microscopic version of the CFT vacuum $|0\rangle_{\text{CFT}}$. Similarly, there is a unique low-energy eigenstate of H, noted $|\phi\rangle_L$, that is viewed as a microscopic version of the CFT state $|\phi\rangle_{\text{CFT}}$.
- the form factor in the microscopic model, ${}_L\langle\phi|\, O(x)\,|0\rangle_L$, is known for arbitrary L. This is often the case thanks to form factors formulas obtained with the algebraic Bethe Ansatz, see e.g. (Slavnov, 1989; Kitanine et al., 1999).

The coefficient $\mathcal{A}_{O\phi}$ is then given by

$$\mathcal{A}_{O\phi}(x) \;=\; \lim_{L\to\infty}\left[\left(\frac{L}{2\pi}\right)^{\Delta_\phi}\frac{{}_L\langle\phi|\, O(x)\,|0\rangle_L}{\sqrt{{}_L\langle 0\,|0\rangle_L\;{}_L\langle\phi\,|\phi\rangle_L}}\right], \tag{3.13}$$

where Δ_ϕ is the scaling dimension of the CFT operator ϕ. Formula (3.13) is obtained by conformal mapping from the complex plane to the cylinder.

To summarize, for operators in the microscopic model such as the density operator $n(x)$, or the boson creator/annihilator operators $\Psi^\dagger(x)$, $\Psi(x)$, exact form factors formulas available in the literature (Slavnov, 1989; Kitanine et al., 1999) allow to extract the non-universal coefficient $\mathcal{A}_{n\,\phi}$, $\mathcal{A}_{\Psi^\dagger\,\phi}$, $\mathcal{A}_{\Psi\,\phi}$, etc. For more details, see e.g. (Shashi et al., 2011,

2012; Kitanine et al., 2011, 2012; Bondesan et al., 2015; Brun and Dubail, 2018; Scopa et al., 2020). These non-universal prefactors, together with the known (or easily computable) field theory correlators, gives access to equal-time ground state correlations in the 1D Bose gas.

3.1.7 Correlations at different times. Propagation of quantum fluctuations in the (linear) Luttinger liquid.

So far we have focused only on equal-time correlations functions. But the Luttinger liquid also gives predictions for correlation functions at different times. For simplicity, consider the ground state of the spatially homogeneous system ($V(x) = 0$), with $n(x,t) = n$ and $u(x,t) = 0$. Linearizing the system (3.3) around that solution leads to the equation of propagation of linear sound waves $(\delta n(x,t), \delta u(x,t))$

$$\left\{ \begin{array}{rcl} \partial_t \delta n + n \partial_x \delta u &=& 0 \\ \partial_t \delta u + \frac{1}{mn} \frac{\partial \mathcal{P}}{\partial n} \partial_x \delta n &=& 0, \end{array} \right. \tag{3.14}$$

or equivalently

$$\left(\frac{\partial}{\partial t} - \begin{pmatrix} +v & 0 \\ 0 & -v \end{pmatrix} \frac{\partial}{\partial x} \right) \begin{pmatrix} v\,\delta n + n\,\delta u \\ v\,\delta n - n\,\delta u \end{pmatrix} = 0, \tag{3.15}$$

with the sound velocity $v = \sqrt{\frac{1}{m}\frac{\partial \mathcal{P}}{\partial n}}$. We see from Eq. (3.15) that there are right- and left-moving sound waves, corresponding to specific linear combinations of δn and δu, traveling at velocity $\pm v$.

In the effective field theory with the quadratic action (3.8), quantum fluctuations propagate in time as linear sound waves. Then correlation functions at different times are obtained from the ones at time $t = 0$ by propagating the operators either to the left or to the right, or combinations of those if the operator is senstive to both left- and right-sound waves.

For instance, the equal-time density-density correlation in the homogeneous ground state of an infinitely long 1D fluid is well-known to be (Giamarchi, 2003; Cazalilla, 2004; Tsvelik, 2007)

$$\langle \delta n(x_1) \delta n(x_2) \rangle_{\text{conn.}} = \frac{-K}{2\pi^2 (x_1 - x_2)^2} \tag{3.16}$$

at the leading order (i.e., keeping only the first operator $\partial_x h$ in the expansion 3.12). This correlation functions can then be propagated in time using the sound wave equation (3.15). It is a combination of two terms, one coming form the right-moving sound wave, the other from the left-moving one:

$$\langle \delta n(x_1,t_1) \delta n(x_2,t_2) \rangle_{\text{conn.}} = \frac{1}{4\pi^2} \left(\frac{-K}{[(x_1 - vt_1) - (x_2 - vt_2)]^2} + \frac{-K}{[(x_1 + vt_1) - (x_2 + vt_2)]^2} \right). \tag{3.17}$$

All other time-dependent correlations can be obtained in a similar way in the framework of (linear) Luttinger liquid theory, see e.g. (Giamarchi, 2003; Cazalilla, 2004; Tsvelik, 2007). These dynamical correlation functions obtained from the propagation of linear sound waves are valid on time scales that are not too long, before non-linear effects kick in. Non-linear effects fall beyond the scope of this habilitation thesis, although they have been studied extensively; see (Imambekov et al., 2012) for a review of 'non-linear Luttinger liquid' theory.

3.2 Zero-entropy GHD, and the sound wave equation

3.2.1 Contour in phase space

It is natural to ask whether the logic of the previous Section can be adapted to GHD, replacing the standard Euler equations at zero temperature (**??**) by the ones of Generalized Hydrodynamics, and adding quantum fluctuations to them. This program was implemented, to some extent, in (Ruggiero et al., 2020), reviewed in the next Section. The starting point of that program is a 'zero-temperature' —more precisely, 'zero-entropy'— form of the GHD equations. Indeed, since we are interested in quantum fluctuations rather than thermal fluctuations, it makes sense to start by investigating the fluid at zero temperature. Just like there is a reduction from the three standard Euler equations (3.1) to two equations (3.3) at zero temperature, there is a drastic simplification of the GHD equations when the gas is initialized in its ground state, as pointed out in (Doyon et al., 2017).

In an external potential $V(x)$, the ground state is modeled by hydrostatics, or equivalently by the local density approximation, which gives the distribution of rapidities $\rho(x,\theta,t=0)$. In the ground state, the Yang-Yang entropy of the gas vanishes. Then, since entropy is always conserved by Euler-scale hydrodynamic equations, it must vanish at all times. This puts very strong restrictions on the class of local stationary states that are explored by the system under GHD evolution: these local states must be either the ground state itself (up to a Galilean boost), or a 'split Fermi sea' (Fokkema et al., 2014; Eliëns and Caux, 2016; Eliëns, 2017). Within the framework of GHD, this is easily understood by using the so-called convective form of the GHD equation (1.55), which gives the evolution of the Fermi occupation ratio $\nu(x,\theta,t)=\rho(x,\theta,t)/\rho_{\rm s}(x,\theta,t)$,

$$\partial_t\nu + v^{\rm eff}(\theta)\partial_x\nu - (\partial_x V)\partial_\theta\nu \;=\; 0. \tag{3.18}$$

In the ground state, the Fermi occupation ratio is either zero or one: $\nu(x,\theta)=1$ if $\theta\in[-\theta_{\rm F}(x),\theta_{\rm F}(x)]$, and $\nu(x,\theta)=0$ otherwise. Here $\theta_{\rm F}(x)$ is a position-dependent Fermi momentum, which depends on the atom density $n(x)$, see Subsection 1.3. This specific form of $\nu(x,\theta,t)$ is preserved under (3.18): at any time, $\nu(x,\theta,t)$ is either zero or one. Consequently, the state of the system at time t is parameterized by a contour Γ_t in phase space (Fig. 2.2, left, and Fig. 3.5, top row), which separates the region where $\nu=1$ from

the one where $\nu = 0$, namely

$$\nu(x,\theta,t) = \begin{cases} 1 & \text{if} \quad (x,\theta) \text{ is inside } \Gamma_t \\ 0 & \text{if} \quad (x,\theta) \text{ is outside } \Gamma_t \,. \end{cases} \tag{3.19}$$

Parameterizing the contour as $\Gamma_t = \{(x_t(s), \theta_t(s));\ s \in [0, 2\pi)\}$, and plugging this into Eq. (3.18) one finds that its evolution equation reads

$$\frac{d}{dt} \begin{pmatrix} x_t(s) \\ \theta_t(s) \end{pmatrix} = \begin{pmatrix} v^{\text{eff}}(\theta_t(s)) \\ -\partial_x V(x_t(s)) \end{pmatrix}. \tag{3.20}$$

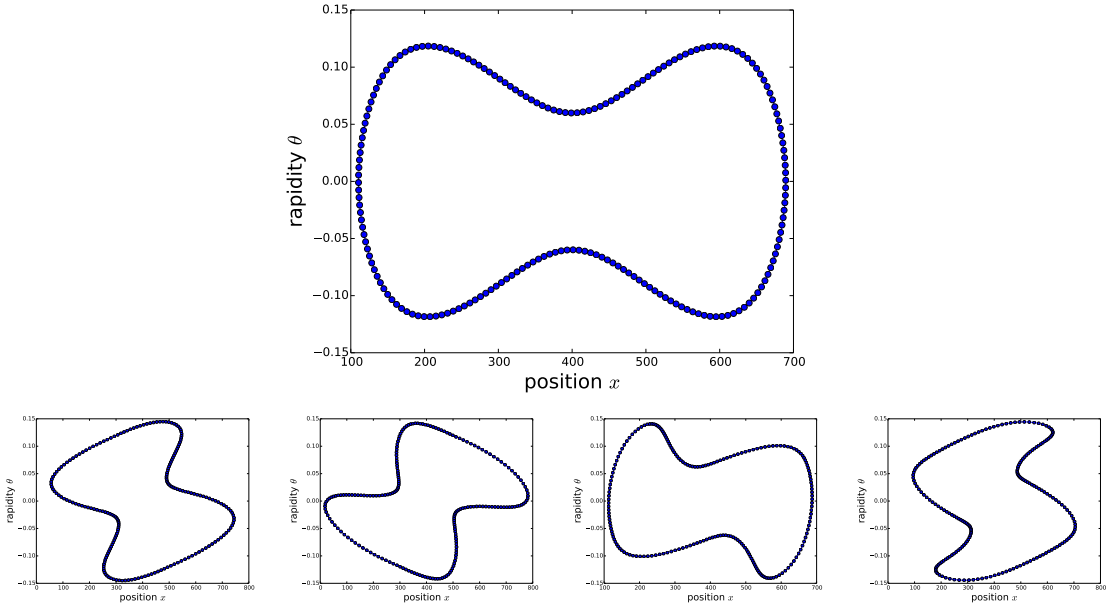

Figure 3.2: Top: the contour is encoded as a list of N points in the (x, θ)-plane. Bottom: the GHD evolution is implemented directly as the motion of each of the N points. Here $N = 200$.

This 'zero-entropy GHD' (Doyon et al., 2017) is very useful for numerical purposes, because it provides a very efficient way of solving the GHD equations: it is easier to compute the evolution of the contour Γ_t, rather than to simulate the evolution of the full distribution $\rho(x, \theta, t)$, even though both formulations are equivalent in the end. A basic algorithm is to numerically evolve the contour is the following, see Fig. 3.2. The contour Γ_t is discretized as a set of points (x_j, θ_j). To go from Γ_t to $\Gamma_{t+\Delta t}$, for every point (x_j, θ_j) one first finds all the segments along the contour which intersect the vertical line $x = x_j$, and calculate the rapidity θ_a, $a = 1, \ldots, 2p$ of their intersection. This gives the local

Fermi sea $\{\theta_a\}$ at position x_j. Then one calculates the corresponding effective velocity $v_j^{\rm eff} = v^{\rm eff}_{\{\theta_a\}}(\theta_j)$. We do this for all points x_j, and then wes evolve them according to

$$x_j \to x_j + v_j^{\rm eff}\Delta t, \qquad \theta_j \to \theta_j - V'(x_j)\Delta t. \tag{3.21}$$

In Fig. 3.2, one can see the evolution of the discretized contour Γ_t when the gas is suddenly released from its ground-state in a double-well potential to a harmonic potential. After a fraction of the period of the harmonic trap frequency, one observes the appearance of local split Fermi seas. Hence, such a setup could not be described by the standard Euler hydrodynamic equations (3.3), because the appearance of such multiple Fermi seas would translate into shock formations for those. GHD, on the other hand, does not have shocks (El and Kamchatnov, 2005; Bulchandani, 2017; Doyon et al., 2017) and remains valid after the appearance of multiple Fermi seas.

3.2.2 Linear sound waves

In Sec. 3.1.7, we saw that, in (linear) Luttinger liquid theory, quantum fluctuations propagate like the linear sound waves of a standard Euler fluid at zero temperature. The idea is now to apply the same logic to an out-of-equilibrium fluid described by GHD. To do this, we first need to derive the equation of propagation of linear sound waves.

Consider a small deformation of the contour Γ_t parameterized as follows (Ruggiero et al., 2020). In an interval $[x, x+\Delta x]$ where the number of Fermi points is constant and equal to $2q$, the contour Γ_t can be locally parameterized by functions $\theta_a(x,t)$, $a = 1, \dots, 2q$, ordered such that $\theta_1(x,t) < \theta_2(x,t) < \cdots < \theta_{2q}(x,t)$. Then the small deformation is written as

$$\theta_a(x,t) \;\to\; \theta_a(x,t) + \delta\theta_a(x,t), \tag{3.22}$$

for the different local Fermi points indexed by a. However, the equation of sound waves is more easily written in terms of small deformations of the Fermi momenta, rather then in terms of those of the rapidities. So we introduce the Fermi point $p_a(x,t)$, $a = 1, \dots, 2q$ such that, at any point (x,t),

$$p_a = \theta_a + \left(\int_{\theta_1}^{\theta_2} + \cdots + \int_{\theta_{2q-1}}^{\theta_{2q}}\right) \frac{d\theta'}{2\pi} \Delta(\theta - \theta') 1^{\rm dr}(\theta'), \tag{3.23}$$

and parameterize small deformations of the contour as

$$p_a(x,t) \;\to\; p_a(x,t) + \delta p_a(x,t). \tag{3.24}$$

This can be interpreted as an excess of fermion density near the Fermi point a,

$$\delta\rho_a(x,t) = \frac{1}{2\pi\hbar}\sigma_a\, \delta p_a(x,t), \tag{3.25}$$

where $\sigma_a = (-1)^a$ corresponds to the chirality of the Fermi point, and the factor $1/(2\pi\hbar)$ is inserted because each quantum state covers an area $2\pi\hbar$ in phase space (x, p). Similarly, one can interpret $\delta\theta_a$ as an excess of *quasi-particle density* at the Fermi point a; however one needs to insert an additional factor taking into account the quasi-particle charge $1^{\rm dr}(\theta_a)$, i.e.

$$\delta\tilde{\rho}_a(x,t) = \frac{1}{2\pi\hbar}\sigma_a\, 1^{\rm dr}(\theta_a)\, \delta\theta_a(x,t). \tag{3.26}$$

The Jacobian of the changes of variables from p_a to θ_a —or from $\delta\rho_a$ to $\delta\tilde{\rho}_a$— defines a useful $2q \times 2q$ matrix M(Eliëns and Caux, 2016; Eliëns, 2017), dubbed the 'Eliëns-Caux matrix' in (Ruggiero et al., 2020), $M_{ab} = \frac{1}{1^{\rm dr}(\theta_b)}\frac{\partial p_a}{\partial\theta_b}$. One can show that M is symplectic in the sense that $M^{-1} = \sigma M^\dagger \sigma$; consequently,

$$\delta\rho_a(x,t) \;=\; \sum [M^\dagger]_{ab}(x,t)\delta\rho_b(x,t). \tag{3.27}$$

In terms of these variables, the sound wave equation reads (Ruggiero et al., 2020)

$$\partial_t\rho_a(x) + \partial_x\left(\sum_b [\sigma M v^{\rm eff}\sigma M^\dagger]_{ab}\rho_b(x)\right) \;=\; 0 \tag{3.28}$$

or equivalently

$$\partial_t\tilde{\rho}_a(x) + \partial_x(v_a^{\rm eff}\tilde{\rho}_a) + (\partial_x\theta_a)[\sigma B(v^{\rm eff} - v_a^{\rm eff}1)\tilde{\rho}]_a \;=\; 0. \tag{3.29}$$

where $B_{ab} = B_{ba} = \frac{1}{2\pi}[\Delta(.-\theta_b)]^{\rm dr}(\theta_a)$.

If we introduce the fermion and quasi-particle densities *along the contour*

$$\delta\rho(s,t) \;=\; \left|\frac{dx_t}{ds}\right|\rho_a(x_t(s),t), \qquad \delta\tilde{\rho}(s,t) \;=\; \left|\frac{dx_t}{ds}\right|\tilde{\rho}_a(x_t(s),t), \tag{3.30}$$

where the index a corresponds to the Fermi point that satisfies $\theta_a = \theta_t(s)$, then the equation for sound waves (3.29) reads

$$\partial_t\tilde{\rho}(s)|ds| + \sigma_a(\partial_x\theta_a)\sum_b B_{ab}(v_b^{\rm eff} - v_a^{\rm eff}1)\tilde{\rho}_b(s)|ds| \;=\; 0. \tag{3.31}$$

It is this equation that we use below for numerical purposes.

3.2.3 Discretization of the equation for sound waves

For numerical purposes, when one works with the discretized contour Γ_t, it is convenient to view $\rho(s)ds$ as a N-component vector with entries P_j whose $j^{\rm th}$ entry is the integrated density on the $j^{\rm th}$ segment along the contour:

$$P_j \;=\; [\rho(s)ds]_{j+\frac{1}{2}} = \int_{\min(x_j,x_{j+1})}^{\max(x_j,x_{j+1})}\rho_a(x)dx, \qquad j = 1,\ldots,N. \tag{3.32}$$

Similarly for the quasi-particle density along the contour, one defines a vector $\tilde{P}$ of 'number of quasi-particles' along each discrete interval,

$$\tilde{P}_j \;=\; [\tilde{\rho}(s)ds]_{j+\frac{1}{2}} \equiv \int_{\min(x_j,x_{j+1})}^{\max(x_j,x_{j+1})} \tilde{\rho}_a(x)dx, \qquad j=1,\ldots,N. \tag{3.33}$$

Then we may discretize the equation of sound waves (3.31) as follows,

$$\tilde{P}(t+\Delta t) \;=\; \left(1-\Delta t\sum_{j=1}^{N}\left[R'_jA_jR_j+L'_jA_jL_j\right]\right)\cdot\tilde{P}(t) \tag{3.34}$$

where the matrix A_j depends on the local Fermi sea and is defined as (we drop the index j)

$$A_{ab}=\sigma_a(\partial_x\theta_a)B_{ab}(v_b^{\rm eff}-v_a^{\rm eff}). \tag{3.35}$$

This is a $(2q_j)\times(2q_j)$ matrix where $2q_j$ is the number of Fermi points at position x_j. The matrices L_j and R_j are of size $(2q_j)\times N$, and they encode the respective weights of the N segments of the contour onto the $2q_j$ left- or right-half-segment touching x_j respectively. B is the above $2q_j\times 2q_j$ matrix. σ and $v^{\rm eff}$ are diagonal $2q_j$ matrices defined as above. L'_j and R'_j are matrices of size $N\times(2q_j)$, which map the $2q_j$ left- or right-half-segments touching x_j to the segments along the contour (the entries of these two matrices are all zero or one). As an example, consider the piece of contour in Fig. 3.3. In this example, L_j and R_j are $4\times N$ matrices with non-zero entries

$$\begin{array}{ll}[R_j]_{1,m+\frac{1}{2}}=\frac{x_R-x_j}{|x_{m+1}-x_m|} & [R_j]_{2,j+\frac{1}{2}}=\frac{x_R-x_j}{|x_{j+1}-x_j|}\\ [R_j]_{3,l+\frac{1}{2}}=\frac{x_R-x_j}{|x_{l+1}-x_l|} & [R_j]_{4,k+\frac{1}{2}}=\frac{x_R-x_j}{|x_{k+1}-x_k|},\end{array} \tag{3.36}$$

$$\begin{array}{ll}[L_j]_{1,m+\frac{1}{2}}=\frac{x_j-x_L}{|x_{m+1}-x_m|} & [L_j]_{2,j+\frac{1}{2}}=\frac{x_j-x_L}{|x_{j+1}-x_j|}\\ [L_j]_{3,l+\frac{1}{2}}=\frac{x_j-x_L}{|x_{l+1}-x_l|} & [L_j]_{4,k+\frac{1}{2}}=\frac{x_j-x_L}{|x_{k+1}-x_k|},\end{array} \tag{3.37}$$

while L'_j and R'_j are $N\times 4$ matrices with non-zero entries

$$\begin{array}{ll}[R'_j]_{m+\frac{1}{2},1}=1 & [R'_j]_{j+\frac{1}{2},2}=1\\ \left[R'_j\right]_{l+\frac{1}{2},3}=1 & \left[R'_j\right]_{k+\frac{1}{2},4}=1,\end{array} \tag{3.38}$$

$$\begin{array}{ll}[L'_j]_{m+\frac{1}{2},1}=1 & [L'_j]_{j+\frac{1}{2},2}=1\\ \left[L'_j\right]_{l+\frac{1}{2},3}=1 & \left[L'_j\right]_{k+\frac{1}{2},4}=1.\end{array} \tag{3.39}$$

Notice that the matrices L_j, L'_j, R_j, R'_j are such that

$$\sum_{j=1}^{N}\left(R'_jR_j+L'_jL_j\right)\;=\;1. \tag{3.40}$$

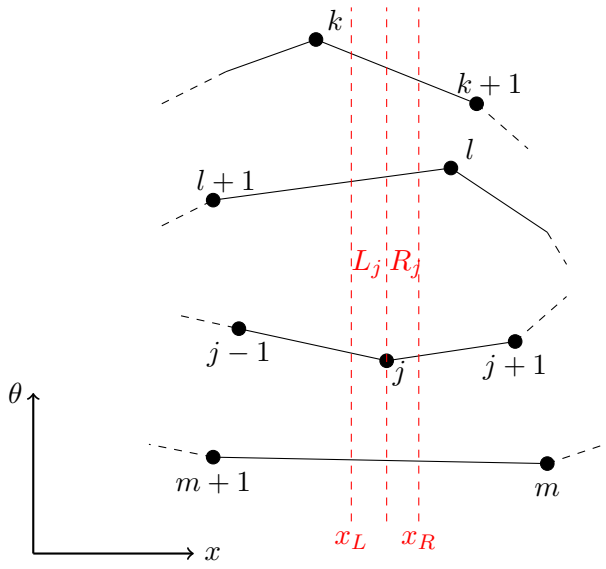

Figure 3.3: Example, to illustrate the definition of matrix L_j, L'_j and R_j, R'_j. On this example there are $2p_j = 4$ Fermi points around point j. Here $x_L = \frac{x_j+x_k}{2}$ and $x_R = \frac{x_j+x_l}{2}$.

3.3 'Quantum' GHD: some results

Now, we put together the ideas of Section 3.1 and of Section 3.2:

- we are interested in zero-point fluctuations in a fluid at zero temperature, modeled by an effective field theory that is quadratic (see Eq. (3.8))
- these quantum fluctuations are propagated in time as linear sound waves that travel on top of a 'hydrodynamic background' that is a solution of the zero-entropy GHD equation (3.20).

This results in a framework, dubbed 'quantum GHD' in (Ruggiero et al., 2020), which is a time-dependent, spatially inhomogeneous, multi-component Luttinger liquid. It provides a practical way of computing large-scale correlation functions of observables, which extends standard Luttinger liquid theory to truly out-of-equilibrium situations.

This procedure results in a time-dependent, spatially inhomogeneous, multi-component Luttinger liquid. In the initial state, assumed to be the ground state of the gas in a potential $V(x)$, the low-energy quantum fluctuations are those of an inhomogeneous Luttinger liquid, see e.g.(Cazalilla, 2004; Dubail et al., 2017; Brun and Dubail, 2018; Bastianello, Dubail and Stéphan, 2020), which are then propagated in time by solving numerically the equation for sound waves.

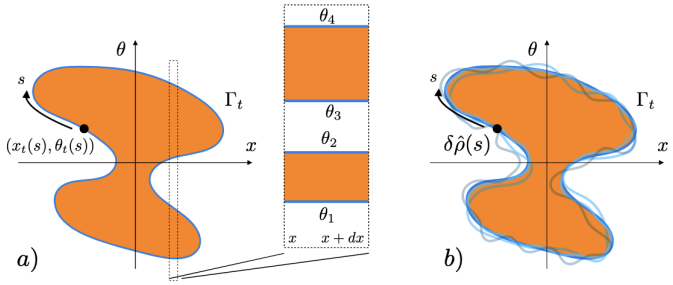

Figure 3.4: *[From (Ruggiero et al., 2020)]* The idea is to take a quantum fluid described by zero-entropy GHD, and to allow the contour Γ_t (in blue) to have zero-point fluctuations at time $t = 0$. These quantum fluctuations are then propagated in time as linear sound wave equation on top of the classical background (orange).

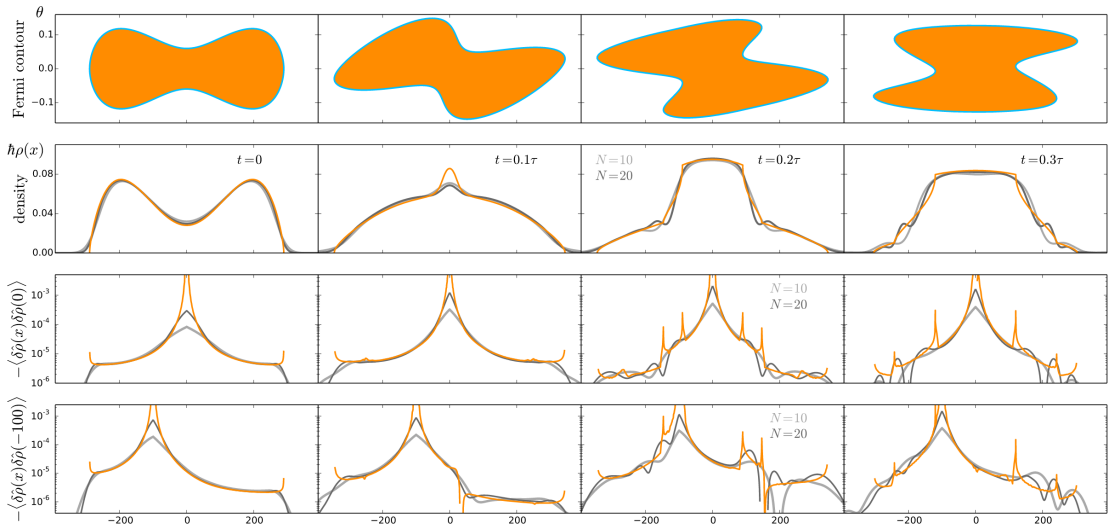

Figure 3.5: [From (Ruggiero et al., 2020)] Quench from a double-well to harmonic potential (with period τ) in a 1D Bose gas at zero temperature and $\gamma \simeq 1$. Top row: evolution of the contour Γ_t according to the zero-entropy GHD equation (3.20). Second row: the corresponding density profiles $n(x, t)$ (orange), compared to t-DMRG results for $N = 10$ and $N = 20$ particles. Third and fourth rows: the equal-time density-density correlation function $\langle\delta n(x_1)\delta n(x_2)\rangle_{\text{conn.}}$ obtained by quantizing the sound waves around zero-entropy GHD.

Fig. 3.5 shows the density-density correlation obtained in this way for the 1D Bose gas at zero temperature, quenched from a double-well to a harmonic potential. The results are in good agreement with DMRG simulations of the gas with small number of particles ($N = 10$ and $N = 20$). So far, apart from the first paper (Ruggiero et al., 2020), not many works have investigated 'quantum GHD' for the interacting 1D Bose gas. This is mainly due to the fact that the numerical implementation is cumbersome. But I plan to do much more on this in the near future, see Section 6.1.

The theory becomes much simpler in the hard-core limit $\gamma \to \infty$, because in that case the small displacements of the Fermi contour at the different Fermi points decouple. Consequently, the equation for sound waves (3.31) simply boils down to

$$(\text{hard} - \text{core limit}) \qquad \partial_t \delta\rho(s) \;=\; 0. \tag{3.41}$$

In other words, any small deformation of the contour simply moves like a single pointlike particle in the potential $V(x)$, regardless of the rest of the system. Since, in that limit, no numerical solution of the sound wave equation is needed, it is much simpler to do calculations, and there exist more works focusing on that particular limit. The results include for instance the calculation of the entanglement entropy after a quench from double-well to harmonic potential, or exact density-density correlations in that case, see Fig. 3.6. Analogous results have also been obtained recently in the XXZ spin chain in various settings, see e.g. (Collura et al., 2020; Scopa et al., 2020, 2021, 2022; Ares et al., 2022) and (Alba et al., 2021) for a recent review.

Finally, let us conclude this Chapter with a comment about the terminology 'quantum GHD'. As explained in this Chapter, this terminology comes from the analogy with the standard Euler fluid. By quantizing the standard Euler fluid, one arrives at Luttinger liquid, which is the universal 'quantum hydrodynamics' of 1D quantum fluids. Analogously, looking at a 'quantum' version of GHD that includes quantum fluctuations and their propagation at the linear level, leads to 'quantum GHD', as outlined in this Chapter.

However, there is, in principle, another approach to quantum fluctuations in GHD (Fagotti, 2017, 2020), which consists in viewing the GHD equation (1.55) as the zeroth order in the evolution equation for the Wigner quasiprobability distribution (Moyal, 1949; Bettelheim et al., 2006; Bettelheim and Wiegmann, 2011; Bettelheim and Glazman, 2012; Protopopov et al., 2013; Doyon et al., 2017; Dean et al., 2018; Ruggiero et al., 2019; Dean et al., 2019; Fagotti, 2020). The evolution equation of the Wigner function may be expanded in powers of $\hbar$ (Moyal, 1949), with higher order terms that give the corrections to the Euler-scale GHD equation. In this approach, it is not only the quantum fluctuations at time zero that are propagated in time as above. Corrections also appear dynamically because of the modified evolution equation. So far, this approach has been limited to the hard-core limit $g \to +\infty$, or more generally to spin chains that map to non-interacting

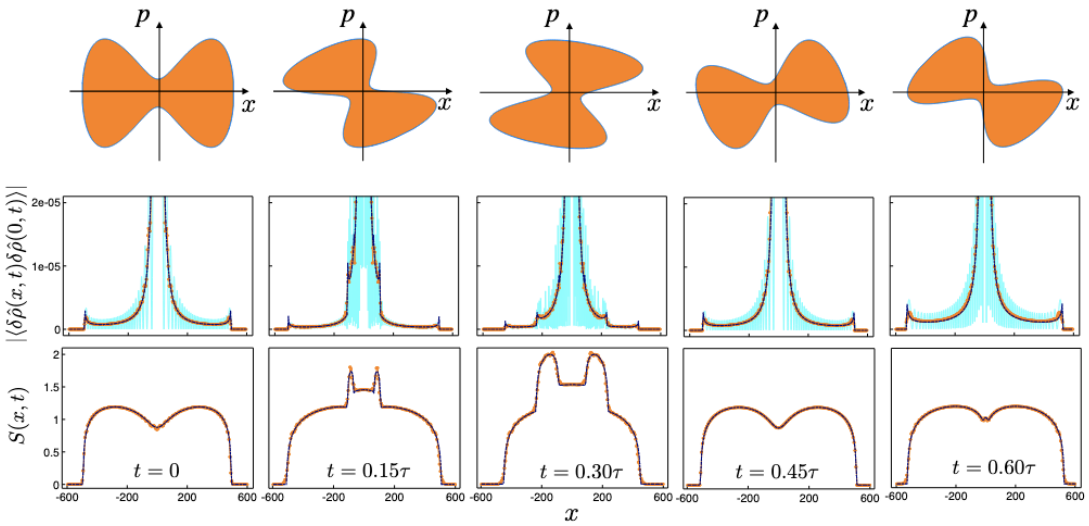

Figure 3.6: *[From (Ruggiero et al., 2021)]* Quench from a double-well to harmonic potential (with period τ) in a 1D hard-core gas at zero temperature ($\gamma \to \infty$). First row: Fermi contour. Second row: absolute value of the connected density-density correlator. Last row: Entanglement entropy. Each row shows the corresponding quantity as a function of the spatial coordinate x, at different times, expressed as a fraction of the period τ (from $t = 0$ in the first column to $t = 0.6\tau$ in the last). Orange symbols are the numerical data (obtained from a lattice model in the dilute limit), whereas dashed blue lines are the 'quantum GHD' predictions. The numerics for the density-density correlator shows large Friedel-type oscillations (cyan continuous line), therefore the analytic prediction is compared with its spatial averaging.

fermions. To our knowledge, the extension of this approach to the interacting case is an open problem. We refer to the aforementioned review (Alba et al., 2021) for a thorough discussion of this topic.

Part II

Other selected results in low-dimensional quantum many-body physics

Chapter 4

Results on Operator Entanglement

Since the early 2000s, quantum many-body theorists have learned a great deal by studying their systems through the prism of quantum entanglement. The entanglement entropy and other quantities coming from quantum information theory (e.g. the mutual information, the negativity, etc.) have become standard diagnostic tools in quantum many-body physics.

For instance, one celebrated fundamental result about the bipartite entanglement entropy is that the ground state of a local, gapped, Hamiltonian satisfies an *area law* (Eisert et al., 2010): for a spatial bipartition of the local degrees of freedom into two parts A and B, the entanglement entropy scales linearly with the length of the boundary of A, as opposed to the volume of A. In 1D, this means that the entanglement entropy is bounded (Hastings, 2007), and in that case it is well established that the boundedness of the entanglement entropy has very important practical consequences. Indeed, the state can be approximated by Matrix Product States (MPS) (Schuch et al., 2008), a class of variational wavefunctions that underly many modern numerical methods for quantum many-body systems Cirac et al. (2021), especially the Density Matrix Renormalization Group (White, 1992; Östlund and Rommer, 1995; Schollwöck, 2005). In contrast, quantum states of 1D systems that possess a large entanglement entropy cannot be well approximated by MPS, and this usually means that there is no known efficient method to represent them on a classical computer. In that sense, the entanglement entropy is a crucial diagnostic tool for computational complexity of quantum states.

Nowadays, there is growing interest in characterizing the complexity of quantum operators, as opposed to quantum states. Just like it is important to know whether a quantum state can be approximated by an MPS (or by a Tensor Network or Projected Entangled Paired State in dimension $D > 1$), it is important to know whether a quantum operator can be approximated by a Matrix Product Operator (MPO). Natural basic questions include, for instance,

1. can the thermal density matrix $\rho = e^{-\beta H}$ of a local 1D Hamiltonian H be approxi-

mated by an MPO?

2. can the evolution operator $U(t) = e^{-iHt}$ be approximated by an MPO?

3. can a local operator evolved in Heisenberg picture, $O(t) = e^{iHt}Oe^{-iHt}$, be approximated by an MPO?

4. after a quantum quench from a shortly-correlated state, can the time-evolved density matrix of a system —or of a subsystem— be approximated by an MPO?

5. and so on.

Contrary to the question of the approximability of pure quantum states in 1D in terms of MPS, where it is well established that the Renyi entanglement entropies are the right quantitifier of approximability —see e.g. (Schuch et al., 2008) for a detailed discussion—, there is not yet a widely accepted quantifier of the approximability of quantum operators in terms of MPO.

In the case when the operator is a density matrix, quantifiers of its 'complexity' used in the literature include the mutual information (Scalet et al., 2021; Kuwahara et al., 2020; Scalet et al., 2021), the negativity (Vidal and Werner, 2002), or the entropy of purification (Nguyen et al., 2018; Jarkovskỳ et al., 2020). However, it is only for the latter quantifier that there is a theorem saying that, if the quantifier is bounded then the density matrix can be approximated by an MPO (Jarkovskỳ et al., 2020).

One reason why the situation is more cumbersome for quantum operators than it is for quantum states is that there are different ways to measure the 'distance' between a quantum operator O and its approximation O_{approx}. If O is a density matrix, then one wants the distance to be measured with respect to the 1-norm, $\|O - O_{\text{approx}}\|_1$ (where $\|A\|_1 = \sum_j |\lambda_j|$ if the λ_j's are the eigenvalues of A), while if O is an observable then the distance should rather be taken with respect to the operator norm $\|O - O_{\text{approx}}\|_\infty$ (where $\|A\|_\infty = \max_j |\lambda_j|$). Therefore, quantifying the 'approximability' of operators really depends on the type of operator one is considering, so the problem is, in general, more subtle than it is for quantum states.

Notwithstanding these subtleties, there is one simple route to quantifying the 'complexity' of an operator O acting on a Hilbert space $\mathcal{H}$, which consists in vectorizing it, $O \in \text{End}(\mathcal{H}) \to |O\rangle \in \mathcal{H} \otimes \mathcal{H}$, and in treating the vectorized operator $|O\rangle$ as a pure quantum state that lives in the 'doubled' Hilbert space $\mathcal{H} \otimes \mathcal{H}$. Then one can ask: Is the pure state $|O\rangle$ approximable by an MPS? To answer that question, one must study the entanglement entropy of the state $|O\rangle$, and if it is found that it satisfies an area law, then the state $|O\rangle$ will be approximable by an MPS, which is equivalent to saying that the operator O is approximable by an MPO (see Fig. 4.1). Notice that, in doing so, one is automatically referring to 'approximability' with respect to the 2-norm $\|O - O_{\text{approx}}\|_2$ (where $\|A\|_2 = \text{tr}[A^\dagger A]$), simply because it is coming from the inner product of states in

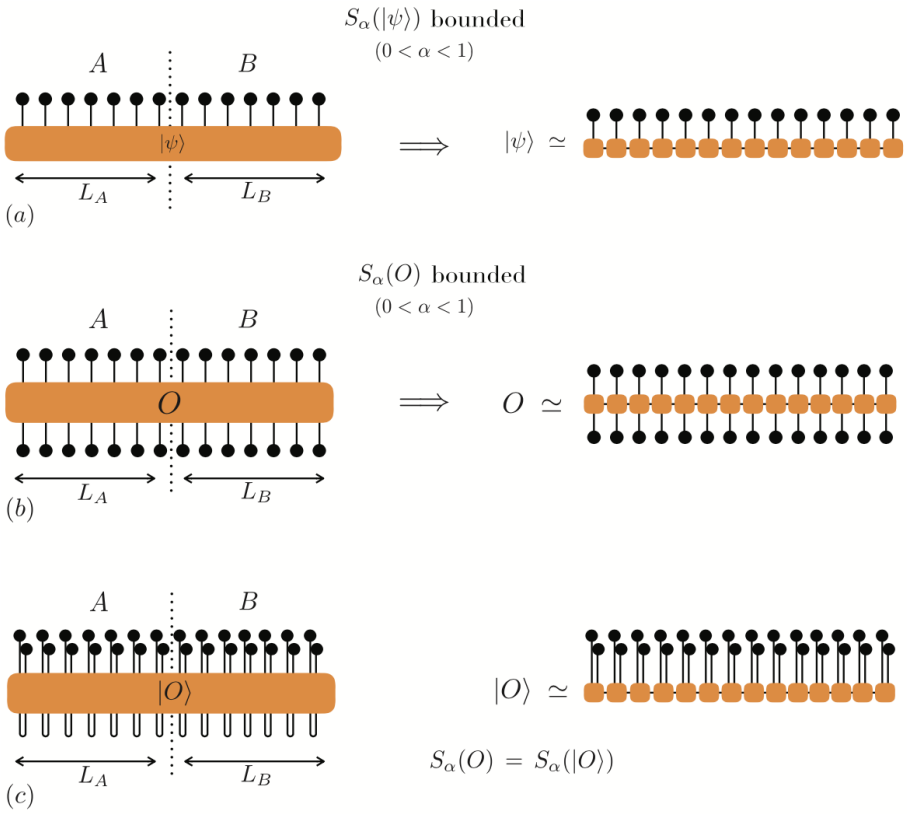

Figure 4.1: *[From (Dubail, 2017)]* Cartoon of the area law/operator area law in 1D and approximability by MPS/MPOs: (a) the states whose entanglement entropy remains bounded when $L_A, L_B \to \infty$ can be well approximated by MPSs with small (finite) bond dimension (b) the operators whose Operator Entanglement remains bounded can be well approximated (in Hilbert Schmidt norm) by MPOs with small (finite) bond dimension. (c) Of course, by viewing $O \in \mathrm{End}(\mathcal{H})$ as a state $|O\rangle \in \mathcal{H} \otimes \mathcal{H}$, the two things are exactly the same. This 'operator-folding' trick is helpful as it allows to use results that are well-established about the entanglement entropy to make analogous claims about the OE; it is also useful numerically, to turn MPS-algorithms into MPO-algorithms and vice versa.

$\mathcal{H} \otimes \mathcal{H}$, $\|O - O_{\text{approx}}\|_2 = \sqrt{\langle O - O_{\text{approx}} | O - O_{\text{approx}} \rangle}$. This is an important point to keep in mind, as the norms $\|O - O_{\text{approx}}\|_1$, $\|O - O_{\text{approx}}\|_2$, and $\|O - O_{\text{approx}}\|_\infty$ are not equivalent in the thermodynamic limit.

That said, this approach to the 'approximability' of operators naturally leads us to the definition of the *Operator Entanglement (OE)*, which mimics the definition of the usual entanglement entropy for pure states. For a bipartition $\mathcal{H} = \mathcal{H}_A \otimes \mathcal{H}_B$, we introduce the 'operator Schmidt decomposition'

$$\frac{O}{\sqrt{\text{tr} O^\dagger O}} = \sum_j \lambda_j O_j^A \otimes O_j^B \tag{4.1}$$

where the O_j^A's and O_j^B's are operators acting on $\mathcal{H}_A$ or $\mathcal{H}_B$ respectively, that are orthogonal (that is, $\text{tr}[O_i^A O_j^A] = \delta_{i,j}$). The coefficients λ_j's are real and positive without loss of generality, and, because of the normalization of the left hand sides, we have $\sum_j \lambda_j^2 = 1$. Then we define the *Operator Entanglement (OE)* of O as

$$S_\alpha(O) := \frac{1}{1-\alpha} \sum_j \lambda_j^{2\alpha}, \tag{4.2}$$

for any Renyi index $\alpha > 0$. The limit $\alpha \to 1$ works as usual, $S_1(O) = -\sum_j \lambda_j^2 \log \lambda_j^2$. Let us pause and stress some nice features of that definition:

- the OE is a quantity that is defined for any operator O, not just for density matrix —as opposed to, say, the negativity—,
- the definition of the OE allows to compute it in a large variety of situations —as opposed to the definition of the entanglement of purification, which requires to solve a hard minimization problem—,
- because of its relation to the standard entanglement entropy, its implications for the approximability of O by MPOs is clear (provided one is happy with 'approximability' with respect to the 2-norm).

The OE was introduced and studied in a few papers in the 2000s (Zanardi et al., 2000; Zanardi, 2001; Prosen and Pižorn, 2007; Pižorn and Prosen, n.d.; Muth et al., 2011), and it has become more and more popular in the past few years. In (Dubail, 2017), I showed that standard twist fields techniques of CFT (Calabrese and Cardy, 2004; Cardy et al., 2008) could be used to compute the OE in 1D quantum critical systems, and I obtained a few basic results on that quantity. The simplest result is about the thermal density matrix

$$\rho_\beta \propto e^{-\beta H} \tag{4.3}$$

of a 1D quantum critical Hamiltonian H whose low-energy spectrum is described by a 1+1D CFT with central charge c. Then, when the system lives on an infinite line, and for

the bipartition $A = (-\infty, 0)$, $B = [0, +\infty)$, the OE of ρ_β has the universal behavior at low temperature

$$S_1(\rho_\beta) \underset{\beta\to\infty}{\simeq} \frac{2c}{3} \log \beta. \tag{4.4}$$

In particular, at finite temperature the OE is finite even though both subsystems A and B are semi-infinite, so the thermal density matrix satisfies an *'operator area law'*. This is of course is stark contrast with the standard entanglement entropy of a thermal density matrix, which satisfies a volume law and is, up to subleading corrections, equal to the thermodynamic entropy of the system.

Another basic result from (Dubail, 2017) is about the 'entangled barrier', discussed in more detail in the next section.

4.1 The entanglement barrier

It is very well established that, after a quantum quench from a shortly correlated state $|\psi_0\rangle$, the entanglement entropy of a subsystem grows linearly —at times not too large compared to the subsytem size— (Calabrese and Cardy, 2005). This implies an exponential blow-up of the complexity (more precisely, of the bond dimension of the MPS in 1D) of a simulation of such a protocol on a classical computer as time increases (Schuch et al., 2008). On the other hand, this exponential growth of complexity with time is seemingly at odds with the intuition that the system should relax to a statistical ensemble with little or no entanglement.

The solution of such conundrum is simply that the relaxation is local (Barthel and Schollwöck, 2008; Cramer et al., 2008; Calabrese et al., 2011) so that we only have to describe the reduced density matrix ρ of a subsystem and not the entire pure state with physically irrelevant correlations. This motivates the introduction of the following tripartition $A_1 \cup A_2 \cup B$ for a 1D system on an infinite line, see the upper inset in Fig. 4.2:

$$B = (-\infty, 0) \cup (L_A, +\infty), \qquad A_1 = [0, x), \qquad B = [x, L_A). \tag{4.5}$$

The idea is the following: we focus on the finite subsytem $A = A_1 \cup A_2$, with the reduced density matrix

$$\rho_A(t) = \mathrm{tr}_B[e^{iHt} |\psi_0\rangle \langle\psi_0| e^{-iHt}]. \tag{4.6}$$

Initially, it is clear that the reduced density matrix can be well approximated by a MPO, because the initial state $|\psi_0\rangle$ can be approximated by an MPS. At late times, since $\rho_A(t)$ is expected to go to a simple statistical ensemble (a simple thermal state if the system is chaotic, or a Generalized Gibbs Ensemble if the system is integrable), it can also be approximated by an MPO with small bond dimension. The question is then: Can the reduced density matrix $\rho_A(t)$ be approximated by an MPO at intermediate times? To answer that question, it is natural to cut the subsystem A into two intervals A_1 and A_2, and to study the OE of $\rho_A(t)$ for the bipartition $\mathcal{H}_{A_1} \otimes \mathcal{H}_{A_2}$.

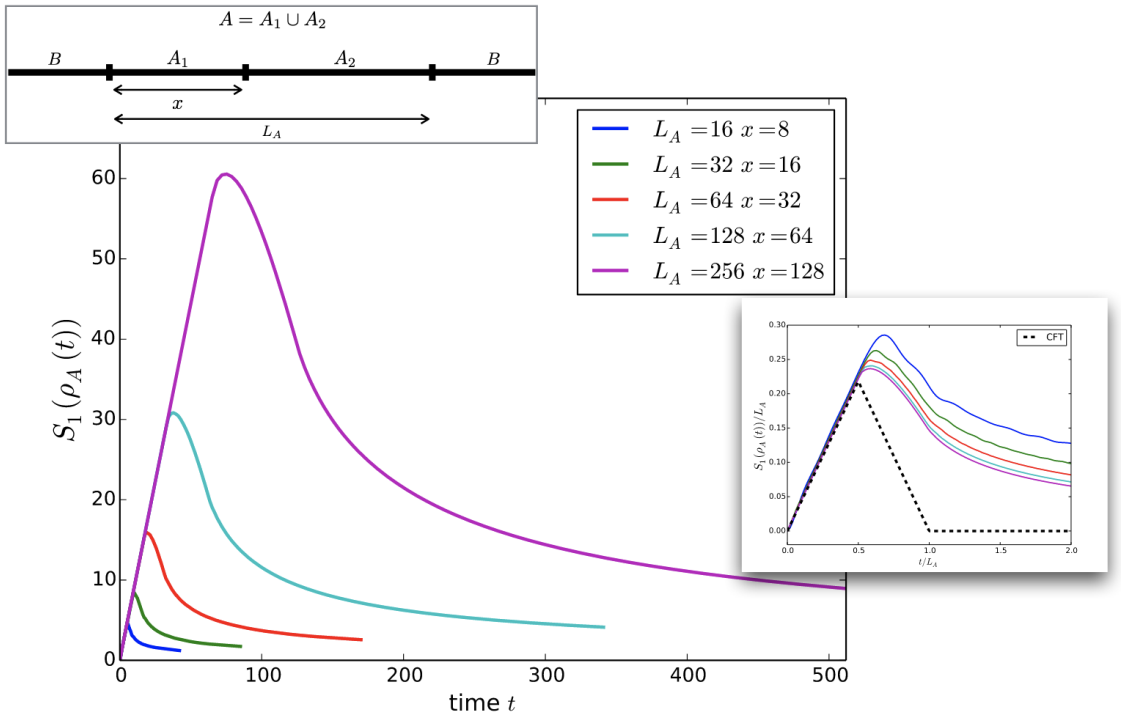

Figure 4.2: *[From (Dubail, 2017)]* OE of the reduced density matrix $\rho_A(t)$, for a bipartition $A = A_1 \cup A_2$, where A_1 and A_2 are of lengths x and $L_A - x$ respectively (here with $x = L_A/2$). The numerical results are obtained for a quench in the XX chain from the Néel state (the calculation is performed in a finite periodic chain of total size $8 \times L_A$; at larger times the system exhibits revivals that are not shown here). The inset shows the rescaled OE, compared to the result of the CFT calculation. The deviations from the CFT result are quite large (due to dispersion effects absent from the CFT description), however the blow-up of the OE, which is the main message of this section, is well captured by the CFT calculation.

The typical result is shown in Fig. 4.2: at intermediate times, the OE exhibits an *entanglement barrier*. The OE of the reduced density matrix initially grows linearly and then decays at longer times, thus displaying a barrier-shaped curve. The initial linear growth is a consequence of the generic linear growth of the (state) entanglement entropy after a quench, while the decay at later times reflects the convergence of the reduced density matrix towards a simple stationary state through the mechanism of thermalization.

In Dubail (2017), I found this entanglement barrier from a CFT calculation, but the result is very general and extends to systems that are not described by CFT. In particular, this entanglement barrier has also been studied in detail in chaotic quantum systems by Wang and Zhou (2019) and Reid and Bertini (2021). The main difference between integrable systems whose dynamics is described by quasi-particles and chaotic ones is that, for $x = L_A/2$ (i.e. for equal-length subsystems A_1 and A_2), the OE has a 'pyramid'-shape for quasi-particle dynamics (as in Fig. 4.2), while it has 'truncated-pyramid'-shape, with a central plateau, for chaotic dynamics. Thus, very interestingly, the shape of the entanglement barrier reflects the underlying dynamics of the quantum system. For more details on this, see (Wang and Zhou, 2019; Reid and Bertini, 2021).

In work currently in preparation with the teams of Pasquale Calabrese in Trieste and of Benoit Vermersch in Grenoble, we are even able to observe the entanglement barrier experimentally for a quench in a trapped ion chain, by performing a new data analysis of the published data of (Brydges et al., 2019).

4.2 Growth of Operator Entanglement of local operators evolving in Heisenberg picture

Another natural question that comes up when one thinks about the OE and the problem of approximability of operators by MPOs is the one of local operators that evolve in Heisenberg picture. Consider an infinite spin chain, and an operator O that is strictly local, in the sense that it acts on a finite number of nearby lattice sites only. Such an operator is obviously an exact MPO with small bond dimension; that bond dimension depends on how many lattice sites are acted upon by O.

It is natural to ask: Can the time-evolved operator

$$O(t) = e^{iHt} O e^{-iHt} \tag{4.7}$$

also be approximated by an MPO with small bond dimension? Or would the bond-dimension blow up? That question is of course very important for numerical purposes. If the bond dimension remained small at all times, then it would be numerically efficient to do 'Heisenberg-picture Density Matrix Renormalization Group' (Hartmann et al., 2009; Muth et al., 2011) to simulate quantum quench dynamics. Indeed, by approximating the shortly-correlated initial state $|\psi_0\rangle$ by an MPS, and the Heisenberg-picture operator $O(t)$

by an MPO, both with small bond dimension, one would be able to efficiently study the relaxation dynamics of the observable $\langle\psi_0|\, O(t)\, |\psi_0\rangle$.

This motivates the question: How does the OE of a Heisenberg picture operator, $S_\alpha(O(t))$, behave as a function of t?

It turns out that the answer depends on whether the underlying dynamics is integrable or chaotic, as pointed out in early numerical studies by Prosen and Žnidarič (2007) and Muth et al. (2011). Numerical simulations for this problem are difficult though, and they are restricted to short times, and it is important to develop an analytical understanding of this phenomenon. The current understanding is as follows. Jonay et al. (2018) used a coarse-grained 'membrane picture' of entanglement growth to argue that, under chaotic dynamics, the OE grows linearly in time,

$$\text{(chaotic dynamics)} \qquad S_1(O(t)) \underset{t\to\infty}{\simeq} \alpha\, t \tag{4.8}$$

with some growth rate α (see also (Kudler-Flam et al., 2021) for related work). This conjectured linear growth for chaotic dynamics is consistent with closely related results obtained in holographic CFTs —which have a large central charge, and exhibit chaotic dynamics— (Caputa et al., 2015), and it is also verified by chaotic dual-unitary circuits (Bertini et al., 2020*a*).

On the other hand, for integrable dynamics, numerical results are compatible with a sublinear growth (Prosen and Žnidarič, 2007; Muth et al., 2011; Dubail, 2017; Alba et al., 2019), probably logarithmic,

$$\text{(integrable dynamics)} \qquad S_1(O(t)) \underset{t\to\infty}{\simeq} \gamma\, \log t. \tag{4.9}$$

The prefactor γ is known for free fermion models (for instance, $\gamma = 1/3$ for the operator σ^+ in the XX chain), and it has recently been conjectured by Alba (2021) to be equal to $1/2$ in several models including the XXZ spin chain, see that reference for details. The conjectured logarithmic growth is supported by a handful of analytical results:

- (Pižorn and Prosen, n.d.) conjectured the logarithmic growth in free fermion chains, and I provided a proof in (Dubail, 2017) which uses a mapping to a domain-wall melting problem, as well as 'inhomogeneous CFT' techniques introduced in (Dubail et al., 2017),
- a proof in the 'Rule 54 qubit chain' (Alba et al., 2019) —see (Buča et al., 2021) for a review of the Rule 54 chain, an important cellular automaton model of classical and quantum dynamics—, obtained by an explicit construction of $O(t)$ in the form of an MPO with bond dimension growing as $\sim t^2$ for all possible single-site operators O. See Fig. 4.3 for an illustration, and also (Gopalakrishnan et al., 2018; Medenjak, 2022) for related results on operator spreading in cellular automata,

- exact results in dual unitary circuits supporting soliton dynamics (Bertini et al., 2020*b*).

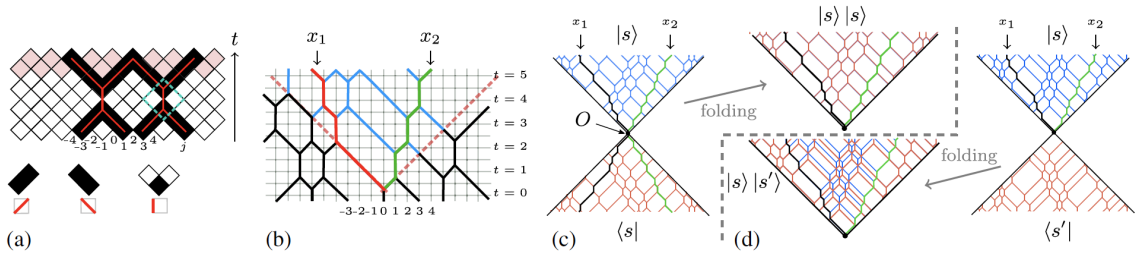

Figure 4.3: *[From (Alba et al., 2019).]* Operator spreading in the Rule 54 chain. (a) Dynamics in the Rule 54 qubit chain, here drawn as a staggered lattice: qubits in the state 1 (0) are drawn as black (white) squares. Red lines superimposed on the black squares show the left and right moving solitons. The dashed box highlights a scattering event, where two solitons get time delayed. The mapping from qubits to solitons is illustrated at the bottom: left and right moving solitons correspond to nearest-neighbor black sites, while a scattering pair corresponds to a single black site surrounded by two white ones. (b) Spacetime picture of a typical evolution. (c) Spreading of a diagonal operator $O = \cdots \otimes \mathrm{I}_2 \otimes \cdots \otimes \mathrm{I}_2 \otimes |010\rangle\langle 010| \otimes \mathrm{I}_2 \otimes \cdots \otimes \mathrm{I}_2 \otimes \ldots$. The forward and backward light cones are present. After folding one is back to the situation (c). The MPO construction of $O(t)$ is based on the fact that a simple algorithm is able to tell whether a soliton configuration contributes or not to $O(t)$. (d) Case of the spreading of the off-diagonal operator $O = \cdots \otimes \mathrm{I}_2 \otimes \cdots \otimes \mathrm{I}_2 \otimes |010\rangle\langle 000| \otimes \mathrm{I}_2 \otimes \cdots \otimes \mathrm{I}_2 \otimes \ldots$. Folding the forward and backward light cones, one sees that they can be related by a simple transformation; this is a key observation of (Alba et al., 2019), which allows to construct MPOs for non-diagonal operators in a similar way as for diagonal ones.

In my opinion, the fact that the OE of local operators in Heisenberg picture clearly distinguishes chaotic from integrable dynamics is important for at least two reasons.

First, it provides a sharp diagnostic tool, at least in principle —that is, provided one is able to compute the OE for large systems at sufficiently long times—. This is important because other quantities that have been proposed as diagnostic tools for quantum chaotic dynamics, such as OTOCs (Out-of-Time-Ordered Correlators) (Larkin and Ovchinnikov, 1969; Maldacena et al., 2016), are usually plagued by the fact that they are inspired from semiclassical considerations. In particular, OTOCs cannot really diverge in locally interacting quantum systems with a finite local Hilbert space dimension, at least not at the level of local operators (Kukuljan et al., 2017; von Keyserlingk et al., 2018), and many features of OTOCs that are supposed to be characteristics of chaotic dynamics are actually found also in integrable systems (see e.g. (Gopalakrishnan et al., 2018; Medenjak, 2022) for more details). The OE does not suffer from such problems, as it does not rely on any

notion of a semiclassical limit. So it is, in my opinion, a better quantifier, more meaningful than OTOCs.

Second, the fact that the OE grows only logarithmically for integrable dynamics implies that, in principle, numerical methods such as Heisenberg-picture DMRG could actually be efficient if one restricts to systems with integrable or nearly integrable dynamics. More generally, this suggests that the computational complexity of the simulation of quantum dynamics on classical computers is fundamentally different depending on whether the dynamics is integrable or chaotic, as already pointed out by Prosen and Žnidarič (2007). So it might be vain to search for general numerical methods —e.g. Tensor Network methods— capable of simulating all kinds of quantum dynamics, and it is probably more promising to try to develop methods specific to integrable (or nearly integrable) dynamics.

4.3 Operator Entanglement of a density matrix under dissipative evolution

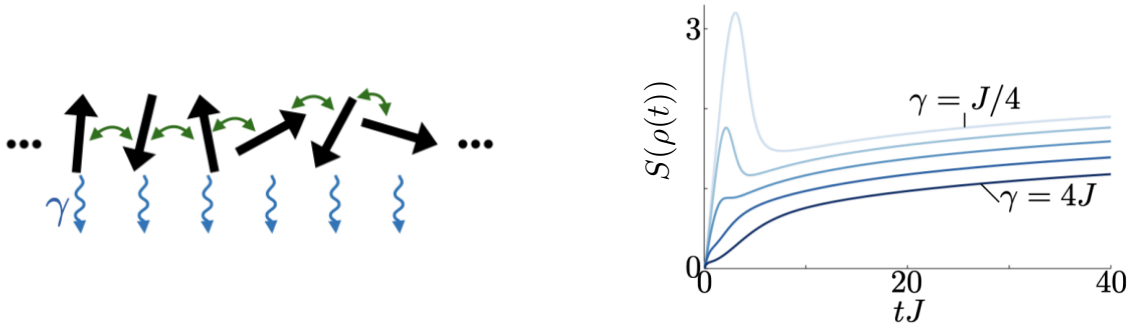

Figure 4.4: *[From (Wellnitz et al., 2022).]* (Left) Cartoon of a spin chain with nearest-neighbor coupling J and on-site dephasing γ. (Right) Operator Entanglement of the density matrix $\rho(t)$ in the XXZ chain after a quantum quench from a product state, as a function of time. The OE initially rises (a linear growth reminiscent of the one of pure state entanglement entropy after a quench), then decreases as dephasing destroys entanglement. The surprising phenomenon found in (Wellnitz et al., 2022) is that the OE rises again at long times. That 'rise again' is much slower though, and the OE goes as $S(\rho(t)) \simeq \frac{1}{4}\log t$ at long times, regardless of the ratio γ/J.

Yet another natural problem that arises when one thinks about MPO approximations of density matrices is the influence of dissipation. Consider an infinite quantum spin chain undergoing dissipative evolution, modeled by the Lindblad equation

$$\frac{d}{dt}\rho \;=\; -i[H,\rho] + \sum_a \left(L_a \rho L_a^\dagger - \frac{1}{2}\{L_a^\dagger L_a, \rho\ \}, \right) \tag{4.10}$$

for a Hamiltonian H and some set of dissipators $\{ L_a \}_{a\in\mathbb{Z}}$. Here we are interested in dissipators L_a that are local, and act homogeneously on all the sites, corresponding for instance to such physical processes as losses or gain, incoherent hopping, or dephasing, see Fig. 4.4.

Let us assume that the spins are initially in a shortly-correlated state $|\psi_0\rangle$, for instance a product state. We know that, in the absence of dissipation, the entanglement entropy of the state $e^{-iHt}|\psi_0\rangle$ between two half-systems $A = (-\infty, 0)$ and $B = [0, +\infty]$ would increase linearly. Consequently, in the absence of dissipation, the OE of $\rho(t) = e^{-iHt}|\psi_0\rangle\langle\psi_0|e^{iHt}$ would also grow linearly in time, as the OE would simply be exactly twice the entanglement entropy.

What happens in the presence of dissipation?

Clearly, dissipative processes are supposed to destroy entanglement in the system, and are expected to bring the density matrix to a simple stationary state at long times, for instance the infinite temperature state, which has vanishing OE. Therefore, the expected scenario in the presence of dissipation is that of an 'entanglement barrier': the OE should increase at short times because of the coherent part of the dynamics, then reach some maximum, and then decrease to some small stationary value because of dissipation. This scenario has been discussed for instance in (Noh et al., 2020) for quantum circuits with dissipation, in relation with the claims of quantum supremacy by Google (Arute et al., 2019) (the argument of Noh et al. (2020) is that, since the OE decreases after many quantum gates have been applied —which corresponds to long time here—, simulating the successive applications of many quantum gates on a classical computer is actually much easier than it seems, provided there is a little bit of dissipation in the experiment).

In (Wellnitz et al., 2022), however, we observed that in spin chains with a U(1) conservation law (conserved magnetization) and under dephasing, this scenario unexpectedly breaks down. Under dephasing, after the initial 'rise and fall' the OE can rise again, increasing logarithmically at long times, see Fig. 4.4. In the XXZ chain initialized in the Néel state, we found that the OE at long time behaves as

$$S(\rho(t)) \underset{t\to\infty}{\simeq} \frac{1}{4}\log t. \tag{4.11}$$

The origin of this slow 'rise again' can be understood easily in the limit of strong dephasing. In that limit, the Lindblad dynamics (4.10) greatly simplifies, as the density matrix effectively remains diagonal in the computational basis at all times,

$$\rho(t) = \sum_\sigma p_\sigma(t)\,|\sigma\rangle\langle\sigma|\,, \tag{4.12}$$

so that one is left with the problem of computing the evolution of the classical probability distribution p_σ over classical spin configurations σ. A simple calculation in second-order

perturbation theory (see (Cai and Barthel, 2013; Bernard et al., 2018) for details) allows to derive the classical master equation satisfied by $p_\sigma(t)$, which turns out to be the one of the Symmetric Simple Exclusion Process (SSEP). Therefore, in the strong-dephasing limit, the problem of computing the OE of the density matrix $\rho(t)$ boils down to understanding correlations between half-systems $A = (-\infty, 0)$ and $B = [0, +\infty)$ in the SSEP with a initial Néel state. It turns out this is a standard problem in the literature, see e.g. (Derrida and Gerschenfeld, 2009) and references therein. The key point is that the correlations between parts A and B are dominated by the fluctuations of the particle number in either part. The difference between the number of particles in A at time t and the one in the initial Néel state typically fluctuates as $\sqrt{\Delta N_A(t)^2} \sim t^{1/4}$, and the anomalous exponent $1/4$ turns out to be directly related to the prefactor $1/4$ in Eq. 4.11.

For finite dephasing strength, no such simple argument has been uncovered yet, however numerical simulations clearly show that the OE still behaves as in Eq. (4.11), with the same prefactor $1/4$ (Fig. 4.4). It would be interesting to learn how to derive that result analytically. I think there is some hope to do that, at least in the XX chain, as the XX chain with dephasing is a model that is exactly solvable by Bethe Ansatz (Medvedyeva et al., 2016).

Chapter 5

Results on 2D chiral topological phases

'2D chiral topological phases' encompass the integer quantum Hall effect, fractional quantum Hall effects (such as the ones described by Laughlin states, hierarchical states or composite fermion constructions, Read-Rezayi states, etc.), $p_x + ip_y$ superconductors, Chern insulators, as well as some other symmetry classes of topological insulators or superconductors.

After my Phd in 2010 and until 2016, I have worked on 2D chiral topological phases from the point of view of their entanglement properties. In this chapter I briefly sketch the main results I obtained on that topic.

A 'topological phase' may be defined as follows. Let $H(\lambda)$ be the hamiltonian of a d-dimensional system in the thermodynamic limit, that depends continuously on some parameter λ (this parameter may be multi-dimensional, $\lambda = (\lambda_1, \lambda_2, \lambda_3 \dots)$). By 'hamiltonian for a d-dimensional system', I mean a hamiltonian that is a sum of *local* terms acting on a collection of degrees of freedom that live in $\mathbb{R}^d$, or on a d-dimensional lattice. If $H(\lambda)$ has an energy gap $\Delta E > 0$ above a finite set of degenerate ground states, then by continuity there exists an open neighborhood of λ in the space of parameters where the gap stays non-zero and the number of ground states is constant. One then says that the system is in a *topological phase*.

A *topological phase* may be *topologically trivial*, in the sense that it can be continuously deformed into the vacuum (or, more generally, a trivial product state) without closing the energy gap. It may also be *topologically non-trivial*. I will give an example of both situations shortly.

In 2d, there exist *topologically non-trivial phases* that possess the following property: when the system has a boundary, there are gapless excitations that are localized along the one-dimensional boundary. When these excitations propagate in one direction only,

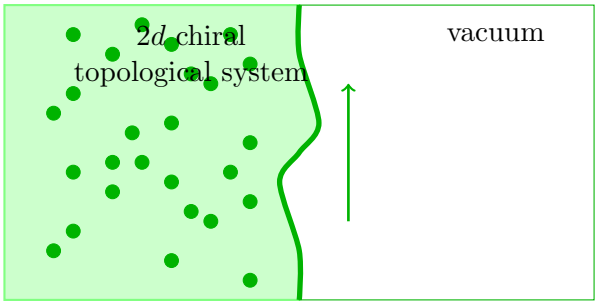

Figure 5.1: Cartoon of an interface between a 2d chiral topological phase (on the left) and the vacuum (on the right) with a small deformation of the fluid at the edge. The energy gap is finite in the bulk, but the edge excitations are gapless and they propagate in one direction only. For many chiral topological phases (including the case of $p_x + ip_y$ superconductors treated in these two lectures), the gapless edge excitations are described by a chiral $1+1d$ CFT.

one talks about a *2d chiral topological phase*. In such a system, time-reversal and parity symmetry must be broken.

5.1 Entanglement spectra and (perturbed) conformal field theory

In an extremely influential paper, Li and Haldane (2008) introduced the idea that the 'entanglement spectrum' —the logarithmic spectrum of the reduced density matrix— of a subsystem A in the bulk of a 2D chiral topological material possesses a universal part which reflects the physical spectrum of the system in the presence of a real physical edge. They stressed that the entanglement spectrum, which can be easily extracted in a numerical simulation, could be used as a 'fingerprint' of a topological phase, thereby providing a very useful new numerical diagnostic tool for the investigation of these systems.

During my postdoctoral years, I worked on these entanglement spectra together with Nick Read and Ed Rezayi. We obtained a complete analytical understanding of the 'Li-Haldane conjecture' about the correspondence between entanglement spectra and the physical edge energy spectrum, in the particular class of trial states given by 2D conformal blocks —which include fractional quantum Hall trial states like the Laughlin state (Laughlin, 1983), the Moore-Read state (Moore and Read, 1991), the Read-Rezayi states (Read and Rezayi, 1999), but also trial states for $p_x + ip_y$ superconductors (Read and Green, 2000; Dubail and Read, 2011)—.

In (Dubail et al., 2012*b*), we introduced a new type of bipartition for states of electrons in the lowest Landau level (the so-called real-space partition, introduced simultaneously by and), which emphasized the role of locality in real space (as opposed to orbital space, which

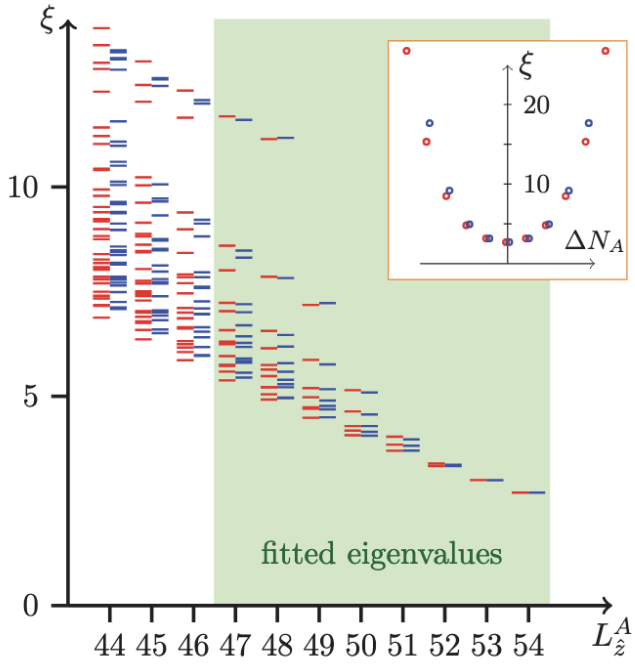

Figure 5.2: *[From (Dubail et al., 2012a)]* Real-space entanglement spectrum for a Laughlin state of $N = 12$ electrons at filling fraction $\nu = 1/3$ on a sphere. Here the subsystem A is the northern hemisphere. The spectrum in red is the exact spectrum exctracted numerically, while the blue spectrum is the spectrum of the perturbed chiral conformal field theory predicted by our theory. The theory has a few free parameters, fitted in order to minimize the total squared distance between the two spectra in the green shaded area. Both spectra are resolved with respect to momentum and to particle number $\Delta N_A = N_A - N/2$. Here we show the entanglement spectrum as a function of the momentum $L_{\hat{z}}^A$, in the charge sector $\Delta N_A = 0$. The inset shows the lowest entanglement level in other charge sectors.

is a mixture of real- and momentum-space in the lowest Landau level). This paved the way for an analytical understanding of entanglement spectra in these systems, for which we provide a full theory in (Dubail et al., 2012*a*). There, we thoroughly analyzed the structure of the vector space of edge states represented by conformal block wavefunctions, as well as the inner product between these edge states.

Conceptually, the most important result of (Dubail et al., 2012*a*) is the emergence of an isomorphism between the space of physical edge states and the Hilbert space of the chiral conformal field theory that underlies the construction of the trial wavefunction. This is a completely general result, which relies solely on the assumption that the CFT trial wavefunction possesses a finite correlation length in the bulk.

The 'Li-Haldane conjecture' is then a simple consequence of that isomorphism. Moreover, our theory shows that the entanglement spectra of trial quantum Hall states are, in general, given by the spectrum of the Hamiltonian of the chiral CFT *perturbed by irrelevant operators*. This is illustrated in Fig. 5.2, where we compare the numerically extracted entanglement spectrum for a Laughlin state to the analytical spectrum of our theory, which has a few free parameters (see (Dubail et al., 2012*a*) for more details). Such analytical understanding of the spectrum was completely new in 2012, as all previous works on entanglement spectra since (Li and Haldane, 2008) had focused on level-counting and on the combinatorics of conformal towers, as opposed to the entanglement levels themselves.

5.2 No-Go theorem for chiral tensor networks

It turns out our 2012 theory of edges states and entanglement spectra in trial states for 2D chiral topological phases (Dubail et al., 2012*a*) is extremely close to similar results previously obtained by Cirac et al. (2011) about 2D Tensor Networks —also called Projected Entangled Paired States (PEPS)—. This suggests that trial wavefunctions constructed as field theory correlators should be regarded as the continuous limit of Tensor Networks —for discussions and extensions of this idea, see e.g. (Dubail et al., 2012*a*; Jennings et al., 2015; Tilloy and Cirac, 2019)—.

This observation also suggests a possible route towards constructing a 2D Tensor Network state (or PEPS) in a chiral topological phase of matter. Indeed, one can start from a trial state for a chiral topological phase given by a correlator in a chiral CFT, and replace the continuous CFT by one of its lattice discretizations. This idea led me to the construction of chiral Tensor Networks for $p_x + ip_y$ superfluids and for Chern insulators in 2013, however these states all have power-law correlations in the bulk. (These states were later published in (Dubail and Read, 2015); similar states were independently constructed by Wahl et al. (2013).) The observation that all the states we could construct at that time unavoidably came with power-law decaying correlations suggested that truly gapped Tensor Network states (with exponentially decaying bulk correlations) in a chiral topological phase could not exist at all.

With Nick Read, we obtained the following No-Go theorem for Tensor Network states of non-interacting fermions, also called Gaussian fermionic Tensor Networks or Gaussian fermionic PEPS.

Theorem (Dubail and Read, 2015) —physics formulation—. A translation-invariant state of non-interacting fermions cannot simultaneously:

1. *be the ground state of a gapped, local, translation-invariant quadratic fermion Hamiltonian,*
2. *be expressible as a 2D Tensor Network with finite bond dimension,*
3. *be in a non-trivial chiral topological phase.*

A significant part of our work on that No-Go theorem consists in reformulating it in precise mathematical terms. It is very well known since Kitaev's work (Kitaev, 2009) that, for classification purposes, translation-invariant states of non-interacting fermions should be regarded mathematically as vector bundles over the Brillouin zone, which is the d-dimensional torus T^d for a d-dimensional physical system. Therefore, mathematically, our No-Go theorem is expressed as follows:

Theorem (Dubail and Read, 2015) —mathematical formulation—. Consider the trivial complex bundle $T^d \times \mathbb{C}^n$, and let $(k_1, k_2, \ldots, k_d) \in (\mathbb{R}/\mathbb{Z})^d$ be the coordinates on the torus. A sub-bundle of that trivial bundle cannot simultaneously:

1. *be an analytic sub-bundle (i.e. a sub-bundle whose components are all real-analytic functions of the coordinates k_a, $a = 1, \ldots, d$)*
2. *be a polynomial sub-bundle (i.e. a sub-bundle whose components are rational functions of $\sin(k_a)$ and $\cos(k_a)$, $a = 1, \ldots, d$)*
3. *have a non-zero Chern number.*

These three properties are in one-to-one correspondance with the three points above. The fact that the state is the ground state of a gapped local Hamiltonian translates into the property that the sub-bundle over the Brioullin is analytic (this essentially the statement of the Payley-Wiener theorem in Fourier analysis). The fact that the state is a Tensor Network with finite bond dimension translates into the fact that its components are expressible as polynomials (this point is non-standard and is a key result of (Dubail and Read, 2015)). Finally, 'topologically non-trivial' translates into 'non-zero Chern number' for the sub-bundle (this is a standard statement in topological band theory).

As of 2022, this No-Go theorem is still the best result available on the question of Tensor Networks for chiral topological phases. Interestingly, its mathematical proof relies on algebraic geometry methods —in particular, on the Hilbert Syzygy theorem (for details, see the published paper reproduced below)— which have so far been remained very

uncommon in theoretical condensed matter physics. Nick Read later extended our results to all symmetry classes of the Altland-Zirnbauer classification (Read, 2017).

Part III

Perspectives

In this Part, I briefly sketch my viewpoint on the future of my research field, and I present some research directions I would like to investigate next.

I believe that, to assist in the fast developments of 'programmable quantum systems', new theoretical tools for precision many-body quantum physics are needed. In the next decade, the design and analysis of the new generation of quantum experiments will rely heavily on benchmarks against theory and simulations made on classical computers. Thus, many-body quantum theorists in the emerging era of programmable quantum systems need to learn how to make precise, reliable, calculations for quantum systems made of N$\sim$100 or 1000 constituents, on currently available classical computers. Obviously this goal cannot be achieved in full generality, but I believe that it can be done for the special class of quantum many-body systems that are 'nearly integrable', meaning that their dynamics on experimental time scales is non-chaotic and is governed by a proximate integrable model. Nearly integrable systems are becoming more and more prominent on the experimental scene, and I believe they will play a key role in many-body quantum science in the next decade, as they will be used as benchmarks for quantum simulators, in addition to raising fascinating fundamental questions.

Some recent exciting questions that have emerged from the interplay between theory and experiments in nearly integrable quantum systems include, for instance, the observation of (Malvania et al., 2020) that GHD is able to reproduce the experimental data for very small atom clouds, containing as few as N=12 atoms, which is clearly at odds with the hydrodynamic approximation that treats the gas as a continuous medium. Is this a mere coincidence, or is there something fundamental, unforeseen, about the GHD framework? Other very recent experiments in spin chains (Wei et al., 2021) raise fundamental questions about charge fluctuations in the 1D Heisenberg magnet (Krajnik et al., 2021), or about new classes of peculiar spin-helix eigenstates in the anisotropic Heisenberg magnet (Jepsen et al., 2021). Theory developments have also triggered outstanding problems: Are there fundamental differences in the entanglement properties of integrable and non-integrable systems? Indeed, indicators of complexity such as the operator entanglement behave very differently (Alba et al., 2019; Bertini et al., 2020*a*,*b*) in both cases; also, the entanglement entropy of high-energy eigenstates seems to follow a different volume law Łydżba et al. (2020). The crucial question is then: Can these special entanglement properties of (nearly) integrable systems lead to their more efficient simulation with Tensor Network methods? Lastly, another exciting perspective is that the newly emerging ideas could finally help us solve fundamental problems that have remained in the theory of quantum integrable systems. For instance (see e.g. (Brandino et al., 2015; Buijsman et al., 2017; Kurlov et al., 2021)): Is there a quantum analog of the famous Kolmogorov-Arnold-Moser theorem for classical dynamical systems, that would govern how quantum integrable dynamics remains

stable to perturbations?

6.1 Momentum distribution of the 1D Bose gas from 'quantum GHD'

A first direction I would like to explore, which is strongly motivated by experiments, is the possibility to compute the momentum distribution of strongly out-of-equilibrium 1D Bose gases,

$$\langle\psi(t)|\, n(p)\, |\psi(t)\rangle = \int dx \int dy\; e^{ipy}\, \langle\psi(t)|\, \Psi^\dagger(x+y/2)\Psi(x-y/2)\, |\psi(t)\rangle \tag{6.1}$$

This is a quantity which is crucial to interpret time-of-flight measurements in experiments, and which is beyond the reach of any existing computational method (it is accessible in quantum Monte Carlo, but only at equilibrium). I believe the theory of quantum fluctuations on top of Generalized Hydrodynamics, which we have started to develop (discussed in Part I of this manuscript) should enable precise calculations if the momentum distribution out of equilibrium. It should also give us access to higher-point correlations, and therefore to higher cumulants of the momentum distribution, e.g. $\langle n(p_1)n(p_2)\rangle$, which are also accessible in atom chip experiments (Fang et al., 2016).

To further establish the relevance of this approach, I would also like to provide a 'smoking-gun' evidence that 'quantum GHD' is necessary to capture true quantum effects. I think this could be done by revisiting the Quantum Newton's Cradle setup, where two atomic clouds periodically collide inside a harmonic trap. I would like to compute the entanglement generated between the two clouds during the collisions. Such entanglement is simply absent from standard GHD, and only 'quantum GHD' should be able to capture it. Although the von Neumann entanglement entropy of one of the two clouds is not an observable that could be easily measured in an experiment, correlations between phase- and density-fluctuations in the two clouds could be measured, and on the theory side we could have access to these as well.

6.2 Weak integrability breaking

I would like to investigate aspects of the dynamics of systems that are not integrable, but whose dynamics is nevertheless governed by their proximity to an integrable model.

I think it should be possible to extend the approach I used recently together with Isabelle Bouchoule and Benjamin Doyon while working on atom losses in the 1D Bose gas Bouchoule et al. (2020); Bouchoule and Dubail (2021), and to turn it into a general method for other problems of nearly integrable dynamics. The basic idea is that when a thermodynamically large integrable system with conserved charges Q_j, $j = 1, 2, 3, \ldots$ is perturbed, its conserved charges are no longer constants of motion, however they evolve

adiabatically if the perturbation is small: the system remains in a *local quasi-stationary state* at all times, with a density matrix $\rho = \rho(\{\langle Q_i \rangle\})$ parameterized by the expectation values of the charges. This gives a closed set of evolution equations for the slow dynamics of the expectation values $\langle Q_j \rangle = \mathrm{tr}\left[Q_j\, \rho(\{\langle Q_i \rangle\}_{i=1,2,\ldots})\right]$, in the form

$$\frac{d}{dt}\langle Q_j \rangle = F_j(\{\langle Q_i \rangle\}_{i=1,2,\ldots}). \tag{6.2}$$

The functions F_j depend on the perturbation. Formal expressions are known both for dissipative perturbations (e.g. losses, dephasing) (Bouchoule et al., 2020) and Hamiltonian perturbations (Durnin et al., 2021). These formal expressions are typically given by the expectation value of the commutator of Q_j with the operator O generating the perturbation, e.g. $F_j \propto \left\langle O^\dagger [Q_j, O] \right\rangle$ (Bouchoule et al., 2020) and the main challenge here is to develop methods, either numerical or analytical, to evaluate such expectation values and to turn this approach into a useful tool to describe the dynamics of nearly integrable systems. It should be possible to implement a tree exploration of the space of eigenstates of the integrable system, based on the weight of their contribution to F_j, which will be evaluated using the machinery of Bethe Ansatz form factors (Slavnov, 1989; Kitanine et al., 1999). The idea is that only a few eigenstates with specific properties (e.g. with a small number of particle-hole excitations compared to a certain reference state) contribute significantly to F_j, so that the F_j's can be evaluated with great accuracy by keeping only the most relevant terms. It should also be possible to develop analytical approximations, whose validity can checked against this numerical method. It would then become possible to apply this toolbox to experimental setups, to model e.g. weak tunneling between 1D tubes in experiments with 3D optical lattices, or dipolar interactions between the atoms.

Another related problem that has prevented analytical progress on the dynamics of the 1D Bose gas with weak integrability breaking is that there is no known 'Wigner operator' whose expectation value gives the spatially-dependent distribution of rapidities. In non-interacting systems such as the XY spin chain or the Tonks-Girardeau gas, it is well known that the distribution of rapidities is obtained from the Wigner function of the underlying non-interacting fermions (Doyon et al., 2017), but no such construction is known for the interacting 1D Bose gas. This has been a major obstacle for analytical approaches to the dynamics of quasi-particles when the system is perturbed away from integrability (Hutsalyuk and Pozsgay, 2021). This seems to be a very difficult problem, but I think there exist at least three ways in which one could attack it. First, one could develop an effective construction of the Wigner operator at low energies, where the Luttinger liquid approach can be used. There, I expect that the quasi-particles should correspond to the refermionization of elementary excitations in the Luttinger liquid, sometimes called 'Rozhkov fermions' (Rozhkov, 2005), which play a central role in the 'non-linear Luttinger liquid' (Imambekov and Glazman, 2009). Writing the Wigner operator in this effective low-energy description is easy, and it gives access to the distribution of rapidities in interacting systems at low energies (Bouchoule et al., 2022). Second, one could try a naive

'few-to-many approach', namely start by constructing the Wigner operator for small systems, for instance in the 1D Bose gas with contact repulsion with $N = 2$ particles (which is very easy), for $N = 3$ (less easy but still doable), etc. The hope there is to be able to identify a general structure that will give the Wigner operator for arbitrary N. Third, one could use to $1/c$ approaches Granet and Essler (2021); Bertini et al. (2022) —where c is the interaction strength between particles—. If successful, the construction of a Wigner operator for the interacting 1D Bose gas would open many new analytical possibilites, for instance it could lead to closed analytic expressions for the functions F_j above, or it could allow to investigate finite-N effects or Moyal-expansion-type corrections to the equations of Generalized Hydrodynamics Fagotti (2020), etc.

6.3 Dynamics of spins in a cavity

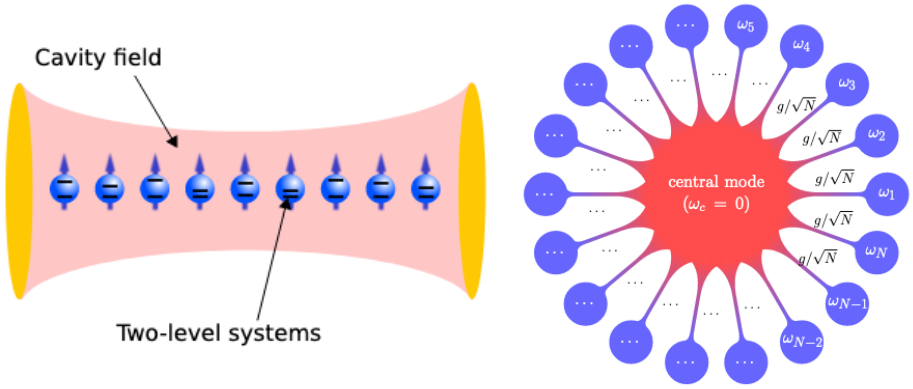

Figure 6.3: *[From (Dubail et al., 2022)]* Left: cartoon of a spin chain (or other two-level systems) coupled to a cavity field. Right: when the spins are coupled to a single cavity mode, then the system takes the form of a 'spin-central' model, where all the spins are coupled to the bosonic degree of freedom in the center.

Another direction I would like to explore is the dynamics of systems of N quantum spins in a cavity (Fig. 6.3), e.g. the Tavis-Cummings (Tavis and Cummings, 1968) or Dicke models (Garraway, 2011) (see the frame below for definitions). In their 'clean' versions —i.e. when the Zeeman energies ω_j of all spins are identical—, these models become semi-classical in the large N limit, and their integrable and chaotic dynamics is relatively well understood using tools of classical dynamical systems (Emary and Brandes, 2003; Altland and Haake, 2012). However, for finite N, or in the presence of disorder (i.e. non-identical ω_j's), no such tools exist, and the influence of integrability on the dynamics of these systems is mysterious to me. The Hamiltonian of these models is, with $g = g'$ (for

the Dicke model) or $g' = 0$ (Tavis-Cummings model),

$$H = \omega_c a^\dagger a + \sum_{j=1}^{N} \omega_j \sigma_j^z + \frac{g}{\sqrt{N}} \sum_{j=1}^{N} (a\sigma_j^+ + a^\dagger \sigma_j^-) + \frac{g'}{\sqrt{N}} \sum_{j=1}^{N} (a\sigma_j^- + a^\dagger \sigma_j^+), \tag{6.3}$$

where $a, a^\dagger$ is the boson creation/annihilation operator, and $\sigma_j^{\pm,z}$ are the Pauli matrices. The disorder prevents the simplification of replacing individual spins by a collective spin operator, hence the need for efficient numerical methods to explore these models. At the Tavis-Cummings point $g' = 0$, the model commutes with the extensive set of (mutually commuting) conserved charges (Faribault et al., 2011; Claeys et al., 2019)

$$Q_j = (\omega_j - \omega_c)\sigma_j^z + \frac{g}{\sqrt{N}}(a\sigma_j^+ + a^\dagger \sigma_j^-) + \sum_{j \neq i}^{N} \frac{2g^2}{N(\omega_i - \omega_j)} \underline{\sigma}_i \cdot \underline{\sigma}_j. \tag{6.4}$$

How do the Q_j's affect the dynamics? Does the system relax to a GGE, of the form $\exp(-\sum_j \beta_j Q_j)$? Or does it relax to something else, as the charges Q_j are not local? When $g' \neq 0$, the model is not integrable, but is there a pre-thermalization effect, so that the dynamis on intermediated time scales is still affected by the Q_j's? It seems that not so much is known about such fundamental questions.

These models are used in a variety of contexts (including dynamical superradiance (Temnov and Woggon, 2005), microcavity polaritons (Szymańska et al., 2006), solid state quantum memories (Diniz et al., 2011), or cold atom in optical cavities with spatial variation of the cavity modes (Zhang et al., 2018)), so I believe there is room for plenty of nice contributions on this topic.

More precisely, I believe it should be possible to investigate the validity of a 'Generalized Eigenstate Thermalization Hypothesis' ('GETH') (Cassidy et al., 2011) in the disordered Tavis-Cummings model. It is not quite clear what *locality* means when the spins are all coupled through the cavity, but probably the concept of 'local charges' in spin chains should now be replaced by 'few-body charges'. Then 'GETH' may be reformulated as the hypothesis that, in any given eigenstate, the expectation value $\langle A \rangle$ of a *few-body observable* A (i.e. involving a finite number of spins, e.g. $\sigma_{j_1}^{a_1}\sigma_{j_2}^{a_2}$ or $\sigma_{j_1}^{a_1}\sigma_{j_2}^{a_2}\sigma_{j_3}^{a_3}$), should be a *smooth* function f_A of the expectation values of the conserved charges for large N,

$$\langle A \rangle \underset{N\to\infty}{\simeq} f_A(\langle Q_1 \rangle, \ldots, \langle Q_N \rangle). \tag{6.5}$$

If this holds, then it should be possible to develop an efficient coarse-grained description of the eigenstates in the thermodynamic limit $N \to \infty$. The idea would be to average over eigenstates and over a few charges Q_j corresponding to Zeeman energies ω_j in the same energy shell $\omega_j \in [\omega - \delta\omega, \omega + \delta\omega]$, so that they become a smooth function $Q(\omega) = Q(\omega_j) = \langle Q_j \rangle$. This would provide an efficient simplified description of the thermodynamics in the

disordered Tavis-Cummings model, analogously to what is achieved by the thermodynamic Bethe Ansatz in 1D systems (Zamolodchikov, 1990).

Then one could study the influence of the integrability-breaking terms in (6.4) when $g' \neq 0$ on the dynamics. For small g', the resulting framework would be an evolution equation for the slow dynamics of the expectation values of the charges $\langle Q_j \rangle$. It would also be interesting to shed light on the transition between nearly-integrable dynamics and chaotic dynamics expected in the clean Dicke model (Buijsman et al., 2017), and to understand whether the effective slow dynamics of the charges is compatible with their relaxation to a thermal state, or if some 'hidden' conserved quantities remain, which could give hints about the form that a quantum analog of the Kolmogoroff-Arnold-Moser theorem should take in these systems.

6.4 Tensor Network methods exploiting the specific features of nearly integrable dynamics

The fundamental obstacle to simulating quantum many-body dynamics on classical computers is the generic linear growth of entanglement, which implies that, when one tries to approximate them with Matrix Product States or Tensor Networks, the required bond dimension blows up as $O(\exp(t))$. The entanglement growth is linear under integrable and chaotic dynamics alike, however the mechanisms at play are different: in integrable systems, entanglement is propagated by quasi-particles (Calabrese and Cardy, 2009; Alba and Calabrese, 2018), while in chaotic systems entanglement follows from a "minimal membrane" in spacetime (Jonay et al., 2018) reminiscent of the Ryu-Takayanagi formula in holography (Ryu and Takayanagi, 2006). I believe it should be possible to exploit that key difference to design novel entanglement quantifiers that distinguish integrable from chaotic dynamics, and use it to design new Tensor Network methods that will be efficient for nearly integrable sytems. One basic idea along these lines is sketched in Fig. 6.4: in an infinite 1D system where entanglement growth is due to pairs of quasi-particles propagating at a velocity v, the reduced density matrix ρ_A of a subsystem A made of n intervals of equal length ℓ ($\ell < 2vt$)

$$A = [0, \ell] \cup [2vt, 2vt + \ell] \cup [4vt, 4vt + \ell] \cup \cdots \cup [2nvt, 2nvt + \ell] \tag{6.6}$$

should have an entanglement entropy $S_A(n, t) = -\mathrm{tr}\rho_A \log \rho_A$ satisfying an *area law*,

$$S_A = C_1\, n + C_2\, t \tag{6.7}$$

for two numerical constants C_1, C_2, as opposed to a *volume law* $S_A \propto nt$. The reason is that the bipartition consists of intervals that contain both members of a pair of quasi-particles emitted by the initial state, except the first and last intervals (see the figure in the frame).

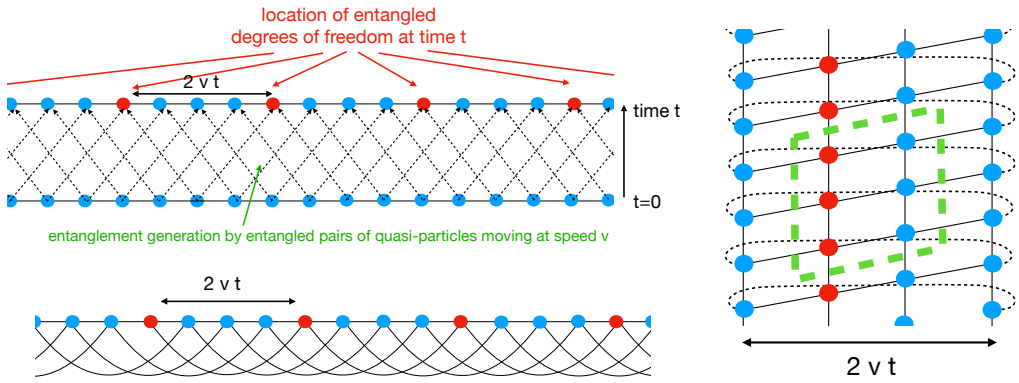

Figure 6.4: Left top: cartoon of quasi-particle dynamics. At time t after a quench from a shortly-correlated state, the degrees of freedom that are entangled are separated by a distance $2vt$, where v is the quasi-particle velocity. Left bottom: consequently, the entanglement structure of the state consists of bonds of length $2vt$. Right: by unraveling that structure, one gets a 2D square lattice network with periodic boundary conditions (right figure). Proving that this is indeed correct will be possible by computing the entanglement entropy of a subsystem corresponding to a connected region in that geometry (dashed green in the figure), which should satisfy an area law.

On the other hand, it is clear that the "minimal membrane" picture of (Jonay et al., 2018) will give a volume law for systems with chaotic dynamics. Therefore, this quantity should somehow measure the amount of entanglement not generated by quasi-particles, and should be able to distinguish quasi-particle from chaotic dynamics. It should be possible to start by investigating this quantity in free fermion chains and in cellular automata models like the Rule 54 qubit chain (Bučа et al., 2021). It could lead to new ideas for designing Tensor Network methods that are specific to (nearly) integrable dynamics. The conjectured area law (6.7) would imply that it is possible to approximate the state of a 1D integrable system after a quench by a 2D Tensor Network, see Fig. 6.4. Other similar ideas could be explored, for instance one could search for efficient encoding of the evolution operator $U(t) = e^{-iHt}$ of systems with quasi-particle dynamics.

Bibliography

Abanov, A. G. (2006), Hydrodynamics of correlated systems, *in* 'Applications of Random Matrices in Physics', Springer, pp. 139–161.

Aizenman, M., Goldstein, S. and Lebowitz, J. L. (1975), 'Ergodic properties of an infinite one dimensional hard rod system', *Communications in Mathematical Physics* **39**(4), 289–301.

Alba, V. (2021), 'Diffusion and operator entanglement spreading', *Physical Review B* **104**(9), 094410.

Alba, V., Bertini, B., Fagotti, M., Piroli, L. and Ruggiero, P. (2021), 'Generalized-hydrodynamic approach to inhomogeneous quenches: correlations, entanglement and quantum effects', *Journal of Statistical Mechanics: Theory and Experiment* **2021**(11), 114004.

Alba, V. and Calabrese, P. (2018), 'Entanglement dynamics after quantum quenches in generic integrable systems', *SciPost Physics* **4**(3), 017.

Alba, V., Dubail, J. and Medenjak, M. (2019), 'Operator entanglement in interacting integrable quantum systems: the case of the rule 54 chain', *Physical review letters* **122**(25), 250603.

Altland, A. and Haake, F. (2012), 'Quantum chaos and effective thermalization', *Physical Review Letters* **108**(7), 073601.

Ares, F., Scopa, S. and Wald, S. (2022), 'Entanglement dynamics of a hard-core quantum gas during a joule expansion', *arXiv preprint arXiv:2204.01664* .

Armijo, J., Jacqmin, T., Kheruntsyan, K. and Bouchoule, I. (2011), 'Mapping out the quasicondensate transition through the dimensional crossover from one to three dimensions', *Phys. Rev. A* **83**(2), 021605.
URL: *http://link.aps.org/doi/10.1103/PhysRevA.83.021605*

Arute, F., Arya, K., Babbush, R., Bacon, D., Bardin, J. C., Barends, R., Biswas, R., Boixo, S., Brandao, F. G., Buell, D. A. et al. (2019), 'Quantum supremacy using a programmable superconducting processor', *Nature* **574**(7779), 505–510.

Barthel, T. and Schollwöck, U. (2008), 'Dephasing and the steady state in quantum many-particle systems', *Phys. Rev. Lett.* **100**.
URL: *https://link.aps.org/doi/10.1103/PhysRevLett.100.100601*

Bastianello, A., Alba, V. and Caux, J.-S. (2019), 'Generalized hydrodynamics with space-time inhomogeneous interactions', *Physical review letters* **123**(13), 130602.

Bastianello, A., Collura, M. and Sotiriadis, S. (2017), 'Quenches from bosonic gaussian initial states to the tonks-girardeau limit: Stationary states and effects of a confining potential', *Physical Review B* **95**(17), 174303.

Bastianello, A., De Luca, A., Doyon, B. and De Nardis, J. (2020), 'Thermalization of a Trapped One-Dimensional Bose Gas via Diffusion', *Phys. Rev. Lett.* **125**(24), 240604. Publisher: American Physical Society.
URL: *https://link.aps.org/doi/10.1103/PhysRevLett.125.240604*

Bastianello, A., De Luca, A. and Vasseur, R. (2021), 'Hydrodynamics of weak integrability breaking', *Journal of Statistical Mechanics: Theory and Experiment* **2021**(11), 114003.

Bastianello, A., Dubail, J. and Stéphan, J.-M. (2020), 'Entanglement entropies of inhomogeneous luttinger liquids', *Journal of Physics A: Mathematical and Theoretical* **53**(15), 155001.

Bergeman, T., Moore, M. and Olshanii, M. (2003), 'Atom-atom scattering under cylindrical harmonic confinement: Numerical and analytic studies of the confinement induced resonance', *Physical review letters* **91**(16), 163201.

Bernard, D., Jin, T. and Shpielberg, O. (2018), 'Transport in quantum chains under strong monitoring', *EPL (Europhysics Letters)* **121**(6), 60006.

Bertini, B., Collura, M., De Nardis, J. and Fagotti, M. (2016), 'Transport in out-of-equilibrium x x z chains: Exact profiles of charges and currents', *Phys. Rev. Lett.* **117**(20), 207201.
URL: *https://link.aps.org/doi/10.1103/PhysRevLett.117.207201*

Bertini, B., Essler, F. H. and Granet, E. (2022), 'Bbgky hierarchy and generalised hydrodynamics', *arXiv preprint arXiv:2201.10549* .

Bertini, B., Kos, P. and Prosen, T. (2020*a*), 'Operator entanglement in local quantum circuits i: Chaotic dual-unitary circuits', *SciPost Physics* **8**(4), 067.

Bertini, B., Kos, P. and Prosen, T. (2020*b*), 'Operator entanglement in local quantum circuits ii: Solitons in chains of qubits', *SciPost Physics* **8**(4), 068.

Bettelheim, E., Abanov, A. and Wiegmann, P. (2006), 'Orthogonality catastrophe and shock waves in a nonequilibrium fermi gas', *Physical review letters* **97**(24), 246402.

Bettelheim, E. and Glazman, L. (2012), 'Quantum ripples over a semiclassical shock', *Physical review letters* **109**(26), 260602.

Bettelheim, E. and Wiegmann, P. B. (2011), 'Universal fermi distribution of semiclassical nonequilibrium fermi states', *Physical Review B* **84**(8), 085102.

Boldrighini, C., Dobrushin, R. L. and Sukhov, Y. M. (1983), 'One-dimensional hard rod caricature of hydrodynamics', *J. Stat. Phys.* **31**(3), 577–616.
URL: *https://doi.org/10.1007/BF01019499*

Boldrighini, C. and Suhov, Y. M. (1997), 'One-dimensional hard-rod caricature of hydrodynamics:"navier–stokes correction" for local equilibrium initial states', *Communications in mathematical physics* **189**(2), 577–590.

Bolech, C., Heidrich-Meisner, F., Langer, S., McCulloch, I., Orso, G. and Rigol, M. (2012), 'Long-time behavior of the momentum distribution during the sudden expansion of a spin-imbalanced fermi gas in one dimension', *Physical review letters* **109**(11), 110602.

Bondesan, R., Dubail, J., Faribault, A. and Ikhlef, Y. (2015), 'Chiral su (2) k currents as local operators in vertex models and spin chains', *Journal of Physics A: Mathematical and Theoretical* **48**(6), 065205.

Bonnes, L., Essler, F. H. and Läuchli, A. M. (2014), '"light-cone" dynamics after quantum quenches in spin chains', *Phys. Rev. Lett.* **113**(18), 187203.
URL: *https://link.aps.org/doi/10.1103/PhysRevLett.113.187203*

Borsi, M., Pozsgay, B. and Pristyák, L. (2020), 'Current operators in bethe ansatz and generalized hydrodynamics: An exact quantum-classical correspondence', *Physical Review X* **10**(1), 011054.

Borsi, M., Pozsgay, B. and Pristyák, L. (2021), 'Current operators in integrable models: a review', *Journal of Statistical Mechanics: Theory and Experiment* **2021**(9), 094001.

Bouchoule, I., Doyon, B. and Dubail, J. (2020), 'The effect of atom losses on the distribution of rapidities in the one-dimensional bose gas', *SciPost Physics* **9**(4), 044.

Bouchoule, I. and Dubail, J. (2021), 'Breakdown of tan's relation in lossy one-dimensional bose gases', *Physical Review Letters* **126**(16), 160603.

Bouchoule, I. and Dubail, J. (2022), 'Generalized hydrodynamics in the one-dimensional bose gas: theory and experiments', *Journal of Statistical Mechanics: Theory and Experiment* **2022**(1), 014003.

Bouchoule, I., Dubail, J., Dubois, L. and Gangardt, D. M. (2022), 'Relaxation of phonons in the lieb-liniger gas by dynamical refermionization', *arXiv preprint arXiv:2206.00112* .

Bouchoule, I. and Schemmer, M. (2020), 'Asymptotic temperature of a lossy condensate', *SciPost Physics* **8**(4), 060.

Brandino, G., Caux, J.-S. and Konik, R. (2015), 'Glimmers of a quantum kam theorem: insights from quantum quenches in one-dimensional bose gases', *Physical Review X* **5**(4), 041043.

Brun, Y. and Dubail, J. (2018), 'The inhomogeneous gaussian free field, with application to ground state correlations of trapped 1d bose gases', *SciPost Phys.* **4**, 037.
URL: *https://scipost.org/10.21468/SciPostPhys.4.6.037*

Brydges, T., Elben, A., Jurcevic, P., Vermersch, B., Maier, C., Lanyon, B. P., Zoller, P., Blatt, R. and Roos, C. F. (2019), 'Probing rényi entanglement entropy via randomized measurements', *Science* **364**(6437), 260–263.

Buča, B., Klobas, K. and Prosen, T. (2021), 'Rule 54: Exactly solvable model of nonequilibrium statistical mechanics', *Journal of Statistical Mechanics: Theory and Experiment* **2021**(7), 074001.

Buijsman, W., Gritsev, V. and Sprik, R. (2017), 'Nonergodicity in the anisotropic dicke model', *Physical Review Letters* **118**(8), 080601.

Bulchandani, V. B. (2017), 'On classical integrability of the hydrodynamics of quantum integrable systems', *J. Phys. A* **50**(43), 435203.
URL: *https://iopscience.iop.org/article/10.1088/1751-8121/aa8c62*

Bulchandani, V. B., Cao, X. and Moore, J. E. (2019), 'Kinetic theory of quantum and classical toda lattices', *J. Phys. A* **52**(33).
URL: *https://iopscience.iop.org/article/10.1088/1751-8121/ab2cf0*

Bulchandani, V. B., Vasseur, R., Karrasch, C. and Moore, J. E. (2017), 'Solvable hydrodynamics of quantum integrable systems', *Physical review letters* **119**(22), 220604.

Bulchandani, V. B., Vasseur, R., Karrasch, C. and Moore, J. E. (2018), 'Bethe-boltzmann hydrodynamics and spin transport in the xxz chain', *Phys. Rev. B* **97**(4), 045407.
URL: *https://link.aps.org/doi/10.1103/PhysRevB.97.045407*

Buljan, H., Pezer, R. and Gasenzer, T. (2008), 'Fermi-bose transformation for the time-dependent lieb-liniger gas', *Physical review letters* **100**(8), 080406.

Cai, Z. and Barthel, T. (2013), 'Algebraic versus exponential decoherence in dissipative many-particle systems', *Physical review letters* **111**(15), 150403.

Calabrese, P. and Cardy, J. (2004), 'Entanglement entropy and quantum field theory', *Journal of statistical mechanics: theory and experiment* **2004**(06), P06002.

Calabrese, P. and Cardy, J. (2005), 'Evolution of entanglement entropy in one-dimensional systems', *Journal of Statistical Mechanics: Theory and Experiment* **2005**(04), P04010.

Calabrese, P. and Cardy, J. (2009), 'Entanglement entropy and conformal field theory', *Journal of physics a: mathematical and theoretical* **42**(50), 504005.

Calabrese, P., Essler, F. H. and Fagotti, M. (2011), 'Quantum quench in the transverse-field ising chain', *Physical review letters* **106**(22), 227203.

Campbell, A., Gangardt, D. and Kheruntsyan, K. (2015), 'Sudden Expansion of a One-Dimensional Bose Gas from Power-Law Traps', *Phys. Rev. Lett.* **114**(12), 125302.
URL: *https://link.aps.org/doi/10.1103/PhysRevLett.114.125302*

Cao, X., Bulchandani, V. B. and Moore, J. E. (2018), 'Incomplete thermalization from trap-induced integrability breaking: lessons from classical hard rods', *Phys. Rev. Lett.* **120**(16), 164101.
URL: *https://link.aps.org/doi/10.1103/PhysRevLett.120.164101*

Cao, X., Bulchandani, V. B. and Spohn, H. (2019), 'The gge averaged currents of the classical toda chain', *Journal of Physics A: Mathematical and Theoretical* **52**(49), 495003.

Caputa, P., Simón, J., Štikonas, A., Takayanagi, T. and Watanabe, K. (2015), 'Scrambling time from local perturbations of the eternal btz black hole', *Journal of High Energy Physics* **2015**(8), 1–36.

Cardy, J., Castro-Alvaredo, O. and Doyon, B. (2008), 'Form factors of branch-point twist fields in quantum integrable models and entanglement entropy', *J. Stat. Phys.* **130**(1), 129–168.
URL: *https://doi.org/10.1007/s10955-007-9422-x*

Cassidy, A. C., Clark, C. W. and Rigol, M. (2011), 'Generalized thermalization in an integrable lattice system', *Physical review letters* **106**(14), 140405.

Castro-Alvaredo, O. A., Doyon, B. and Yoshimura, T. (2016), 'Emergent hydrodynamics in integrable quantum systems out of equilibrium', *Phys. Rev. X* **6**(4), 041065.
URL: *https://link.aps.org/doi/10.1103/PhysRevX.6.041065*

Caux, J.-S., Doyon, B., Dubail, J., Konik, R. and Yoshimura, T. (2019), 'Hydrodynamics of the interacting Bose gas in the Quantum Newton Cradle setup', *SciPost Phys.* **6**, 70.
URL: *https://scipost.org/10.21468/SciPostPhys.6.6.070*

Caux, J.-S., Klauser, A. and van den Brink, J. (2009), 'Polarization suppression and non-monotonic local two-body correlations in the two-component bose gas in one dimension', *Physical Review A* **80**(6), 061605.

Caux, J.-S. and Konik, R. M. (2012), 'Constructing the generalized gibbs ensemble after a quantum quench', *Physical review letters* **109**(17), 175301.

Cazalilla, M. (2004), 'Bosonizing one-dimensional cold atomic gases', *J. Phys. B* **37**(7), S1.
URL: *https://iopscience.iop.org/article/10.1088/0953-4075/37/7/051*

Cirac, J. I., Perez-Garcia, D., Schuch, N. and Verstraete, F. (2021), 'Matrix product states and projected entangled pair states: Concepts, symmetries, theorems', *Reviews of Modern Physics* **93**(4), 045003.

Cirac, J. I., Poilblanc, D., Schuch, N. and Verstraete, F. (2011), 'Entanglement spectrum and boundary theories with projected entangled-pair states', *Physical Review B* **83**(24), 245134.

Claeys, P. W., Dimo, C., De Baerdemacker, S. and Faribault, A. (2019), 'Integrable spin-richardson–gaudin xyz models in an arbitrary magnetic field', *Journal of Physics A: Mathematical and Theoretical* **52**(8), 08LT01.

Collura, M., De Luca, A., Calabrese, P. and Dubail, J. (2020), 'Domain wall melting in the spin-1 2 xxz spin chain: Emergent luttinger liquid with a fractal quasiparticle charge', *Physical Review B* **102**(18), 180409.

Cramer, M., Dawson, C. M., Eisert, J. and Osborne, T. J. (2008), 'Exact relaxation in a class of nonequilibrium quantum lattice systems', *Phys. Rev. Lett.* **100**, 030602.
URL: *https://link.aps.org/doi/10.1103/PhysRevLett.100.030602*

Cubero, A. C. (2020), 'How generalized hydrodynamics time evolution arises from a form factor expansion', *arXiv preprint arXiv:2001.03065* .

Cubero, A. C. and Panfil, M. (2020), 'Generalized hydrodynamics regime from the thermodynamic bootstrap program', *SciPost Phys* **8**(004).

Cubero, A. C., Yoshimura, T. and Spohn, H. (2021), 'Form factors and generalized hydrodynamics for integrable systems', *Journal of Statistical Mechanics: Theory and Experiment* **2021**(11), 114002.

Davies, B. (1990), 'Higher conservation laws for the quantum non-linear schrödinger equation', *Physica A: Statistical Mechanics and its Applications* **167**(2), 433–456.

Davies, B. and Korepin, V. E. (2011), 'Higher conservation laws for the quantum non-linear schrödinger equation', *arXiv preprint arXiv:1109.6604* .

De Nardis, J., Bernard, D. and Doyon, B. (2018), 'Hydrodynamic diffusion in integrable systems', *Phys. Rev. Lett.* **121**(16), 160603.
URL: *https://link.aps.org/doi/10.1103/PhysRevLett.121.160603*

De Nardis, J., Bernard, D. and Doyon, B. (2019), 'Diffusion in generalized hydrodynamics and quasiparticle scattering', *SciPost Phys.* **6**(4), 049.

De Nardis, J. and Panfil, M. (2018), 'Edge singularities and quasilong-range order in nonequilibrium steady states', *Physical review letters* **120**(21), 217206.

Dean, D. S., Le Doussal, P., Majumdar, S. N. and Schehr, G. (2018), 'Wigner function of noninteracting trapped fermions', *Physical Review A* **97**(6), 063614.

Dean, D. S., Le Doussal, P., Majumdar, S. N. and Schehr, G. (2019), 'Nonequilibrium dynamics of noninteracting fermions in a trap', *EPL (Europhysics Letters)* **126**(2), 20006.

Del Campo, A. (2008), 'Fermionization and bosonization of expanding one-dimensional anyonic fluids', *Physical Review A* **78**(4), 045602.

Derrida, B. and Gerschenfeld, A. (2009), 'Current fluctuations in one dimensional diffusive systems with a step initial density profile', *Journal of Statistical Physics* **137**(5), 978–1000.

Diniz, I., Portolan, S., Ferreira, R., Gérard, J., Bertet, P. and Auffeves, A. (2011), 'Strongly coupling a cavity to inhomogeneous ensembles of emitters: Potential for long-lived solid-state quantum memories', *Physical Review A* **84**(6), 063810.

Doyon, B. (2017), 'Thermalization and pseudolocality in extended quantum systems', *Communications in Mathematical Physics* **351**(1), 155–200.

Doyon, B. (2019*a*), 'Generalized hydrodynamics of the classical toda system', *Journal of Mathematical Physics* **60**(7), 073302.

Doyon, B. (2019*b*), 'Lecture notes on generalised hydrodynamics', *arXiv preprint arXiv:1912.08496* .

Doyon, B., Dubail, J., Konik, R. and Yoshimura, T. (2017), 'Large-scale description of interacting one-dimensional bose gases: generalized hydrodynamics supersedes conventional hydrodynamics', *Phys. Rev. Lett.* **119**(19), 195301.
URL: *https://link.aps.org/doi/10.1103/PhysRevLett.119.195301*

Doyon, B. and Spohn, H. (2017*a*), 'Drude weight for the lieb-liniger bose gas', *SciPost Phys.* **3**, 039.
URL: *https://scipost.org/10.21468/SciPostPhys.3.6.039*

Doyon, B. and Spohn, H. (2017*b*), 'Dynamics of hard rods with initial domain wall state', *Journal of Statistical Mechanics: Theory and Experiment* **2017**(7), 073210.

Doyon, B. and Yoshimura, T. (2017), 'A note on generalized hydrodynamics: inhomogeneous fields and other concepts', *SciPost Phys.* **2**(2), 014.
URL: *https://scipost.org/10.21468/SciPostPhys.2.2.014*

Doyon, B., Yoshimura, T. and Caux, J.-S. (2018), 'Soliton gases and generalized hydrodynamics', *Phys. Rev. Lett.* **120**(4), 045301.
URL: *https://link.aps.org/doi/10.1103/PhysRevLett.120.045301*

Dubail, J. (2016), 'A more efficient way to describe interacting quantum particles in 1d', *Physics* **9**, 153.

Dubail, J. (2017), 'Entanglement scaling of operators: a conformal field theory approach, with a glimpse of simulability of long-time dynamics in 1+ 1d', *Journal of Physics A: Mathematical and Theoretical* **50**(23), 234001.

Dubail, J., Botzung, T., Schachenmayer, J., Pupillo, G. and Hagenmüller, D. (2022), 'Large random arrowhead matrices: multifractality, semilocalization, and protected transport in disordered quantum spins coupled to a cavity', *Physical Review A* **105**(2), 023714.

Dubail, J. and Read, N. (2011), 'Entanglement spectra of complex paired superfluids', *Physical Review Letters* **107**(15), 157001.

Dubail, J. and Read, N. (2015), 'Tensor network trial states for chiral topological phases in two dimensions and a no-go theorem in any dimension', *Physical Review B* **92**(20), 205307.

Dubail, J., Read, N. and Rezayi, E. (2012*a*), 'Edge-state inner products and real-space entanglement spectrum of trial quantum hall states', *Physical Review B* **86**(24), 245310.

Dubail, J., Read, N. and Rezayi, E. (2012*b*), 'Real-space entanglement spectrum of quantum hall systems', *Physical Review B* **85**(11), 115321.

Dubail, J., Stéphan, J.-M., Viti, J. and Calabrese, P. (2017), 'Conformal field theory for inhomogeneous one-dimensional quantum systems: the example of non-interacting fermi gases', *SciPost Phys.* **2**(1), 002.
URL: *https://arxiv.org/abs/1606.04401*

Dubessy, R., Polo, J., Perrin, H., Minguzzi, A. and Olshanii, M. (2021), 'Universal shockwave propagation in one-dimensional bose fluids', *Physical Review Research* **3**(1), 013098.

Durnin, J., Bhaseen, M. and Doyon, B. (2021), 'Nonequilibrium dynamics and weakly broken integrability', *Physical Review Letters* **127**(13), 130601.

Dymarsky, A. and Pavlenko, K. (2019), 'Generalized eigenstate thermalization hypothesis in 2d conformal field theories', *Physical review letters* **123**(11), 111602.

Eisenbud, L. (1948), 'The formal properties of nuclear collisions.', *PhDT* .

Eisert, J., Cramer, M. and Plenio, M. B. (2010), 'Colloquium: Area laws for the entanglement entropy', *Reviews of modern physics* **82**(1), 277.

El, G. and Kamchatnov, A. (2005), 'Kinetic equation for a dense soliton gas', *Phys. Rev. Lett.* **95**(20), 204101.
URL: *https://link.aps.org/doi/10.1103/PhysRevLett.95.204101*

Eliëns, I. S. (2017), On quantum seas, PhD thesis.

Eliëns, S. and Caux, J.-S. (2016), 'General finite-size effects for zero-entropy states in one-dimensional quantum integrable models', *J. Phys. A* **49**(49), 495203.
URL: *https://iopscience.iop.org/article/10.1088/1751-8113/49/49/495203*

Emary, C. and Brandes, T. (2003), 'Chaos and the quantum phase transition in the dicke model', *Physical Review E* **67**(6), 066203.

Fabbri, N., Clément, D., Fallani, L., Fort, C. and Inguscio, M. (2011), 'Momentum-resolved study of an array of one-dimensional strongly phase-fluctuating bose gases', *Physical Review A* **83**(3), 031604.

Fagotti, M. (2017), 'Higher-order generalized hydrodynamics in one dimension: The noninteracting test', *Physical Review B* **96**(22), 220302.

Fagotti, M. (2020), 'Locally quasi-stationary states in noninteracting spin chains', *SciPost Phys* **8**, 048.

Fang, B., Johnson, A., Roscilde, T. and Bouchoule, I. (2016), 'Momentum-space correlations of a one-dimensional bose gas', *Physical review letters* **116**(5), 050402.

Faribault, A., El Araby, O., Sträter, C. and Gritsev, V. (2011), 'Gaudin models solver based on the correspondence between bethe ansatz and ordinary differential equations', *Physical Review B* **83**(23), 235124.

Fokkema, T., Eliëns, I. and Caux, J.-S. (2014), 'Split fermi seas in one-dimensional bose fluids', *Phys. Rev. A* **89**(3), 033637.
URL: *https://link.aps.org/doi/10.1103/PhysRevA.89.033637*

Folman, R., Krüger, P., Cassettari, D., Hessmo, B., Maier, T. and Schmiedmayer, J. (2000), 'Controlling cold atoms using nanofabricated surfaces: atom chips', *Physical Review Letters* **84**(20), 4749.

Francesco, P., Mathieu, P. and Sénéchal, D. (2012), *Conformal field theory*, Springer Science & Business Media.

Garraway, B. M. (2011), 'The dicke model in quantum optics: Dicke model revisited', *Philosophical Transactions of the Royal Society A: Mathematical, Physical and Engineering Sciences* **369**(1939), 1137–1155.

Gaudin, M. (2014), *The Bethe Wavefunction*, Cambridge University Press.

Giamarchi, T. (2003), *Quantum physics in one dimension*, Vol. 121, Clarendon press.

Girardeau, M. (1960), 'Relationship between systems of impenetrable bosons and fermions in one dimension', *J. Math. Phys.* **1**(6), 516–523.
URL: *https://doi.org/10.1063/1.1703687*

Gopalakrishnan, S., Huse, D. A., Khemani, V. and Vasseur, R. (2018), 'Hydrodynamics of operator spreading and quasiparticle diffusion in interacting integrable systems', *Phys. Rev. B* **98**(22), 220303.
URL: *https://link.aps.org/doi/10.1103/PhysRevB.98.220303*

Granet, E. and Essler, F. (2021), 'Systematic strong coupling expansion for out-of-equilibrium dynamics in the lieb-liniger model', *SciPost Physics* **11**(3), 068.

Haldane, F. (1981), 'Effective harmonic-fluid approach to low-energy properties of one-dimensional quantum fluids', *Physical Review Letters* **47**(25), 1840.

Haller, E., Gustavsson, M., Mark, M. J., Danzl, J. G., Hart, R., Pupillo, G. and Nägerl, H.-C. (2009), 'Realization of an Excited, Strongly Correlated Quantum Gas Phase', *Science* **325**(5945), 1224–1227.
URL: *http://www.sciencemag.org/content/325/5945/1224*

Hartmann, M. J., Prior, J., Clark, S. R. and Plenio, M. B. (2009), 'Density matrix renormalization group in the heisenberg picture', *Phys. Rev. Lett.* **102**, 057202.
URL: *https://link.aps.org/doi/10.1103/PhysRevLett.102.057202*

Hastings, M. B. (2007), 'An area law for one-dimensional quantum systems', *Journal of statistical mechanics: theory and experiment* **2007**(08), P08024.

He, K., Santos, L. F., Wright, T. M. and Rigol, M. (2013), 'Single-particle and many-body analyses of a quasiperiodic integrable system after a quench', *Physical Review A* **87**(6), 063637.

Hutsalyuk, A. and Pozsgay, B. (2021), 'Integrability breaking in the one-dimensional bose gas: Atomic losses and energy loss', *Physical Review E* **103**(4), 042121.

Ilievski, E., Medenjak, M., Prosen, T. and Zadnik, L. (2016), 'Quasilocal charges in integrable lattice systems', *Journal of Statistical Mechanics: Theory and Experiment* **2016**(6), 064008.

Imambekov, A. and Glazman, L. I. (2009), 'Universal theory of nonlinear luttinger liquids', *Science* **323**(5911), 228–231.

Imambekov, A., Schmidt, T. L. and Glazman, L. I. (2012), 'One-dimensional quantum liquids: Beyond the luttinger liquid paradigm', *Rev. Mod. Phys.* **84**(3), 1253.
URL: *https://link.aps.org/doi/10.1103/RevModPhys.84.1253*

Jacqmin, T., Armijo, J., Berrada, T., Kheruntsyan, K. V. and Bouchoule, I. (2011), 'Sub-Poissonian Fluctuations in a 1D Bose Gas: From the Quantum Quasicondensate to the Strongly Interacting Regime', *Phys. Rev. Lett.* **106**(23), 230405.
URL: *http://link.aps.org/doi/10.1103/PhysRevLett.106.230405*

Jarkovskỳ, J. G., Molnár, A., Schuch, N. and Cirac, J. I. (2020), 'Efficient description of many-body systems with matrix product density operators', *PRX Quantum* **1**(1), 010304.

Jennings, D., Brockt, C., Haegeman, J., Osborne, T. J. and Verstraete, F. (2015), 'Continuum tensor network field states, path integral representations and spatial symmetries', *New Journal of Physics* **17**(6), 063039.

Jepsen, P. N., Lee, Y. K., Lin, H., Dimitrova, I., Margalit, Y., Ho, W. W. and Ketterle, W. (2021), 'Catching bethe phantoms and quantum many-body scars: Long-lived spin-helix states in heisenberg magnets', *arXiv preprint arXiv:2110.12043* .

Jonay, C., Huse, D. A. and Nahum, A. (2018), 'Coarse-grained dynamics of operator and state entanglement', *arXiv:1803.00089* .
URL: *https://arxiv.org/abs/1803.00089*

Jukić, D., Pezer, R., Gasenzer, T. and Buljan, H. (2008), 'Free expansion of a lieb-liniger gas: Asymptotic form of the wave functions', *Physical Review A* **78**(5), 053602.

Kinoshita, T., Wenger, T. and Weiss, D. S. (2005), 'Local Pair Correlations in One-Dimensional Bose Gases', *Phys. Rev. Lett.* **95**(19), 190406.
URL: *http://link.aps.org/doi/10.1103/PhysRevLett.95.190406*

Kinoshita, T., Wenger, T. and Weiss, D. S. (2006), 'A quantum newton's cradle', *Nature* **440**(7086), 900.
URL: *https://www.nature.com/articles/nature04693*

Kitaev, A. (2009), Periodic table for topological insulators and superconductors, *in* 'AIP conference proceedings', Vol. 1134, American Institute of Physics, pp. 22–30.

Kitanine, N., Kozlowski, K., Maillet, J. M., Slavnov, N. and Terras, V. (2011), 'A form factor approach to the asymptotic behavior of correlation functions in critical models', *Journal of Statistical Mechanics: Theory and Experiment* **2011**(12), P12010.

Kitanine, N., Kozlowski, K., Maillet, J. M., Slavnov, N. and Terras, V. (2012), 'Form factor approach to dynamical correlation functions in critical models', *Journal of Statistical Mechanics: Theory and Experiment* **2012**(09), P09001.

Kitanine, N., Maillet, J. and Terras, V. (1999), 'Form factors of the xxz heisenberg spin-12 finite chain', *Nuclear Physics B* **554**(3), 647–678.

Klauser, A. and Caux, J.-S. (2011), 'Equilibrium thermodynamic properties of interacting two-component bosons in one dimension', *Physical Review A* **84**(3), 033604.

Klümper, A. and Pâţu, O. I. (2011), 'Efficient thermodynamic description of multicomponent one-dimensional bose gases', *Physical Review A* **84**(5), 051604.

Korepin, V. E., Bogoliubov, N. M. and Izergin, A. G. (1997), *Quantum inverse scattering method and correlation functions*, Vol. 3, Cambridge university press.

Krajnik, Ž., Ilievski, E. and Prosen, T. (2021), 'Breakdown of the large deviation principle in an integrable magnet', *arXiv preprint arXiv:2109.13088* .

Kudler-Flam, J., Nozaki, M., Ryu, S. and Tan, M. T. (2021), 'Entanglement of local operators and the butterfly effect', *Physical Review Research* **3**(3), 033182.

Kukuljan, I., Grozdanov, S. and Prosen, T. (2017), 'Weak quantum chaos', *Physical Review B* **96**(6), 060301.

Kurlov, D. V., Malikis, S. and Gritsev, V. (2021), 'Quasi-conserved charges in the perturbed spin-1/2 xxx model', *arXiv preprint arXiv:2107.04505* .

Kuwahara, T., Kato, K. and Brandão, F. G. (2020), 'Clustering of conditional mutual information for quantum gibbs states above a threshold temperature', *Physical Review Letters* **124**(22), 220601.

Lang, G., Hekking, F. and Minguzzi, A. (2017), 'Ground-state energy and excitation spectrum of the lieb-liniger model: accurate analytical results and conjectures about the exact solution', *SciPost Phys* **3**(003).

Larkin, A. and Ovchinnikov, Y. N. (1969), 'Quasiclassical method in the theory of superconductivity', *Sov Phys JETP* **28**(6), 1200–1205.

Laughlin, R. B. (1983), 'Anomalous quantum hall effect: an incompressible quantum fluid with fractionally charged excitations', *Physical Review Letters* **50**(18), 1395.

Lebowitz, J. and Percus, J. (1967), 'Kinetic equations and density expansions: exactly solvable one-dimensional system', *Physical Review* **155**(1), 122.

Li, C., Zhou, T., Mazets, I., Stimming, H.-P., Møller, F. S., Zhu, Z., Zhai, Y., Xiong, W., Zhou, X., Chen, X. et al. (2020), 'Relaxation of bosons in one dimension and the onset of dimensional crossover', *SciPost Physics* **9**(4), 058.

Li, H. and Haldane, F. D. M. (2008), 'Entanglement spectrum as a generalization of entanglement entropy: Identification of topological order in non-abelian fractional quantum hall effect states', *Physical review letters* **101**(1), 010504.

Lieb, E. H. and Liniger, W. (1963), 'Exact analysis of an interacting bose gas. i. the general solution and the ground state', *Phys. Rev.* **130**(4), 1605.
URL: *https://link.aps.org/doi/10.1103/PhysRev.130.1605*

Love, E. (1949), 'The electrostatic field of two equal circular co-axial conducting disks', *The Quarterly Journal of Mechanics and Applied Mathematics* **2**(4), 428–451.

Łydżba, P., Rigol, M. and Vidmar, L. (2020), 'Eigenstate entanglement entropy in random quadratic hamiltonians', *Physical review letters* **125**(18), 180604.

Maldacena, J., Shenker, S. H. and Stanford, D. (2016), 'A bound on chaos', *Journal of High Energy Physics* **2016**(8), 1–17.

Malvania, N., Zhang, Y., Le, Y., Dubail, J., Rigol, M. and Weiss, D. S. (2020), 'Generalized hydrodynamics in strongly interacting 1d bose gases', *arXiv preprint arXiv:2009.06651* .

Marino, M. and Reis, T. (2019), 'Exact perturbative results for the lieb–liniger and gaudin–yang models', *Journal of Statistical Physics* **177**(6), 1148–1156.

Medenjak, M. (2022), 'Operator spreading in quantum hardcore gases', *arXiv preprint arXiv:2201.00395* .

Medenjak, M., Nardis, J. D. and Yoshimura, T. (2020), 'Diffusion from Convection', *SciPost Phys.* **9**, 75.
URL: *https://scipost.org/10.21468/SciPostPhys.9.5.075*

Medvedyeva, M. V., Essler, F. H. and Prosen, T. (2016), 'Exact bethe ansatz spectrum of a tight-binding chain with dephasing noise', *Physical review letters* **117**(13), 137202.

Mei, Z., Vidmar, L., Heidrich-Meisner, F. and Bolech, C. (2016), 'Unveiling hidden structure of many-body wave functions of integrable systems via sudden-expansion experiments', *Physical Review A* **93**(2), 021607.

Minguzzi, A. and Gangardt, D. (2005), 'Exact coherent states of a harmonically confined tonks-girardeau gas', *Physical review letters* **94**(24), 240404.

Møller, F., Li, C., Mazets, I., Stimming, H.-P., Zhou, T., Zhu, Z., Chen, X. and Schmiedmayer, J. (2021), 'Extension of the generalized hydrodynamics to the dimensional crossover regime', *Physical Review Letters* **126**(9), 090602.

Møller, F. S. and Schmiedmayer, J. (2020), 'Introducing ifluid: a numerical framework for solving hydrodynamical equations in integrable models', *SciPost Phys* **8**, 041.

Moore, G. and Read, N. (1991), 'Nonabelions in the fractional quantum hall effect', *Nuclear Physics B* **360**(2-3), 362–396.

Moyal, J. E. (1949), Quantum mechanics as a statistical theory, *in* 'Mathematical Proceedings of the Cambridge Philosophical Society', Vol. 45, Cambridge University Press, pp. 99–124.

Muth, D., Unanyan, R. G. and Fleischhauer, M. (2011), 'Dynamical simulation of integrable and nonintegrable models in the heisenberg picture', *Phys. Rev. Lett.* **106**, 077202.
URL: *https://link.aps.org/doi/10.1103/PhysRevLett.106.077202*

Nguyen, P., Devakul, T., Halbasch, M. G., Zaletel, M. P. and Swingle, B. (2018), 'Entanglement of purification: from spin chains to holography', *Journal of High Energy Physics* **2018**(1), 1–41.

Noh, K., Jiang, L. and Fefferman, B. (2020), 'Efficient classical simulation of noisy random quantum circuits in one dimension', *Quantum* **4**, 318.

Olshanii, M. (1998), 'Atomic Scattering in the Presence of an External Confinement and a Gas of Impenetrable Bosons', *Phys. Rev. Lett.* **81**(5), 938–941.
URL: *http://link.aps.org/doi/10.1103/PhysRevLett.81.938*

Östlund, S. and Rommer, S. (1995), 'Thermodynamic limit of density matrix renormalization', *Physical review letters* **75**(19), 3537.

Palmai, T. and Konik, R. M. (2018), 'Quasilocal charges and the generalized gibbs ensemble in the lieb-liniger model', *Physical Review E* **98**(5), 052126.

Panfil, M. and Pawełczyk, J. (2019), 'Linearized regime of the generalized hydrodynamics with diffusion', *arXiv:1905.06257* .

Pâţu, O. I. and Klümper, A. (2015), 'Thermodynamics, density profiles, and correlation functions of the inhomogeneous one-dimensional spinor bose gas', *Physical Review A* **92**(4), 043631.

Percus, J. (1976), 'Equilibrium state of a classical fluid of hard rods in an external field', *Journal of Statistical Physics* **15**(6), 505–511.

Pethick, C. J. and Smith, H. (2008), *Bose–Einstein condensation in dilute gases*, Cambridge university press.

Pižorn, I. and Prosen, T. (n.d.), 'Operator space entanglement entropy in xy spin chains'.

Popov, V. N. (1977), 'Theory of one-dimensional bose gas with point interaction', *Teoreticheskaya i Matematicheskaya Fizika* **30**(3), 346–352.

Pozsgay, B. (2011), 'Mean values of local operators in highly excited bethe states', *Journal of Statistical Mechanics: Theory and Experiment* **2011**(01), P01011.

Pozsgay, B. (2014), 'Failure of the generalized eigenstate thermalization hypothesis in integrable models with multiple particle species', *Journal of Statistical Mechanics: Theory and Experiment* **2014**(9), P09026.

Pozsgay, B. (2020*a*), 'Algebraic construction of current operators in integrable spin chains', *Physical Review Letters* **125**(7), 070602.

Pozsgay, B. (2020*b*), 'Current operators in integrable spin chains: lessons from long range deformations', *SciPost Phys* **8**(016), 1910–12833.

Prolhac, S. (2017), 'Ground state energy of the δ-bose and fermi gas at weak coupling from double extrapolation', *Journal of Physics A: Mathematical and Theoretical* **50**(14), 144001.

Prosen, T. and Žnidarič, M. (2007), 'Is the efficiency of classical simulations of quantum dynamics related to integrability?', *Phys. Rev. E* **75**, 015202(R).
URL: *https://link.aps.org/doi/10.1103/PhysRevE.75.015202*

Prosen, T. and Pižorn, I. (2007), 'Operator space entanglement entropy in a transverse ising chain', *Physical Review A* **76**(3), 032316.

Protopopov, I., Gutman, D., Schmitteckert, P. and Mirlin, A. (2013), 'Dynamics of waves in one-dimensional electron systems: Density oscillations driven by population inversion', *Physical Review B* **87**(4), 045112.

Rauer, B., Grišins, P., Mazets, I. E., Schweigler, T., Rohringer, W., Geiger, R., Langen, T. and Schmiedmayer, J. (2016), 'Cooling of a one-dimensional bose gas', *Physical Review Letters* **116**(3), 030402.

Read, N. (2017), 'Compactly supported wannier functions and algebraic k-theory', *Physical Review B* **95**(11), 115309.

Read, N. and Green, D. (2000), 'Paired states of fermions in two dimensions with breaking of parity and time-reversal symmetries and the fractional quantum hall effect', *Physical Review B* **61**(15), 10267.

Read, N. and Rezayi, E. (1999), 'Beyond paired quantum hall states: Parafermions and incompressible states in the first excited landau level', *Physical Review B* **59**(12), 8084.

Reichel, J., Hänsel, W. and Hänsch, T. (1999), 'Atomic micromanipulation with magnetic surface traps', *Physical Review Letters* **83**(17), 3398.

Reichel, J. and Vuletic, V. (2011), *Atom chips*, John Wiley & Sons.

Reid, I. and Bertini, B. (2021), 'Entanglement barriers in dual-unitary circuits', *Physical Review B* **104**(1), 014301.

Rigol, M., Dunjko, V. and Olshanii, M. (2008), 'Thermalization and its mechanism for generic isolated quantum systems', *Nature* **452**(7189), 854–858.

Rigol, M., Dunjko, V., Yurovsky, V. and Olshanii, M. (2007), 'Relaxation in a completely integrable many-body quantum system: An ab initio study of the dynamics of the highly excited states of 1d lattice hard-core bosons', *Phys. Rev. Lett.* **98**(5), 050405.
URL: *https://link.aps.org/doi/10.1103/PhysRevLett.98.050405*

Rigol, M. and Muramatsu, A. (2005), 'Fermionization in an expanding 1d gas of hard-core bosons', *Physical review letters* **94**(24), 240403.

Robinson, N., Caux, J.-S. and Konik, R. (2016), 'Exact nonequilibrium dynamics of a class of initial states in one-dimensional two-component integrable quantum gases'.

Robinson, N. J. and Konik, R. M. (2017), 'Excitations in the yang–gaudin bose gas', *Journal of Statistical Mechanics: Theory and Experiment* **2017**(6), 063101.

Rozhkov, A. (2005), 'Fermionic quasiparticle representation of tomonaga-luttinger hamiltonian', *The European Physical Journal B-Condensed Matter and Complex Systems* **47**(2), 193–206.

Ruggiero, P., Brun, Y. and Dubail, J. (2019), 'Conformal field theory on top of a breathing one-dimensional gas of hard core bosons', *SciPost Phys.* **6**, 51.
URL: *https://scipost.org/10.21468/SciPostPhys.6.4.051*

Ruggiero, P., Calabrese, P., Doyon, B. and Dubail, J. (2020), 'Quantum generalized hydrodynamics', *Physical review letters* **124**(14), 140603.

Ruggiero, P., Calabrese, P., Doyon, B. and Dubail, J. (2021), 'Quantum generalized hydrodynamics of the tonks–girardeau gas: density fluctuations and entanglement entropy', *Journal of Physics A: Mathematical and Theoretical* **55**(2), 024003.

Ryu, S. and Takayanagi, T. (2006), 'Holographic derivation of entanglement entropy from the anti–de sitter space/conformal field theory correspondence', *Physical review letters* **96**(18), 181602.

Scalet, S. O., Alhambra, Á. M., Styliaris, G. and Cirac, J. I. (2021), 'Computable rényi mutual information: Area laws and correlations', *Quantum* **5**, 541.

Schemmer, M. and Bouchoule, I. (2018), 'Cooling a bose gas by three-body losses', *Physical review letters* **121**(20), 200401.

Schemmer, M., Bouchoule, I., Doyon, B. and Dubail, J. (2019), 'Generalized hydrodynamics on an atom chip', *Phys. Rev. Lett.* **122**(9), 090601.
URL: *https://link.aps.org/doi/10.1103/PhysRevLett.122.090601*

Schollwöck, U. (2005), 'The density-matrix renormalization group', *Reviews of modern physics* **77**(1), 259.

Schuch, N., Wolf, M. M., Verstraete, F. and Cirac, J. I. (2008), 'Entropy scaling and simulability by matrix product states', *Physical review letters* **100**(3), 030504.

Scopa, S., Calabrese, P. and Dubail, J. (2022), 'Exact hydrodynamic solution of a double domain wall melting in the spin-1/2 xxz model', *SciPost Physics* **12**(6), 207.

Scopa, S., Krajenbrink, A., Calabrese, P. and Dubail, J. (2021), 'Exact entanglement growth of a one-dimensional hard-core quantum gas during a free expansion', *Journal of Physics A: Mathematical and Theoretical* **54**(40), 404002.

Scopa, S., Piroli, L. and Calabrese, P. (2020), 'One-particle density matrix of a trapped lieb–liniger anyonic gas', *Journal of Statistical Mechanics: Theory and Experiment* **2020**(9), 093103.

Shashi, A., Glazman, L. I., Caux, J.-S. and Imambekov, A. (2011), 'Nonuniversal prefactors in the correlation functions of one-dimensional quantum liquids', *Physical Review B* **84**(4), 045408.

Shashi, A., Panfil, M., Caux, J.-S. and Imambekov, A. (2012), 'Exact prefactors in static and dynamic correlation functions of one-dimensional quantum integrable models: Applications to the calogero-sutherland, lieb-liniger, and x x z models', *Physical Review B* **85**(15), 155136.

Slavnov, N. A. (1989), 'Calculation of scalar products of wave functions and form factors in the framework of the algebraic bethe ansatz', *Teoreticheskaya i Matematicheskaya Fizika* **79**(2), 232–240.

Spohn, H. (2012), *Large scale dynamics of interacting particles*, Springer Science & Business Media.

Spohn, H. (2020), 'Collision rate ansatz for the classical toda lattice', *Physical Review E* **101**(6), 060103.

Szymańska, M., Keeling, J. and Littlewood, P. (2006), 'Nonequilibrium quantum condensation in an incoherently pumped dissipative system', *Physical review letters* **96**(23), 230602.

Takahashi, M. (1975), 'On the validity of collective variable description of bose systems', *Progress of Theoretical Physics* **53**(2), 386–399.

Tavis, M. and Cummings, F. W. (1968), 'Exact solution for an n-molecule—radiation-field hamiltonian', *Physical Review* **170**(2), 379.

Temnov, V. V. and Woggon, U. (2005), 'Superradiance and subradiance in an inhomogeneously broadened ensemble of two-level systems coupled to a low-q cavity', *Physical review letters* **95**(24), 243602.

Tilloy, A. and Cirac, J. I. (2019), 'Continuous tensor network states for quantum fields', *Physical Review X* **9**(2), 021040.

Tsvelik, A. M. (2007), *Quantum field theory in condensed matter physics*, Cambridge university press.

van Amerongen, A. H., van Es, J. J. P., Wicke, P., Kheruntsyan, K. V. and van Druten, N. J. (2008), 'Yang-Yang Thermodynamics on an Atom Chip', *Phys. Rev. Lett.* **100**(9), 090402.
URL: *http://link.aps.org/doi/10.1103/PhysRevLett.100.090402*

Van den Berg, R., Wouters, B., Eliëns, S., De Nardis, J., Konik, R. and Caux, J.-S. (2016), 'Separation of time scales in a quantum newton's cradle', *Physical review letters* **116**(22), 225302.

Vidal, G. and Werner, R. F. (2002), 'Computable measure of entanglement', *Physical Review A* **65**(3), 032314.

Vidmar, L. and Rigol, M. (2016), 'Generalized gibbs ensemble in integrable lattice models', *Journal of Statistical Mechanics: Theory and Experiment* **2016**(6), 064007.

von Keyserlingk, C. W., Rakovszky, T., Pollmann, F. and Sondhi, S. L. (2018), 'Operator hydrodynamics, otocs, and entanglement growth in systems without conservation laws', *Phys. Rev. X* **8**, 021013.
URL: *https://link.aps.org/doi/10.1103/PhysRevX.8.021013*

Vu, D.-L. and Yoshimura, T. (2019), 'Equations of state in generalized hydrodynamics', *SciPost Phys.* **6**(2), 023.
URL: *https://arxiv.org/abs/1809.03197*

Wahl, T. B., Tu, H.-H., Schuch, N. and Cirac, J. I. (2013), 'Projected entangled-pair states can describe chiral topological states', *Physical review letters* **111**(23), 236805.

Wang, H. and Zhou, T. (2019), 'Barrier from chaos: operator entanglement dynamics of the reduced density matrix', *Journal of High Energy Physics* **2019**(12), 1–44.

Wei, D., Rubio-Abadal, A., Ye, B., Machado, F., Kemp, J., Srakaew, K., Hollerith, S., Rui, J., Gopalakrishnan, S., Yao, N. Y. et al. (2021), 'Quantum gas microscopy of kardar-parisi-zhang superdiffusion', *arXiv preprint arXiv:2107.00038* .

Wellnitz, D., Preisser, G., Alba, V., Dubail, J. and Schachenmayer, J. (2022), 'The rise and fall, and slow rise again, of operator entanglement under dephasing', *arXiv preprint arXiv:2201.05099* .

White, S. R. (1992), 'Density matrix formulation for quantum renormalization groups', *Physical review letters* **69**(19), 2863.

Wigner, E. P. (1955), 'Lower limit for the energy derivative of the scattering phase shift', *Physical Review* **98**(1), 145.

Wilson, J. M., Malvania, N., Le, Y., Zhang, Y., Rigol, M. and Weiss, D. S. (2020), 'Observation of dynamical fermionization', *Science* **367**(6485), 1461–1464. Publisher: American Association for the Advancement of Science Section: Report.
URL: *https://science.sciencemag.org/content/367/6485/1461*

Wouters, B., De Nardis, J., Brockmann, M., Fioretto, D., Rigol, M. and Caux, J.-S. (2014), 'Quenching the anisotropic heisenberg chain: exact solution and generalized gibbs ensemble predictions', *Physical review letters* **113**(11), 117202.

Yang, C.-N. (1967), 'Some exact results for the many-body problem in one dimension with repulsive delta-function interaction', *Physical Review Letters* **19**(23), 1312.

Yang, C.-N. and Yang, C. P. (1969), 'Thermodynamics of a one-dimensional system of bosons with repulsive delta-function interaction', *Journal of Mathematical Physics* **10**(7), 1115–1122.

Yoshimura, T. and Spohn, H. (2020), 'Collision rate ansatz for quantum integrable systems', *SciPost Phys.* **9**, 40.
URL: *https://scipost.org/10.21468/SciPostPhys.9.3.040*

Zamolodchikov, A. B. (1990), 'Thermodynamic bethe ansatz in relativistic models: Scaling 3-state potts and lee-yang models', *Nuclear Physics B* **342**(3), 695–720.

Zanardi, P. (2001), 'Entanglement of quantum evolutions', *Phys. Rev. A* **63**, 040304(R).
URL: *https://link.aps.org/doi/10.1103/PhysRevA.63.040304*

Zanardi, P., Zalka, C. and Faoro, L. (2000), 'Entangling power of quantum evolutions', *Physical Review A* **62**(3), 030301.

Zhang, Z., Lee, C. H., Kumar, R., Arnold, K., Masson, S. J., Grimsmo, A., Parkins, A. and Barrett, M. (2018), 'Dicke-model simulation via cavity-assisted raman transitions', *Physical Review A* **97**(4), 043858.

Part IV

Appendices

Appendix A

Reproduction of selected publications

Note: the manuscript used for the Habilitation defense contained reproductions of the following scientific articles. I do not reproduce them in this version of the manuscript made available online, but the preprints of all these articles can be found on the arXiv.

A.1 Main publications on Generalized Hydrodynamics

- M.Schemmer, I. Bouchoule, B. Doyon and J. Dubail, "Generalized HydroDynamics on an Atom Chip", Phys. Rev. Lett. 122, 090601 (2019), arXiv:1810.07170
- N. Malvania, Y. Zhang, Y. Le, J. Dubail, M. Rigol, D. Weiss, "Generalized hydrodynamics in strongly interacting 1D Bose gases", Science 373, 1129 (2021), arXiv:2009.06651
- B. Doyon, J. Dubail, R. Konik, T. Yoshimura, "Large-scale description of interacting one- dimensional Bose gases: generalized hydrodynamics supersedes conventional hydrodynamics", Phys. Rev. Lett. 119, 195301 (2017), arXiv:1704.04151
- J.-S. Caux, B. Doyon, J. Dubail, R. Konik, T. Yoshimura, "Hydrodynamics of the interacting Bose gas in the Quantum Newton Cradle setup", Scipost Phys. 6, 070 (2019), arXiv:1711.00873

A.2 Main publications on quantum fluctuations of 1D gases

- P. Ruggiero, P. Calabrese, B. Doyon, J. Dubail, "Quantum Generalized Hydrodynamics", Phys. Rev. Lett. 124, 140603 (2020), arXiv:1910.00570

- J. Dubail, J.-M. Stéphan, J. Viti et P. Calabrese, "Conformal Field Theory for Inhomogeneous One-dimensional Quantum Systems: the Example of Non-Interacting Fermi Gases", SciPost Phys. 2, 002 (2017). arXiv:1606.04401

- Y. Brun and J. Dubail, "The Inhomogeneous Gaussian Free Field, with application to ground state correlations of trapped 1d Bose gases", SciPost Phys. 4, 037 (2018). arXiv:1712.05262

A.3 Main publications on Operator Entanglement

- V. Alba, J. Dubail, M. Medenjak, "Operator Entanglement in Interacting Integrable Quantum Systems: the Case of the Rule 54 Chain", Phys. Rev. Lett. 122, 250603 (2019), arXiv:1901.04521

- J. Dubail, "Entanglement scaling of operators: a conformal field theory approach, with a glimpse of simulability of long-time dynamics in 1+1d", J. Phys. A: Math. Theor. 50 234001 (2017). arXiv:1612.08630

A.4 Main publications on chiral topological phases

- J. Dubail et N. Read, "Tensor network trial states for chiral topological phases in two dimensions and a no-go theorem in any dimension", Phys. Rev. B 92, 205307 (2015), arXiv: 1307.7726

- J. Dubail, N. Read et E. Rezayi, "Edge state inner products and real-space entanglement spectrum of trial quantum Hall states", Phys. Rev. B 86, 245310 (2012), arXiv:1207.7119

Appendix B

Curriculum, list of publications and of communications

Curriculum Vitae

Jérôme DUBAIL

Born November 24, 1984 in Mulhouse, France. French nationality.

Married, two children born 2015 and 2017.

POSITIONS

Since 2013 CNRS permanent researcher (chargé de recherche) at the Laboratoire de Physique et Chimie Théoriques (LPCT), CNRS and University of Lorraine, Nancy, France.
(Before the LPCT was created in 2018, my research team was affiliated with the Institut Jean Lamour, another Institute in Nancy).

2010–2013 Postdoctoral fellow in the Condensed Matter Theory Group, Yale University, New Haven, United States.
I held a 'Yale Postdoctoral Prize Fellowship' (one such Fellowship awarded per year) and worked mostly with Nick Read.

EDUCATION

2007-2010 PhD from Université Paris Sud-Orsay, prepared at the Institute for Theoretical Physics (IPhT), CEA Saclay, France.
My PhD work was supervised by Hubert Saleur (CEA Saclay) and Jesper Jacobsen (Ecole Normale Supérieure, Paris).

2007-2006 Master in Theoretical Physics, Physics Department, Ecole Normale Supérieure, Paris, France. Highest honours, rank: 1.

2003-2006 Undergraduate studies at Ecole Polytechnique, Palaiseau, France.

ACADEMIC PROFILE

I am a theoretical physicist working on low-dimensional quantum many-body physics. Over the past five years I have been focusing mainly on the out-of-equilibrium dynamics of one-dimensional cold atom gases, in particular on a new theory called 'Generalized hydrodynamics', in collaboration with other theorists in Europe and with experimentalists in France and in the US. I have also been interested in the simulability of quantum many-body systems with Tensor Networks methods, and on how to characterize it by their entanglement properties, in particular by a computable quantity dubbed 'operator entanglement'.

Before that, I worked on topological insulators and superconductors and on the fractional quantum Hall effect, with a strong focus on entanglement, and on one-dimensional quantum critical points in spin chains. I also obtained results on Tensor Networks, in particular on the fundamental problem of Tensor Networks for chiral topological phases.

During my PhD I worked on classical loop gases in two dimensions and on their relation with critical interfaces of percolation clusters or magnetic domains in the Ising model, and with the Schramm-Löwner evolution.

I have **co-authored ∽50 papers**, published in such journals as Science, Phys. Rev. Lett., Scipost, Eur. Phys. Lett., Phys. Rev. A, Phys. Rev. B, J. Stat. Mech., J. Phys. A, J. High Energy Phys., Nucl. Phys. B, etc. For bibliometrics, see my Google Scholar profile.

I have been invited to give presentations in ∽**30 international conferences and workshops**, and ∽**40 seminars** in various research groups and Physics Departments, mainly in Europe and in the United States.

RESEARCH GRANTS, AWARDS

- PI of CNRS International Emerging Action project "QuDOD" (2021-2022). 10 000 euros.

- member of the project "QUADY" (2021-2024) funded by the Agence Nationale de la Recherche (main PI: Isabelle Bouchoule). Total amount of the project: 250 000 euros.

- member of the project "DIMERS" (2019-2022) funded by the Agence Nationale de la Recherche (PIs: Cédric Boutillier and Jérémie Bouttier). Total amount of the project: approx. 350 000 euros.

- PI of Interdisciplinary challenge "InFiNiTi" of CNRS (2018). 6000 euros.

- Starting Funds from the Conseil Regional and the Universite de Lorraine (2015-2016). 20 000 euros.

- PI of Interdisciplinary challenge " InPhyNiTi" of CNRS (2015). 4000 euros.

- Outstanding Referee for Nucl. Phys. B (2014)

- Laureate of the TOR program of the French Ambassy in Sweden (2014) (five laureates among more than a hundred candidates, for a project between France and Sweden). 2000 euros.

- Invited Scientist at the Max Planck Institut für Physik komplexer Systeme, Dresden, for 2 months in October and November 2014.

- Yale Postdoctoral Prize Fellowship, awarded by the Physics Department at Yale University 2010-2013 (150 000 US dollars)

-J. Phys. A Best Paper Prize 2011, together with J. Jacobsen and H. Saleur, for the paper 'Critical exponents of domain walls in the two-dimensional Potts model'

SUPERVISION OF STUDENTS

PhD students

Francois Riggio (PhD started in 2020, defense expected 2023). Co-supervised with Dragi Karevski (LPCT). 1 joint publication.

Yannis Brun (PhD defended in 2019, now in the private sector). Co-supervised with Christophe Chatelain. 4 joint publications.

Master students

Yasser Bezzaz, April 2021 to July 2021 (now a PhD student in Birmingham)

Francois Riggio, January 2020 to July 2020 (he is now doing his PhD with me)

Oscar le Noan, January 2019 to July 2019 (then left academia to work for an NGO)

Louise Budzinski, from September 2016 to February 2017 (then did her PhD at Ecole Normale Supérieure, Paris). 1 joint publication.

Yannis Brun: from January 2016 to July 2016 (then did his PhD with me)

Vendana Revathi Venkateswaran: January 2015 to February 2015 (then did her PhD at the Max Planck Institut for Evolutionary Biology, Plön, Germany)

Joel Moreno, from January 2015 to February 2015 (graduated, now in the private sector)

TEACHING

2021-2022: Master 2 - fundamental physics at Université de Lorraine. 'Introduction to theoretical physics: classical and quantum phase transitions' (16 hours)

2020-2021: Master 2 - fundamental physics at Université de Lorraine. 'Introduction to theoretical physics: classical and quantum phase transitions' (16 hours)

Lectures in international Winter/Summer Schools:

2019: Winter School 'Statistical Field Theories' at Galileo Galilei Institute, Florence, Italy. 'Three lectures on classical and quantum hydrodynamics applied to 1D trapped gases' (8 hours)

2017: Summer School 'Exact Methods in Low Dimensional Statistical Physics' in Cargèse, France. 'CFT and chiral topological phases: an introduction' (2 hours)

RESPONSIBILITIES

Local

- Head of the 'Dynamics and Symmetry' team, one of the five scientific teams that compose the LPCT, since 2018. The team has 12 permanent researchers, plus PhD and master students.

- Member of the Scientific Council of the LPCT since 2018.

International

- Since 2019, I am a member of the Editorial Board of Journal of Physics A

ORGANIZATION OF CONFERENCES, WORKSHOPS, SCHOOLS

2020 - … I am a co-organizer of the Winter School 'Statistical Field Theories' held yearly at the Galileo Galilei Institute in Florence, Italy.

2022 I co-organized a 4-week international program «Programmable Quantum Matter: Many-Body Physics in the Era of Quantum Advantage», at the Aspen Center of Physics, Aspen, Colorado, Etats-Unis (with S. Gopalakrishnan, A. Kaufman, M. Schleier-Smith, D. Stamper-Kurn).

2019 I co-organized a 3-week international workshop at the International Institute of Physics, Natal, Brazil, on the 'Emergent hydrodynamics in quantum systems' (with B. Doyon, J. Viti, G. Mussardo, M. Rajabpour)

2018	I co-organized a 2-day conference on low-dimensional quantum systems (with C. Chatelain and D. Karevski from Nancy, G. Morigi from Saarbrücken, T. Schmidt from Luxembourg)
2018	I co-organized a 'topical day' on hydrodynamics of quantum systems at the Ecole Normale Supérieure, Paris (with D. Bernard and M. Fagotti)
2014-15-16 -18-19-20 -21-22	Together with my colleagues from Nancy and Metz, I co-organize our yearly 3-day conference 'Statistical Physics and Low-Dimensional Systems' held at the Abbaye des Prémontrés in Pont-à-Mousson, France.
2014-15-16	I organized three editions of a Topical School in Theoretical Physics in Nancy, aimed at PhD students from the Université de Lorraine, and other neighboring universities (with participants from Paris, Lyon, Strasbourg, Luxembourg, Toulouse, Sarrebrücken, Utrecht). The School lasted for 3 days, with approximately 25 participants. The topic was 'topological phases' in 2014 (lectures by Nicolas Regnault, Gunnar Möller, Andreas Schnyder), 'out-of-equilibrium quantum dynamics' in 2015 (lectures by Benjamin Doyon, Ivan Protopopov, Mario Collura), and 'Many-body localization' in 2016 (lectures by Antonello Scardicchio, Fabien Alet, Gabriel Lemarié).

OTHER ACTIVITIES

- I am a referee for several journals, including Phys. Rev. Lett. Phys. Rev. X, Scipost, Phys. Rev. B, Phys. Rev. A, J. Stat. Mech., Nucl. Phys. B, Annals of Physics, and others.

- I have reviewed grant applications for national funding agencies, including the french Agence Nationale de la Recherche, the belgian FWO (Fonds Wetenschappelijk Onderzoek), and the polish national agency

- in 2021, I co-edited a Special Issue of J. Phys. A on the 'Hydrodynamics of low-dimensional quantum systems' together with A. Abanov (Stony Brook, USA), A. Kamenev (U. Minnesota, USA), B. Doyon (King's College, UK), and H. Spohn (Munich, Germany).

PARTICIPATION TO PHD COMMITTEES

- Nadir Samos, Universidad Autonoma de Madrid, Spain, February 2022. Advisors: German Sierra and J. Rodriguez-Laguna

- Romain Daviet, Sorbonne Université, Paris, France, June 2021. Advisor: Nicolas Dupuis.

- Yannis Brun, Université de Lorraine, Nancy, France, Septembre 2019. Advisor: myself

- Maximilian Schemmer, Université Paris-Saclay, Palaiseau, France, June 2019. Advisor: Isabelle Bouchoule

- Thomas Dupic, Université Pierre et Marie Curie, Paris, France, October 2018. Advisors: Benoît Estienne and Yacine Ikhlef

- Alvise Bastianello, SISSA, Trieste, Italy, October 2018. Advisor: Giuseppe Mussardo

- Matthias Bal, University of Ghent, Belgium, February 2018. Advisor: Frank Verstraete

List of publications

Breakdown of publications

Publications in peer-reviewed journals	Science	1
	Physical Review Letters	9
	SciPost Physics	8
	Euro Physics Letters	2
	Phys. Rev. B + PRB Rapid Comm.	5 + 1
	Phys. Rev. A	1
	J. Phys. A: Math. Theor.	7
	J. of Statistical Mechanics	8
	J. of High Energy Physics	1
	J. of Statistical Physics	1
	Nucl. Phys. B	4
Under review (with preprints on the arXiv)		3
Other	1 invited viewpoint in Physics (journal for highlights of the APS) 2 sets of lecture notes at Summer Schools, available on the web	

Published papers

[48] D. Wellnitz, G. Preisser, V. Alba, J. Dubail, J. Schachenmayer, "The rise and fall, and slow rise again, of operator entanglement under dephasing", Phys. Rev. Lett., in press, arXiv:2201.05099

[47] S. Scopa, P. Calabrese, J. Dubail, "Exact hydrodynamic solution of a double domain wall melting in the spin-1/2 XXZ model", Scipost Phys. 12, 207 (2022), arXiv:2109.05249

[46] I. Bouchoule, J. Dubail, "Generalized Hydrodynamics in the 1D Bose gas: theory and experiments", Review article for J. Stat. Mech. Special Issue on Generalized Hydrodynamics, J. Stat. Mech. (2022) 014003, arXiv:2108.02509

[45] P. Ruggiero, P. Calabrese, B. Doyon, J. Dubail, "Quantum Generalized Hydrodynamics of the Tonks-Girardeau gas: density fluctuations and entanglement entropy", J. Phys. A: Math. Theor. 55 024003 (2022), arXiv:2107.05655

[44] P. Calabrese, J. Dubail, S. Murciano, "Symmetry-resolved entanglement entropy in Wess-Zumino-Witten models", J. High Energy Physics 2021, 67 (2021), arXiv:2106.15946

[43] J. Dubail, T. Botzung, J. Schachenmayer, G. Pupillo, D. Hagenmuller, "Large Random Arrowhead Matrices: Multifractality, Semi-Localization, and Protected Transport in Disordered Quantum Spins Coupled to a Cavity", Phys. Rev. A 105, 023714 (2022), arXiv:2105.08444

[42] S.Scopa, A. Krajenbrink, P. Calabrese, J. Dubail, “Exact entanglement growth of a one-dimensional hard-core quantum gas during a free expansion”, J. Phys. A: Math. Theor. 54, 404002 (2021), arXiv:2105.05054

[41] I.Bouchoule, J. Dubail, “Breakdown of Tan's relation in lossy one-dimensional Bose gases”, Phys. Rev. Lett. 126, 160603 (2021), arXiv:2011.13250

[40] N. Malvania, Y. Zhang, Y. Le, J. Dubail, M. Rigol, D. Weiss, “Generalized hydrodynamics in strongly interacting 1D Bose gases”, Science 373, 1129 (2021), arXiv:2009.06651

[39] I. Bouchoule, B. Doyon, J. Dubail, “The effect of atom losses on the distribution of rapidities in the one-dimensional Bose gas”, SciPost Phys. 9, 044 (2020), arXiv:2006.03583

[38] T. Botzung, D. Hagenmuller, S. Schütz, J. Dubail, G. Pupillo, J. Schachenmayer, “Dark state semilocalization of quantum emitters in a cavity”, Phys. Rev. B 102, 144202 (2020), arXiv:2003.07179

[37] M. Collura, A. de Luca, P. Calabrese, J. Dubail, “Domain-wall melting in the spin-1/2 XXZ spin chain: emergent Luttinger liquid with fractal quasi-particle charge”, Phys. Rev. B 102, 180409(R) 2020, arXiv:2001.04948

[36] A. Bastianello, J. Dubail, J.-M. Stéphan, “Entanglement entropies of inhomogeneous Luttinger liquids”, J. Phys. A: Math. Theor.53 155001 (2020), arXiv:1910.09967

[35] P. Ruggiero, P. Calabrese, B. Doyon, J. Dubail, “Quantum Generalized Hydrodynamics”, Phys. Rev. Lett. 124, 140603 (2020), arXiv:1910.00570

[34] T. Botzung, D. Hagenmüller, G. Masella, J. Dubail, N. Defenu, A. Trombettoni, G. Pupillo, “Effects of energy extensivity on the quantum phases of long-range interacting systems”, Phys. Rev. B 103, 155139 (2021), arXiv:1909.12105

[33] P. Ruggiero, Y. Brun, J. Dubail, “Conformal field theory on top of a breathing one-dimensional gas of hard core bosons”, Scipost Phys. 6, 051 (2019), arXiv:1901.08132.

[32] V. Alba, J. Dubail, M. Medenjak, “Operator Entanglement in Interacting Integrable Quantum Systems: the Case of the Rule 54 Chain”, Phys. Rev. Lett. 122, 250603 (2019), arXiv:1901.04521.

[31] M.Schemmer, I. Bouchoule, B. Doyon and J. Dubail “Generalized HydroDynamics on an Atom Chip”, Phys. Rev. Lett. 122, 090601 (2019), arxiv:1810.07170.

[30] E. Granet, L. Budzynski, J. Dubail, J. Jacobsen, “Inhomogeneous Gaussian Free Field inside the interacting arctic curve”, J. Stat. Mech. (2019) 013102, arXiv:1807.07927.

[29] E. Basor, J. Dubail, T. Emig, R. Santachiara, “Modified Szego-Widom Asymptotics for Block Toeplitz Matrices with Zero Modes”, J. Stat. Phys. (2019) 174, 28. arXiv:1806.09494

[28] Y. Brun and J. Dubail, “The Inhomogeneous Gaussian Free Field, with application to ground state correlations of trapped 1d Bose gases”, SciPost Phys. 4, 037 (2018). arXiv:1712.05262

[27] J.-S. Caux, B. Doyon, J. Dubail, R. Konik, T. Yoshimura, “Hydrodynamics of the interacting Bose gas in the Quantum Newton Cradle setup”, Scipost Phys. 6, 070 (2019), arXiv:1711.00873.

[26] J. Dubail, J.-M. Stéphan, P. Calabrese, “Emergence of curved light-cones in a class of inhomogeneous Luttinger liquids”, SciPost Phys. 3, 019 (2017). arXiv:1705.00679

[25] B. Doyon, J. Dubail, R. Konik, T. Yoshimura, “Large-scale description of interacting one-dimensional Bose gases: generalized hydrodynamics supersedes conventional hydrodynamics”, Phys. Rev. Lett. 119, 195301 (2017). arXiv:1704.04151

[24] Y. Brun and J. Dubail, “One-particle density matrix of trapped one-dimensional impenetrable bosons from conformal invariance”, SciPost Phys. 2, 012 (2017). arXiv:1701.02248

[23] J. Dubail, “Entanglement scaling of operators: a conformal field theory approach, with a glimpse of simulability of long-time dynamics in 1+1d”, J. Phys. A: Math. Theor. 50 234001 (2017). arXiv:1612.08630

[22] J. Rodriguez-Laguna, J. Dubail, G. Ramirez, P. Calabrese et G. Sierra, “More on the rainbow chain: entanglement, space-time geometry and thermal states”, J. Phys. A: Math. Theor. 50 164001 (2017). arXiv:1611.08559

[21] J. Dubail, R. Santachiara, T. Emig, “Conformal field theory of critical Casimir forces between surfaces with alternating boundary conditions in two dimensions”, J. Stat. Mech. (2017) 033201. arXiv:1611.04814

[20] J. Dubail, J.-M. Stéphan, J. Viti et P. Calabrese, “Conformal Field Theory for Inhomogeneous One-dimensional Quantum Systems: the Example of Non-Interacting Fermi Gases”, SciPost Phys. 2, 002 (2017). arXiv:1606.04401

[19] N. Allegra, J. Dubail, J.-M. Stéphan, J. Viti, “Inhomogeneous field theory inside the arctic circle”, J. Stat. Mech. (2016) 053108. arXiv:1512.02872

[18] J. Viti, J.-M. Stéphan, J. Dubail et M. Haque, “Inhomogeneous quenches in a fermionic chain: exact results”, EuroPhysics Letters 115 (2016) 40011. arXiv:1507.08132

[17] J. Dubail, R. Santachiara et T. Emig, “Critical Casimir Force between Inhomogeneous Boundaries”, EuroPhysics Letters 112 (2015) 66004. arXiv:1505.02145

[16] R. Bondesan, J. Dubail, A. Faribault et Y. Ikhlef, “Chiral SU(2)_k currents as local operators in vertex models and spin chains”, J. Phys. A: Math. Theor. 48 (2015) 065205. arXiv:1409.8590

[15] J. Dubail et N. Read, “Tensor network trial states for chiral topological phases in two dimensions and a no-go theorem in any dimension”, Phys. Rev. B 92, 205307 (2015). arXiv:1307.7726

[14] J.-M. Stéphan et J. Dubail, “Logarithmic corrections to the free energy from sharp corners with angle 2pi”, J. Stat. Mech. (2013) P09002. arXiv:1303.3633

[13] J. Dubail, N. Read et E. Rezayi, “Edge state inner products and real-space entanglement spectrum of trial quantum Hall states”, Phys. Rev. B 86, 245310 (2012). arXiv:1207.7119

[12] J. Dubail, N. Read et E. Rezayi, “Real-space entanglement spectrum of quantum Hall systems”, Phys. Rev. B 85, 115321 (2012). arXiv:1111.2811

[11] R. Bondesan, J. Dubail, J. Jacobsen et H. Saleur,“Conformal boundary state for the rectangular geometry”, Nucl. Phys. B 862, 553-575 (2012). arXiv:1110.6861

[10] J.-M. Stéphan et J. Dubail, “Local quantum quenches in critical one-dimensional systems: entanglement, the Loschmidt echo, and light-cone effects”, J. Stat. Mech. (2011) P08019, arXiv:1105.4846

[9] J. Dubail et N. Read, “Entanglement spectra of complex paired superfluids”, Phys. Rev. Lett. 107, 157001 (2011), arXiv:1105.4808

[8] J. Dubail et J.-M. Stéphan, “Universal behavior of a bipartite fidelity at quantum criticality”, J. Stat. Mech. (2011) L03002, arXiv:1010.3716

[7] J. Dubail, J. Jacobsen et H. Saleur, “Bulk and boundary critical behaviour of thin and thick domain walls in the two-dimensional Potts model”, J. Stat. Mech. (2010) P12026 , arXiv:1010.1700

[6] J. Dubail, J. Jacobsen et H. Saleur, “Critical exponents of domain walls in the two-dimensional Potts model”, J. Phys. A: Math. Theor. 43 482002, arXiv:1008.1216

[5] J. Dubail, J. Jacobsen et H. Saleur, “Conformal field theory at central charge c=0: a measure of the indecomposability (b) parameters”, Nucl. Phys. B 834 399-422 (2010), arXiv:1001.1151

[4] J. Dubail, J. Jacobsen et H. Saleur, “Exact solution of the anisotropic special transition in the O(n) model in 2D”, Phys. Rev. Lett. 103 (2009) 145701, arXiv:0909.2949

[3] J. Dubail, J. Jacobsen et H. Saleur, “Conformal boundary conditions in the critical O(n) model and dilute loop models”, Nucl. Phys. B 827, 457-502 (2010). arXiv:0905.1382

[2] J. Dubail, J. Jacobsen et H. Saleur, “Conformal two-boundary loop model on the annulus”, Nucl. Phys. B 813, 430-459 (2009), arXiv:0812.2746

[1] A. Saint-Jalmes, S. Marze, H. Ritacco, D. Langevin, S. Bail, J. Dubail, L. Guingot, G. Roux, P. Sung, and L. Tosini, “Diffusive liquid propagation in porous and elastic materials: the case of foams under microgravity conditions” , Phys. Rev. Lett. 98, 058303 (2007).

arXiv preprints, under review

[51] A. Rath, V.Vitale, S. Murciano, M. Votto, J. Dubail, R. Kueng, C. Branciard, P. Calabrese, B. Vermersch, “Entanglement barrier and its symmetry resolution: theory and experiment”, arXiv:2209.04393

[50] I. Bouchoule, J. Dubail, L. Dubois, D. Gangardt, “Relaxation of phonons in the Lieb-Liniger gas by dynamical refermionization”, arXiv:2206.00112

[49] F. Riggio, Y. Brun, A. Faribault, D. Karevski, J. Dubail, “Gradient corrections to the local density approximation in the one-dimensional Bose gas”, arXiv:2204.06658

Other

A Viewpoint on two articles by O. Castro-Alvaredo, B. Doyon, T. Yoshimura and by B. Bertini, M. Collura, J. de Nardis, M. Fagotti published in PRX and PRL:

[A1] J. Dubail, “A More Efficient Way to Describe Interacting Quantum Particles in 1D”, Physics 9, 153 (2016)

Lecture notes (available on the web)

[A2] “CFT and chiral topological phases, an introduction”, notes de cours pour l'école “Exact Methods in Low-Dimensional Statistical Physics”, Cargèse, France (2017)

[A3] "Three lectures on classical and quantum hydrodynamics applied to trapped 1d quantum gases", notes de cours pour l'école "Lectures on Statistical Field Theories", Florence, Italie (2019)

List of presentations

Invited presentations in international conferences and workshops

September 2022	workshop "Mathematical developments in Tensor Networks", Schrödinger Institut, Vienna, Austria
June 2022	conference "Many-body quantum systems in the presence of an environment", Cergy-Pontoise, France
April 2022	workshop 'Randomness, integrability and universality', GGI Florence, Italy
March 2022	invited talk at APS March Meeting, Chicago, USA
September 2021	conference 'Universality in out-of-equilibrium quantum systems', KITP, Santa Barbara, California, USA (online)
September 2021	Birthday conference 'Hubert Saleur is 60', CEA Saclay, France
November 2020	online conference 'CoolMe' organised by the 'Groupement de Recherche Atomes Froids', ENS Lyon, France
June 2020	online conference 'Out-of-equilibrium integrable systems and beyond', ICTP, Trieste, Italy
November 2019	workshop 'Out-of-equilibrium systems, many-body localization, hydrodynamics', Bangalore, India
September 2019	conference 'Entangle This IV', Madrid, Spain
June 2019	conference 'Low-Dimensional Quantum Systems', Amsterdam, Netherlands
February 2019	invited lecture, Winter School 'Statistical Field Theory', GGI Florence, Italy
November 2018	conference 'Eniqma', ENS Lyon, France
September 2018	conference 'Non-equilibrium behaviour of isolated classical and quantum systems', SISSA Trieste, Italy
Juillet 2018	workshop «Small and medium sized quantum systems», Benasque, Spain
Juin 2018	conference 'Entanglement in Quantum Systems', GGI Florence, Italy
Avril 2018	workshop 'Quantum Paths', Schrödinger Insitut, Vienna, Austria
November 2017	conference 'Eniqma, Entanglement and Interactions in Cold Atoms', Lille, France
July 2017	invited lecture, Summer School 'Exact methods in low-dimensional systems', Cargèse, France

September 2016	workshop and summer school “Quantum integrable systems, CFTs and stochastic processes”, Cargèse, France
May 2016	workshop “From quantum field theories to numerical methods”, Nordita, Stockholm, Suède
December 2015	workshop “Geometric aspects of the Quantum Hall Effect”, Cologne University, Allemagne
March 2015	workshop “Many-body Dynamics out of Equilibrium”, MPIPKS Dresden, Allemagne
September 2014	workshop “Numerical and analytical methods for strongly correlated systems”, Benasque, Espagne
August 2014	workshop “Topological phases of matter”, Schrödinger Institut, Vienna, Austria
Juin 2013	workshop “Topological phases in condensed matter and cold atom systems”, Cargèse, France
Juin 2013	workshop “Topological phases of matter”, Simons Center, Stony Brook, USA
Nov. 2012	workshop “Entanglement spectra in complex quantum wavefunctions”, Dresden, Germany
September 2012	Symposium “Topological Quantum Information”, Oxford University, UK.
August 2012	workshop “Topological States of Matter: Insulators, Superconductors, and Quantum Hall Liquids”, Nordita, Sweden
April 2012	workshop “New Quantum Phases of Matter in and out of Equilibrium”, GGI, Florence, Italy
November 2011	conference “CFT, Topology and Information”, Institut Poincaré, Paris, France.
March 2010	conference “Physics in the plane: from condensed matter to string theory”, Les Houches, France.

Invited seminars

June 2022	IRMA, University of Strasbourg (analysis seminar), France.
May 2022	King's College London (statistical physics seminar), UK.
Décembre 2021	LPT (séminaire du laboratoire), Toulouse, France.
Novembre 2021	SISSA (statistical physics seminar), Trieste, Italy.
Juin 2021	Université de Genève (séminaire de théorie de la matière condensée), Genève, Suisse.
Janvier 2021	Université de Budapest (hungarian integrability seminar), Budapest, Hungary.
Janvier 2021	Université Catholique de Louvain (math. Physics seminar), Louvain-la-Neuve, Belgique.
Novembre 2020	Penn State University (atomic physics seminar), State College, Pennsylvania, Etats-Unis.

Avril 2019	Brown University (condensed matter seminar), Providence, Rhode Island, Etats-Unis
Mars 2019	Laboratoire de Physique Quantique, ISIS, Strasbourg, France.
Mars 2018	Institut d'Optique (séminaire de théorie des atomes froids), Palaiseau, France.
Février 2018	Université de Ghent (quantum physics seminar), Belgique.
Janvier 2018	Université Joseph Fourier Grenoble (colloquium), France.
Déc. 2017	Institut de Physique Théorique, CEA Saclay (séminaire de physique statistique), France.
Nov. 2017	King's College London (mathematical physics seminar), UK.
Juin 2017	Université Paris XIII-Villetaneuse (séminaire de théorie des atomes froids), France.
Mai 2017	University of Luxembourg (séminaire de théorie de la matière condensée), Luxembourg.
Mai 2017	Oxford University (condensed matter theory seminar), Oxford, UK.
Jan. 2017	LPTHE (séminaire de théorie de la matière condensée), Univ. Pierre et Marie Curie, Paris, France.
Nov. 2016	Université Catholique de Louvain (math. physics seminar), Louvain-la-Neuve, Belgium.
Sept. 2016	Max Planck Institute for Quantum Optics (MPQ–theory division seminar), Garching, Germany.
Juin 2016	Cambridge University (condensed matter seminar), Cambridge, UK.
Mars 2016	SISSA (condensed matter seminar), Trieste, Italy.
Juin 2015	Université Paris Cergy-Pontoise (condensed matter theory seminar), France.
Nov. 2014	MPIPKS Dresden (condensed matter theory seminar), Germany.
Mars 2014	University of Cologne (mathematical physics seminar), Germany.
Fév. 2013	Yale University (condensed matter seminar), New Haven, USA.
Jan. 2013	Université Paul Sabatier (séminaire de théorie de la matière condensée), Toulouse, France.
Nov. 2012	LPTMS (séminaire de théorie de la matière condensée), Université Paris Sud, Orsay, France.
Sept. 2012	Université d'Amsterdam (condensed matter theory seminar), Hollande.
Juin 2012	Microsoft Station Q (“Q-Seminar”), Santa Barbara, USA.
Avril 2012	Ecole Normale Supérieure (séminaire de physique statistique), Paris, France.
Mars 2012	Princeton University (condensed matter theory seminar), USA.
Janvier 2012	Institut de Physique Théorique Saclay (séminaire phys. math.), Gif-Sur-Yvette, France.
Mars 2011	Microsoft Station Q (quantum physics seminar), Santa Barbara, Californie, USA.
Mars 2011	University of Southern California (quantum physics seminar), Los Angeles, USA.
Janvier 2011	University of North Carolina (string theory seminar), Chapel Hill, North Carolina, USA.
Mars 2010	International Center for Theoretical Physics (statistical physics seminar) Trieste, Italie.
Février 2010	University of Chicago (condensed matter theory seminar), Chicago, USA.
Février 2010	Yale University (condensed matter theory seminar), New Haven, Connecticut, USA.
Janvier 2010	Université de Cologne (séminaire de théorie de la matière condensée), Cologne, Allemagne.
Janvier 2010	Université Rome III (séminaire de physique mathématique), Rome, Italie.
October 2009	Journées du LPT ENS, Royaumont, France.